universität
wien

DIPLOMARBEIT

Titel der Diplomarbeit

Human Dermal Mesenchymal Stem Cell Subsets Induce FoxP3 in Naive T cells

angestrebter akademischer Grad

Magistra der Naturwissenschaften (Mag.rer.nat.)

Verfasserin:	Karin Pfisterer
Studienrichtung /Studienzweig (lt. Studienblatt):	Genetik / Mikrobiologie
Betreuer / Betreuerin:	Thomas Decker
	Adelheid Elbe-Bürger

Wien, am 11. 11. 2010

Zusammenfassung

Für die moderne Medizin gewinnt die Stammzellforschung zunehmend an Bedeutung. Mesenchymale Stammzellen (MSZ) sind multipotente adulte Stammzellen, welche in Adipozyten, Osteoblasten und Chondrozyten differenzieren können und immunsuppressive Eigenschaften besitzen. Kürzlich konnten wir verschiedene MSZ-Subtypen in der humanen Dermis identifizieren und isolieren, welche einzigartige Differenzierungskapazitäten aufwiesen und dabei eine Reihe von MSZ Markern exprimierten, die auch auf MSZ aus dem Knochenmark präsent sind. Aufgrund der relativ einfachen Zugänglichkeit der Haut, stellen MSZ in Zukunft eine interessante Möglichkeit für vielfältige Einsatzmöglichkeiten in der Medizin dar. Um jedoch MSZ für therapeutische Zwecke verwenden zu können, werden weitere Informationen über ihre funktionellen Eigenschaften benötigt. Da die Aktivität von Stammzellen eng mit deren Mikroumgebung zusammenhängt, haben wir MSZ-Subtypen in jugendlicher menschlichen Haut mittels Immunfluoreszenz-Färbungen lokalisiert. Dabei haben wir mehrere Zellen und Zellstrukturen gefunden, welche die typischen MSZ-Marker CD73, CD90 und CD271 exprimierten. Weiters fanden wir eine bevorzugte perivaskuläre Verteilung von CD271$^+$ Zellen, welche häufig Kollagen Typ-IV koexprimierten. Zellen, die neuronale und gliale Marker aufwiesen, wurden von CD271$^+$ Zellstrukturen umgeben. Vereinzelt konnten CD271$^+$ Zellen identifiziert werden, welche diese neuralen/glialen Marker koexprimierten. Da bekannt ist, dass MSZ aus verschiedenen Geweben in vitro und in vivo immunsuppressives Potenzial aufweisen, untersuchten wir die immunsuppressiven Fähigkeiten spezifischer MSZ-Subtypen aus der Haut, welche mit Hilfe der Expression der Marker CD73, CD90 und CD271 isoliert wurden. Außerdem stellten wir uns die Frage, ob regulatorische T-Zellen für die Inhibierung der T-Zellproliferation verantwortlich sein können oder zumindest beteiligt sind. Die immunsuppressive Eigenschaft dermaler MSZ wurde in funktionellen in vitro Experimenten untersucht, wobei die gesamte dermale Fraktion, definierte dermale MSZ Populationen und, als Kontrolle, MSZ aus dem Knochenmark verwendet wurden. Es muss betont werden, dass keine dieser Zelltypen kostimulatorische Moleküle, wie CD80/86, exprimiert. Diese Zellen wurden mit CD25-depletierten, naiven T-Helferzellen kultiviert und mit anti-CD3 oder anti-CD3/CD28 Antikörpern stimuliert. Mittels Durchflusszytometrie, wurde sowohl die T-Zell Proliferation mittels Carboxyfluorescein Succinimidylester Verdünnung visualisiert, als auch die Induktion regulatorischer T-Zellen durch Gegenfärbung des Transkriptionsfaktors Foxp3 evaluiert. Anti-CD3/CD28-stimulierte naive T-Helferzellen wiesen nach Kokultur mit Hautzellen oder MSZ aus dem Knochenmark nur eine marginale Erhöhung der Foxp3-Expression in T-Zellen auf, während die Stimulierung mit anti-CD3 alleine die Foxp3-Expression, sowohl nach Kokultur mit dermalen Zellen als auch mit MSZ aus dem Knochenmark, signifikant erhöhte. Außerdem

beobachteten wir eine, wenn auch nicht signifikante Tendenz, dass CD90$^+$ Hautzellen mehr FoxP3 in T-Helferzellen induzieren als CD90-depletierte Zellen. Weiters, fanden wir einen höheren Anteil von Foxp3-exprimierenden T-Helferzellen nach Kokultur mit CD271-depletierten dermalen Zellen verglichen mit CD271$^+$-Zellen. Zusammenfassend konnten wir die enge Assoziation von nicht-follikulären MSZ aus humaner Haut mit dem dermalen Gefäßsystem demonstrieren, welches die Besiedelung einer perivaskulären Nische nahe legt. Diese Lokalisation lässt den Schluss zu, dass sie direkt mit Lymphozyten in der Peripherie interagieren können. Gemeinsam mit den funktionellen Daten weisen unsere Ergebnisse auf eine entscheidende Rolle für dermale MSZ zur Erhaltung der immunologischen Homöostase in der Haut hin, um so möglicherweise exzessive Immunantworten zu verhindern.

Abstract

Stem cell-based therapies are anticipated to be part of modern clinical medicine. Mesenchymal stem cells (MSCs) are multipotent adult stem cells, which can differentiate into adipocytes, osteoblasts and chondrocytes and have immunosuppressive features. Recently, we identified and isolated different MSC subsets in human dermis, which possess unique differentiation capacities and express several markers known to be expressed by bone marrow-derived (BM-)MSCs. Given the easy accessibility of skin, resident MSCs are a very promising autologous source for future stem cell therapies. To make better use of dermal MSCs in therapies, we need a greater in-depth knowledge about their physiological role. Since the activity and functionality of MSCs are closely related with their microenvironment, we localized MSC subsets in human skin cryosections by immunofluorescence staining and found some cells and cell structures to be positive for MSC markers such as CD73, CD90 and CD271. Further, we identified a preferential perivascular distribution of CD271$^+$ cells, frequently coexpressing collagen type-IV. Cells expressing neuronal and glial markers were found to be surrounded by CD271$^+$ cells but rarely CD271$^+$ cells coexpressed these neural crest-related markers. As MSCs from various tissues are known to have immunomodulatory potential in vitro and in vivo, we aimed to investigate the immunosuppressive capacities of specific dermal-derived MSC subsets, separated via the expression of the markers CD73, CD90 and CD271. Further, we wanted to unravel whether regulatory T cells are involved in the inhibition of T cell proliferation. For this purpose, dermal MSCs were subjected to functional in vitro assays. Total adherent dermal cells, defined dermal MSC subsets and, as a control, BM-MSCs, which all lack the expression of CD80/86, were cocultured with naive CD25-depleted, helper T (T$_h$) cells and stimulated with either anti-CD3 or anti-CD3/CD28 mAbs. Using flow cytometry, T cell proliferation and potential induction of regulatory T cells was visualized via carboxyfluorescein succinimidyl ester dilution and counterstaining of the transcription factor FoxP3, respectively. We showed that stimulation of naive T$_h$ cells with anti-CD3/CD28 and coculture with dermal cells or BM-MSCs led to a marginal increase of FoxP3-expressing T cells, while stimulation with anti-CD3 alone and coculture with dermal cells or BM-MCSs significantly increased FoxP3 expression in T cells. Moreover, we found a tendency, though not significant, for CD90$^+$ dermal cells to induce more FoxP3 in T$_h$ cells than CD90$^-$ cells and a higher percentage of FoxP3-expressing T$_h$ cells upon coculture with CD271$^-$ dermal cells compared with CD271$^+$ cells. In summary, we uncovered a close association of human, non-follicular dermal MSC subsets with skin vasculature, suggesting their homing in a perivascular niche. This enhances the probability of a direct interaction with lymphocytes in the periphery. Together with the demonstration of a yet unexplored pathway for FoxP3 induction in naive T$_h$ cells through dermal MSC subsets without the engagement of

known costimulatory molecules, our data suggest a crucial role for dermal MSCs to maintain the immune homeostasis in skin and to prevent excessive immunopathology.

Acknowledgements

First and foremost, I would like to thank my supervisor Adelheid Elbe-Bürger for giving me the opportunity to perform my diploma thesis in her lab. Her open ear for ideas, her passion for science and encouraging and insightful character have been direfully inspiring and highly motivating throughout my working period.

I want to thank my colleagues Marion, Christopher, Waltraud and Nousheen, the SIBs and many other members of the VCC for fruitful scientific and non-scientific discussions and for the numerous happy "Happy hours" we spent together. Especially, I want to thank my former lab member Christine for introducing me into lab-life, for constructive critics, her patience and kind advice in every possible situation.

Moreover, I want to thank my family for believing in me at all stages of my life. In particular, I want to thank my mum, for being proud of me, whatever comes and for taking care of Jakob during the weekends and/or holidays with an extraordinary lovable passion. Furthermore, I want to thank Matthias for enjoyable scientific discussions, his unlimited patience and understanding. By going with me together through the ups and downs of our diploma thesis, he played an invaluable role in finishing this work.

My special thanks go to Matthias and Jakob, for loving me the way I am. I do so too.

Table of content

1   Abbreviations

[^{3}H]-TdR	[^{3}H]-thymidine
7-AAD	7-amino-actinomycin D
Ab(s)	Antibody(ies)
AF	Alexa Fluor
APC	Allophycocyanine
BM	Bone marrow
BSA	Bovine serum albumin
CCL	CC-chemokine ligand
CCR	Chemokine receptor
CD	Cluster of differentiation
CLA	Common leukocyte antigen
CLSM	Confocal laser scanning microscopy
Col-IV	Collagen type IV
DC(s)	Dendritic cell(s)
DMSO	Dimethylsulfoxide
EDTA	Ethylenediaminetetraacetic acid
ESC(s)	Embryonic stem cell(s)
FACS	Fluorescence-activated cell sorter/sorting
FCS	Fetal calf serum
FITC	Fluorescein-isothiocyanate
FoxP3	Forkhead box P3
GFAP	Glial fibrillary acidic protein
GPI	Glycophosphatidyl inositol
Gy	Gray
HLA	Human leukocyte antigen
HSC(s)	Hematopoietic stem cell(s)
IDO	Indolamin-2,3-dioxygenase
IFN	Interferon(s)
Ig	Immunoglobulin(s)
IL	Interleukin(s)
iPS	Induced pluripotent stem cells
iTreg	induced Treg
LC(s)	Langerhans cell(s)
LNGFR	Low-affinity nerve growth factor receptor
mAb(s)	Monoclonal antibody(ies)

MACS	Magnetic cell sorting
MHC	Major histocompatibility complex
min	Minute(s)
mm	Millimeter
MSC(s)	Mesenchymal stem/stomal cell(s)
NCAM	Neural cell adhesion molecule
NK cell	Natural killer cell(s)
nTreg(s)	natural regulatory T cell(s)
o/n	Overnight
PBMC(s)	Peripheral blood mononuclear cell(s)
PBS	Phosphate-buffered saline
PE	Phycoerythrin
PFA	Paraformaldehyde
RCF	Relative centrifugal force
RNA	Ribonucleic acid
rpm	revolutions per minute
RPMI	Roswell Park Memorial Institute
RT	Room temperature
SC(s)	Stem cell(s)
sec	Second(s)
SKP(s)	Skin-derived precursor(s)
TCR	T cell receptor(s)
T_{fh}	T follicular helper cell
TGF	Transforming growth factor
T_h cell(s)	T helper cell(s)
Thy-1	Thymocyte differentiation antigen-1
TR1	T regulatory type 1
TRAIL	Tumor necrosis factor-related apoptosis-inducing ligand
Treg(s)	Regulatory T cell(s)
α-SMA	Alpha-smooth muscle actin

2   Introduction

2.1   The human immune system

The human immune system is an important and powerful defense network against bacteria, viruses, fungi or parasites that reached its actual complexity by co-evolution in conjunction with its invaders. It consists of an inherited part, the innate immunity, and the flexible adaptive immunity, which combined act against early and proceeding infections[1].

The innate immune system, to which the skin and all mucous membranes belong, is a non-specific defense line against microbes and viruses. All epithelia of the body build the first barrier, which prevents pathogens from invading and colonizing the tissues of the body via physical, chemical and microbiological features. If the seal against the exterior is disrupted or weakened, microbes can intrude into the organism, where they either are worsted immediately and non-specific by cells of the innate immune system or, in case they evade, trigger an adaptive immune response, which is by then already "alarmed" by the innate activators[1, 2]. Once the infection is cured, the resulting memory cells can cause a lifelong lasting immunity against this specific pathogen / antigen that ensures a faster and stronger reaction for future infections. Both systems depend on the capability to discriminate between "self" and "non-self", to allow exclusive elimination of foreign pathogens, while tissues of the host are left unhampered[3].

Table 1 | Defense cascade of the human immune system at a glance

Line of defense	Invader's opposition	Features	
1st	Surface barrier	Mechanical	– dense cell network of skin or mucosal epithelia
		Chemical	– antimicrobial peptides, enzymes, acidic body fluids
		Biological	– normal bacterial flora
2nd	Innate & early adaptive	Patrolling phagocytes (macrophages, neutrophiles), complement, natural killer cells;	
		Antibodies secreted at epithelial surfaces, lymphocytes in epithelia;	
3rd	Adaptive	Specific antibodies and lymphocytes	

(adapted from A. Abbas et al.[1])

2.1.1   Adaptive immune system

Responses of the adaptive immune system can be separated into a humoral and a cellular type. The main players of the humoral immunity are antibodies (Abs) that circulate in the blood and lymph and are produced by B lymphocytes that interact and crosstalk with the global players of the cell-mediated immune response system, the T lymphocytes or T cells.

2.1.2 T cells

T cells are produced in the bone marrow along with hematopoietic cells, get preselected in the thymus, to ensure non-reactivity to self-antigens, and spread hereafter throughout the body. T cells can be distinguished from other lymphocytes through their unique expression of the T cell receptor (TCR) on their cell surface, which is composed of an $\alpha\beta$ heterodimer in 90-99% of T cells, compared with a minute number of T cells with $\gamma\delta$ chains (1-10%)[4, 5]. The TCR is associated with non-polymorphic polypeptides (ε, γ, δ and ζ chains) that constitute the cluster of differentiation (CD)3 complex. Early investigations in T cell signaling led to the hypothesis that the TCR initially transduces the signal after peptide (p)MHC binding, whereas recent studies out-dated these models. It was shown by mutagenesis of the immunoreceptor tyrosine-based activation motives (ITAMs) on the cytoplasmatic part of CD3 that the phosphorylation of these tyrosines is an early and mandatory step in T cell activation[6]. Additionally, T cells own costimulatory receptor binding sites along the TCR-complex that interact with CD80 or CD86. For T cell activation, both receptors have to be engaged, to ensure specifity of the immune system, although this is controversial in literature[7]. In vivo, this is performed by professional antigen-presenting cells (APCs), like dendritic cells (DCs), B cells or macrophages that express MHC class I and II, to present foreign peptides via pMHC complexes for initiation of adaptive immune responses of T cells[1]. The simultaneous ligation of the costimulatory receptor molecule CD28, which is constitutively expressed on all T cells, with the costimulatory molecules CD80 or CD86 strongly enhances the T cell signaling and subsequent proliferative response[7]. In vitro, one makes use of Abs directed against CD3 and CD28 to provide both signals and to ensure adequate stimulation of T cell proliferation[8].

Basically, T cells can be divided into two different subgroups, the cytotoxic T cells and the helper T (T_h) cells. $CD8^+$ cytotoxic T cells detect and destroy tumor cells and cells infected by viruses or other invaders via recognition of pathogen peptides presented on MHC-I molecules, which are present on all nucleated host cells. By contrast, T_h cells that express the characteristic coreceptor CD4 and can therefore interact solely with MHC-II, establish and orchestrate immune responses via their interaction with professional APCs, cytotoxic T cells and macrophages, mainly via secretion of various cytokines[1, 2].

2.1.3 Naive T_h cells

Naive T_h cells bear, beneath the TCR, CD45RA, which results from alternative splicing of CD45[9] and classifies the cell as "naive", compared with CD45RO-expressing cells that resemble memory T cells. They play a major role in the maintenance of adaptive immune responses by interacting with B lymphocytes or cytotoxic T cells as well as in the activation of cells of the innate immune system, like macrophages[1]. Further, they have the ability to differentiate into several subsets of T_h cells with different cytokine secretion patterns,

depending on the type of pathogen encountered. CD4$^+$ T cells also play a major role in the development of autoimmune diseases, asthma, allergies or even cancer[10]. As naive T$_h$ cells have never encountered an antigen, they preferentially colonize sites of pathogen entrance or circulate in the lymphatic system, including lymph nodes. The existence of two different subtypes of T$_h$ cells was first described by Mosmann et al., who named and distinguished T$_h$1 from T$_h$2 cells by the different expression of cytokines, primarily interferon (IFN-)γ and interleukin (IL-)4/IL-13, respectively[11]. To date, the dualistic model of T$_h$ cells has been expanded by a broad spectrum of T$_h$ subtypes, like T$_h$17 that secrete IL-17, T$_h$22 expressing IL-22, T follicular helper (T$_{fh}$) cells that produce IL-21 and a regulatory T cell subset, which is thought to be involved in maintaining tolerance by secreting IL-10, IL-35 and transforming growth factor (TGF-)β[10]. The classical monolithic model of T$_h$ cell differentiation is still prevalent, although there is growing evidence that differentiated T$_h$ cells are not terminally restricted to their subtype in reference to the cytokine secretion (**Fig. 1|**). For most studies, however, where the influence of diverse cells, substances or pathogens on the differentiation of naive T$_h$ cells is investigated, predominantly the culture determined phenotype of T$_h$ cells is of note[12]. Whether these T$_h$ cells are flexible and possess the plasticity to change their secreted cytokines or even the expression of their master regulators, is of peripheral interest for many questions asked, but still a very momentous finding for therapeutic implications, as autoimmune diseases or allergic inflammatory disorders, where special T cell subsets are involved, these could be switched to other, less self-reactive and thus less harmful subsets[10].
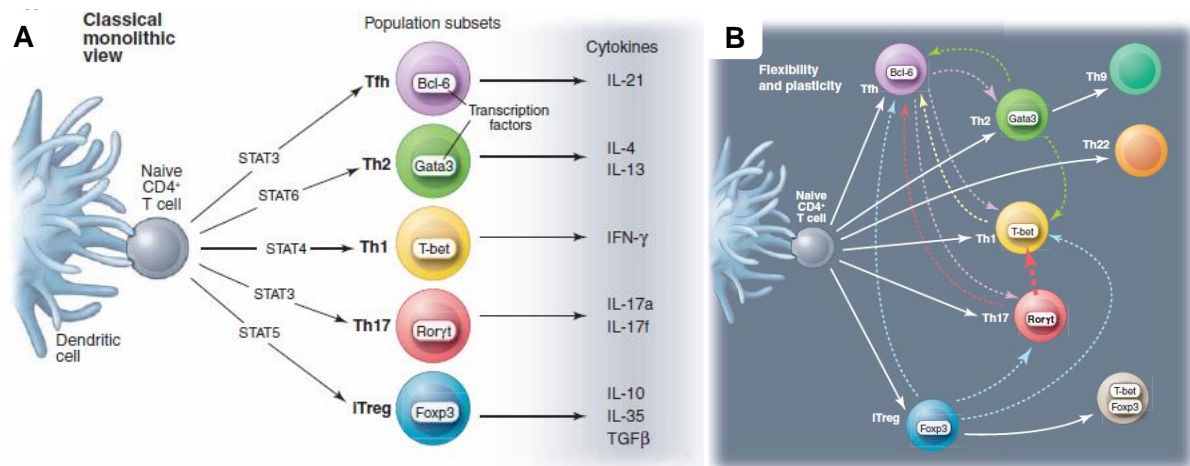
Fig. 1| Differentiation of naive T$_h$ cells. A| The classical monolithic model of CD4$^+$ T cell differentiation that displays the different subsets as terminally committed with specific cytokines expressed and unique master transcription factors. **B|** Emerging evidences raise the question, if a flexible model of T$_h$ cell subsets would be more accurate. This would suggest that different stages of differentiation could be changed in response to intrinsic and extrinsic signals. This flexibility would open new fields for therapeutic approaches. (adopted from O'Shea et al.[10])

2.1.4 Regulatory T cells

The border between fast, effective and potent immune responses, with subsequent clearance of pathogenic microorganisms and misguided deleterious effector functions against self proteins, which can destroy host tissues and lead to severe inflammatory responses (i.e. autoimmunity diseases), is very narrow and must be tightly controlled. The human immune system employs numerous sophisticated regulatory mechanisms to accomplish this indispensable balance and to maintain homeostasis. One of the most prominent cellular guards of peripheral tolerance are regulatory T cells (Tregs)[13], which control the activation and subsequent expansion of aberrant, over- or self-reactive lymphocytes[14]. Further, Tregs suppress effectively allograft rejection, allergy and play an important role in tumor immunity[15]. Like for T_h cells in general, distinct types of Tregs exist, including the adaptively induced T_h3 cells[16], which produce TGF-β, the IL-10 secreting T regulatory type 1 (TR1) and regulatory cells that are CD8$^{+[17]}$ and CD4$^-$CD8$^{-[18]}$, which all acquire their regulatory functions upon specific stimulation with antigens and cytokine messengers. The great majority of Tregs can be described phenotypically as CD4$^+$ T cells, which bear the TCR$\alpha\beta$ and express high levels of CD25, also known as IL-2 receptor alpha. As CD25 is also upregulated upon activation of T cells under neutral TCR stimulation conditions[19, 20], the identification of the transcription factor forkhead box P3 (FoxP3), a master regulator[21] of development[22] and function[21, 23] in naturally occurring (n)Tregs lead to a more defined picture, although the obligatory linkage of FoxP3 expression with the inhibitory activity is controversial in literature. Recent findings showed that activation of human CD4$^+$ and CD8$^+$ T cells subsequently leads to transient and low FoxP3 expression[24], without suppressive capacity. The inclusion of the extracellular marker CD127, whose low expression in Tregs inversely correlates with FoxP3 expression (up to 90%)[25, 26] and the suppressive potency, is one essential finding that helps to clearly delineate and purify nTregs in combination with the expression of CD4, CD25 and FoxP3. nTregs are principally generated in the thymus from CD4$^+$CD25^{low}CD45RA$^+$FoxP3$^-$ T cells, by a mechanism that requires high-affinity interactions between the TCR and self-peptide-MHC complexes presented by thymus-resident stromal cells[18]. Further, thymic DCs[27] and/or stromal cells[14] are thought to regulate the positive selection of self-reactive thymocytes and induce the differentiation into FoxP3$^+$ Tregs via provision of costimulatory molecules, like CD80 or CD86, whose ligation to the T cell molecule CD28 is essential for FoxP3 induction in the thymus. However, the molecular mechanisms that drive the selection and differentiation of nTregs in humans are still unknown and have to be elucidated in more detail. Alternatively, FoxP3$^+$ expression can also be induced in naive T_h cells in the periphery[28-35] with DCs[15, 36] in the presence of TGF-β in vitro[28, 37]. Furthermore, several in vivo studies showed that the conversion of naive T_h cells into Tregs can also occur in the periphery[31, 38, 39]. In vitro-induced Tregs (iTregs) show the same inhibitory potential as thymus selected nTregs, but it

still has to be clarified, whether iTregs are functionally stable over longer periods and to what extend and under what conditions they are generated in vivo[14]. Nevertheless, several factors have been identified that facilitate and enhance the differentiation of naive T_h cells into iTregs and maintain their survival and function, although exogenous cytokines are not mandatory[40]. Most prominent, along with the most critical factor TGF-β, is the cytokine IL-2, which is the ligand for the receptor CD25 and has been shown in vitro[41-43] and in mouse models[44, 45] to be an enhancer of the TGF-β-induced differentiation pathway in the periphery, but most important, a key factor of nTreg growth and survival[46]. Other members of the common cytokine-receptor γ-chain family, to which beneath IL-2 belong for instance IL-7 or IL-15[47], may substitute partly the maintenance activity of IL-2 and might contribute to Treg development[48] and function[49, 50]. Further, it has been shown that tryptophan catabolism through indolamin-2,3-dioxygenase (IDO) matures DCs, with the help of IFN-γ[51], to induce FoxP3+ Tregs in humans[52] and that retinoic acid[53] plays an auxiliary role in DC-mediated Treg conversion in the presence of TGF-β[54-57]. Although many mechanisms have been investigated and found to be involved in adaptive Treg development, it seems that a great variety of rapid induction models exist in inflamed peripheral tissues[58], but also during normal maintenance of homeostasis, and remain elusive.

2.2   Stem cells

The term stem cell was originally introduced by the Russian histologist A. Maximow at the beginning of the 20th century[59], for describing hematopoietic progenitor or stem cells (HSCs), which are now known to be the initiators of a well-organized developmental hierarchy[60], called hematopoiesis. Generally, stem cells are defined as unspecialized cells with an nearly unlimited ability to renew themselves by mitotic cell divisions, even after long phases of inactivity. Further, they possess the plasticity to differentiate into any organ- or tissue-specific cell under specific conditions, induced by the microenvironment in vivo, or artificially in an experimental system in vitro. Stem cells can be isolated from embryonic [embryonic stem cells (ESCs)] and non-embryonic tissues[61], whereas the latter gives rise to two different stem cells, the naturally occurring somatic or adult stem cells, like HSCs or mesenchymal stem cells (MSCs) and the induced pluripotent stem cells (iPS) that can be generated from adult tissue cells, like fibroblasts. Fulfilling the criteria of long-term self-renewal and pluripotency, as they are able to differentiate into cells of the ectoderm, mesoderm and endoderm, ESCs are promising candidates for cell therapy applications, like regenerative medicine and tissue replacement. Further, this cell type resembled for years the only model to investigate the mechanisms of early developmental differentiation events for humans. However, since the first success in culturing human-derived ESCs in vitro, they are a matter of debate[62], as they are derived from preimplanted embryos[63], more precisely from

blastocysts. Moreover, cell transplantation therapies with ESCs are still challenging, predominantly facing the problems of graft rejection with allogeneic cells and tumorgenicity. The recent achievement of K. Takahashi and coworkers in 2007, who retrovirally introduced four essential transcription factors (Sox2, c-Myc, Oct-3/4 and Klf4)[64] into differentiated somatic human cells (fibroblasts), which resulted in restored pluripotency, with cells exhibiting the morphology, dividing potential and expression profile of ESCs[65], could have solved ethical concerns and rejection problems by using patient-derived cells. Since then, the original experimental setup has been improved manifold, regarding safety (c-Myc is oncogenic and retroviral vectors are not the delivery method of choice for human studies) and efficiency, through worldwide extensive work in this field. But up to date the clinical use of iPS cells is still far away from routine applications, as transplanted iPS cells have the same or even higher potential to form teratomas as ESCs[66, 67]. Furthermore, transcription-factor-based reprogrammed somatic cells keep residual signatures of DNA and histone methylation patterns[68], which are typical of the tissue origin (fibroblasts or blood), but this cell type still resembles an effective tool for basic developmental research.

2.2.1 MSCs

Friedenstein and his colleagues[69] discovered bone marrow-resident, non-hematopoietic adult stem cells in the 1970ies, called MSCs, and pioneered the tremendous work on these adult stem cells till this day. As the name implies, these cells are derived from immature embryonic connective tissue, the mesenchyme. MSCs are fibroblast-like cells[70] that have a limited capacity for self-renewal[61] and exclusively possess multipotency, which means that they are primarily restricted to differentiate into cells of their origin, like chondrocytes, adipocytes and osteoblasts, but can also give rise to tendon, ligament, muscles, dermis and connective tissue[71]. The potential to give rise to neuro-ectodermal cells, like neurons and astrocytes, and endodermal cell types, like hepatocytes, broadens the in vitro differentiation repertoire of MSCs tremendously[72-74]. Although the majority of MSCs resides in the bone marrow, many studies report about the existence of MSCs in multiple organs and tissues in animals[75, 76] and humans[77], like adipose tissue, amniotic fluid, cultured pancreatic islets[78], periostium, fetal tissues[79] (i.e. aorta-gonad-mesonephros and yolk sac[80]), placental tissues, and others. This suggests a perpetual reservoir of tissue-specific stem cells in virtually all post-natal tissues for the regeneration of injured tissues and the replacement of damaged cells[81]. The migration capacity towards inflamed tissues in response to chemotactic factors[82], has already been evaluated in pre-clinic studies via infusion of MSCs into animals and showed local engraftment in damaged tissues with repair potential to a greater or lesser extent in different disease settings[82, 83]. Therefore, MSCs are believed to be the adult stem cell with highest therapeutic potential[84].

2.2.2 MSC markers

MSCs are a very heterogeneous subset of stroma cells, expressing a great variety of markers, most of which are also present on multiple miscellaneous cell types. Due to the lack of specific antigens that clearly define MSCs, the "International Society for Cellular Therapy" postulated the minimal criteria to define MSCs[85], which facilitates a uniform phenotypic description. Beneath the potential to differentiate into osteoblasts, adipocytes and chondrocytes in vitro, MSCs must be plastic-adherent and have to express the membrane-bound antigens CD73, CD90 and CD105. Further, the expression of CD11b or CD14, CD19 or CD79α, CD34 and CD45 should be absent[85]. The lack of HLA-DR and the costimulatory molecules CD80 or CD86 renders MSCs as hypo-immunogenic cells, not able to induce allogeneic immune responses[86].

2.2.2.1 CD73

CD73, also known as Ecto-5'-nucleotidase (NT5E), dephosphorylates nucleotides, such as adenosinmonophosphate, thereby creating nucleosides[2, 87, 88], like adenosine. This glycophosphatidyl inositol (GPI)-linked dimer[1] is expressed on B and T cell subsets, like Tregs[89] and primed uncommitted T_h cells[90], endothelial cells, fibroblasts[91], germinal centre follicular DCs[1], epithelial cells[88] and MSCs from bone marrow[92] and other tissues. CD73 seems to be implicated in the protection against tumor necrosis factor related apoptosis inducing ligand (TRAIL)-induced apoptosis[93] and might therefore be widely expressed on many tumor cell lines and cancerous tissues[94].

2.2.2.2 CD90

The thymocyte differentiation antigen-1 (Thy-1) or CD90, is a highly conserved GPI-anchored cell surface protein, which belongs to the immunoglobulin superfamily[1]. Originally detected on thymocytes, CD90 is now widely used as a surrogate marker to identify and isolate immature CD34$^+$ HSCs from peripheral blood[95], but also other stem cells, like keratinocyte stem cells[96] and MSCs. Further, this marker is expressed on T cells, neurons, activated endothelial cells[97, 98] and partly on fibroblasts[99, 100]. It has been shown to be involved in the regulation of various nonimmunologic processes, as cell adhesion, tumor growth, migration and apoptosis[98].

2.2.2.3 CD105

The homodimer[1] CD105 or endoglin is mainly expressed on endothelial cells, especially in the vasculature of solid tumors, inflamed tissues and healing wounds[101]. Further, it is present on activated monocytes, macrophages and bone marrow subsets[2], like MSCs[92]. It is a component of the TGF-β receptor complex[102] and capable to bind TGF-β and modulate cellular responses to this growth factor[1].

2.2.2.4 CD271

The low-affinity nerve growth factor receptor (LNGFR or CD271) is a specific marker for cells of the central and peripheral nervous system. Recently, it has been reported to be expressed on melanoma-initiating cells in humans[103], which started again the discussion, whether cancer stem cells may originate from the transformation of tissue-specific stem and progenitor cells. Formerly, the marker CD271 was described for the isolation of neural crest stem cells from peripheral nerves[104]. Currently, it is a very promising candidate for the prospective isolation of high clonogenic MSC subsets from bone marrow[105, 106]. Isolated CD271+ cells from bone marrow coexpress the well established MSC markers CD73 and CD105[106].

2.2.2.5 CD56

Beneath its expression on the surface of neurons, glial cells, skeletal muscle and neuromuscular junctions[88], the neural cell adhesion molecule (NCAM), or CD56, is expressed on virtually all resting and activated natural killer (NK) cells and subsets of B and T cells[1]. The expression of CD56 in combination with the mesenchymal stem cell antigen-1 and CD271 has been shown to define a distinct subtype of BM-MSCs, with distinct morphologic characteristics, a high clonogenic potential and enhanced differentiation capacity towards the chondrocyte lineage[107].

2.2.3 Immunomodulatory potential of BM-MSCs

The immunomodulatory properties of BM-MSCs have been demonstrated manifold in vitro and in vivo, but the mechanisms that drive this potential still remain elusive. Widespread in vitro studies have shown the hypo-immunogenic and profound immunosuppressive capacities of MSCs, through interactions with cells of the innate and adaptive immune system[108, 109]. In vivo, MSCs are thought to maintain peripheral tolerance[110], regulate autoimmunity[111] and fetal-maternal tolerance[112] and might play a major role in tumor evasion[113]. Further, autologous or syngeneic MSCs from bone marrow or blood[109] have been proven in clinical trials to be safe and partly reduce graft-versus-host disease and ameliorate the reconstitution of several patients hematopoietic system, when cotransplanted in HSC-therapies[114-116]. Moreover, MSCs were demonstrated to have vigorous immunomodulatory activity on cells of the innate and adaptive immunity, including the inhibition of monocyte maturation and function[117] and the in vitro differentiation of CD34+ HSCs into DCs[118]. Further, DC activity is down-regulated upon coculture with MSCs, regarding the expression of HLA-DR, costimulatory molecules and secretion of cytokines[119, 120]. The cytotoxic activity of NK cells, another important player of the innate immunity, was shown to be down-regulated through human MSCs in vitro[121]. But also cells of the adaptive immunity are modulated by MSCs, including the suppression of B cell proliferation[122] and

differentiation into Ab-producing cells and affect their chemotactic properties[122]. As B cell responses are mainly T cell-dependent, the effect of MSCs on T cells has accumulated major interest in the last years. MSCs have been reported to inhibit proliferation of CD4$^+$ and CD8$^+$ T cells stimulated with alloantigens, mitogens or specific Abs in vitro[123-125] and are able to induce peripheral T cell tolerance in mice models for autoimmunity diseases[126]. This suppression is not obligatory the result of induced apoptosis[83], as T cell survival has been shown to be sustained in a quiescent state through MSCs, which leads to an overstimulation and subsequent activation-induced cell death[127]. Further, it has been shown that BM-MSCs recruit, regulate[128] and stimulate the proliferation of CD4$^+$ and CD8$^+$ Tregs[129] and induce the differentiation of naive T$_h$ cells towards a regulatory phenotype[130], with expression of FoxP3[131]. The MSC-mediated immunomodulation is not solely cell contact dependent, as various soluble factors have been shown, to be, at least partly, implicated in the mechanism, like TGF-β1, prostaglandine E2, IDO, human leukocyte antigen G5[109], inducible nitric oxide synthase, heme oxigenase 1[132] or cytokines such as IL-10[133].

2.2.4 MSC niche

The concept of a stem cell niche for HSCs was already introduced in 1978 by Schofield et al.[134] and has been supported from thereon, creating a new research field focussing on the in vivo identity and anatomic location of adult stem cells. BM-MSCs share their microenvironment with HSC and have been shown in murine studies to differentiate into cells producing the functional components that support hematopoiesis[135], like pericytes, myofibroblasts, stromal cells, osteoblasts and endothelial cells[83]. Three types of niches have been described for HSCs[81], which are provided by cells originating from MSCs. The endosteal niche is formed by osteoblasts[136] in the trabecular area of the large bones, whereas the pericyte niche is composed of perivascular cells, which express alpha-smooth muscle actin (α-SMA)[137]. The third hypothesized niche is the vascular niche, which is built up by endothelial cells and CD146$^+$ sub-endothelial stromal cells[83]. However, stromal cells of every supposed niche provide the environment that prevents HSC differentiation, proliferation and apoptosis and maintains their self-renewal capacity[83] by keeping them in a quiescent state. Recently, Méndez-Ferrer et al. reported about a close association of MSCs and HSCs in rodent bone marrow. Nestin$^+$ MSCs did not express vascular endothelial markers, like CD31 or CD34, but were distributed perivascular, mainly outside the endosteal region, which supports the theory of a perivascular niche[138].

2.3 Skin

The skin, with a surficial area between 1.5-1.8 m^2, is the largest sensory organ of the human body[139] and constitutes the first effective barrier against external physical, chemical or biological offenses[140]. Schematically the skin structure is arranged in three main layers: (i) epidermis, including its specialized epithelial structures, namely the appendages, which is connected to the (ii) dermis or cutis by the dermal-epidermal basement membrane and the lowermost layer, which is called (iii) hypodermis or subcutis and anchors the skin to the deep fascia.

2.3.1 Epidermis

The superficial epidermis is a malpighian epithelium[140] that forms the first line of defense of the human body and has self-renewal capacities via proliferating resident stem cells[141, 142] that differentiate during their migration from the Stratum basale, through the Stratum spinosum, Stratum granulosum and Stratum lucidum to the Stratum corneum[143] (**Fig. 2|**). The epidermis originates from the ectoderm[140] and is non-vascularized, but contains many cutaneous appendages like hair and pilosebaceous follicles, sweat gland endings and nails[140, 144]. The majority of epidermal cells is comprised of keratinocytes that are interspersed with professional APCs, called the Langerhans cells[143], which are specialized, mobile DCs. Another epidermal cell type, the melanocyte, is derived from the neural crest, produce the skin pigment melanin[140, 143] and can be found in the basal layer. Merkel cells[145] function as mechanotransducers[146] by contacting dermal sensory axons and are localized in the basal layer and around hair follicles[140]. Lymphocytes are very infrequent in the epidermis and express mostly memory/effector T cell molecules[140, 147].

2.3.2 Dermis

The dermis can be separated into the papillary part underneath the epidermis that forms cones[140], which extend into the epidermis and provide additional stability, and the reticular or deep dermis. The main structural components that characterize this supportive, compressible and elastic connective tissue, are dermal fibres that are made of interstitial collagen and resist mechanical stress, elastic fibers that are responsible for the retractile characteristics[140] and the extrafibrillar matrix, which consists of proteoglycans and glycoproteins[140]. The dermis is vascularized and nerved, contains vessels of the peripheral lymphatic system and the deep part of skin appendages[140]. The fundamental cells of the dermis are the fibroblasts[143], which are the main producers of fibres and ground substance[140] and are also thought to have immunomodulatory functions[148, 149]. Further, cells of the immune system, such as DCs (interstitial and plasmacytoid), mast cells,

macrophages, NK cells and T cells[147] (NKT cells, cytotoxic T cells and T_h cells), can be found in low numbers in healthy human dermis[144, 150].

2.3.3 Hypodermis

The hypodermis - the innermost layer of the skin - connects the dermis to the fascia laying underneath and acts as energy reservoir via the fat storing adipocytes, which represent the main characteristic cell type[140].
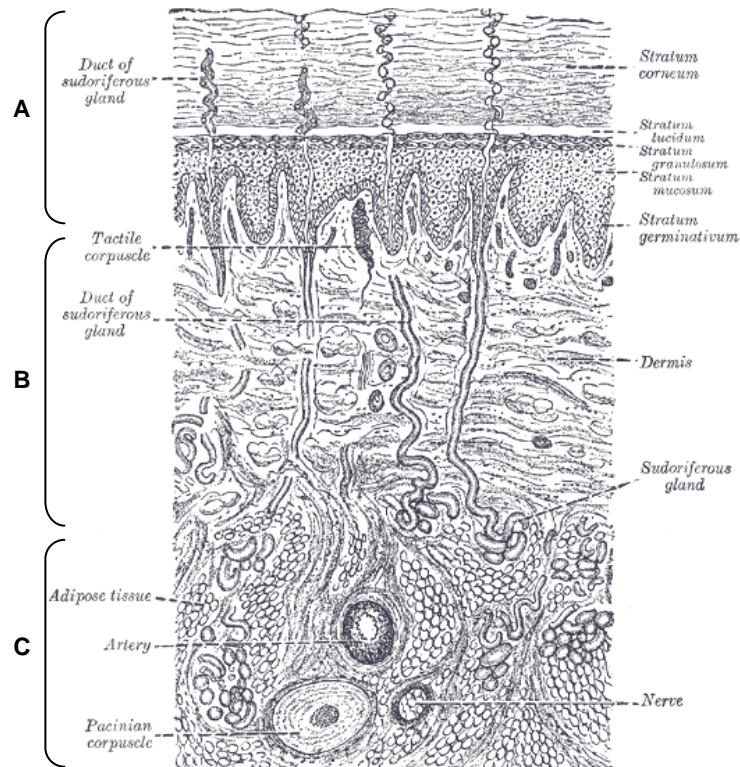
Fig. 2| Schematic overview of human skin. The outermost layer of the skin is built by **A|** the stratified epidermis, followed by **B|** the dermis and **C|** the subcutis. (Adopted from Gray[151])

2.3.4 Skin homing T cells

Normal healthy skin harbors more than 2×10^{10} resident T cells[150] that are critical for cutaneous immunosurveilance[152] and are thought to play a major role in many inflammatory skin diseases, like psoriasis, atopic dermatitis or melanoma. The predominant T cell type in the epidermis expresses the markers CD8 and CD45RO, bears the common $TCR\alpha\beta$[153] and is located in the basal and suprabasal layer of keratinocytes[150]. In contrast, the dermis contains around 90% CD4- and only 10% CD8-positive cells[154], predominantly of a memory phenotype that mainly express, amongst others, a skin-homing receptor, called cutaneous lymphocyte antigen (CLA)[154], which is the ligand for E-selectin. Dermal T cells are located around postcapillary venules, close to the epidermal-dermal junction and in proximity to skin appendages[150]. The vast majority of CD3+ T cells in fetal skin are naive CD4+ T cells, while only ~5% CD45RA+ T cells are found in adult non-inflamed skin under resting conditions[147].

Among conventional T cells in human skin, like T_h1, T_h2 and T_h17 cells, there exist also a small proportion of TCRγδ cells and invariant NKT cells, which both have been reported to be involved in skin inflammatory diseases and cancer, but further studies are required to determine their specific functions[150]. Approximately 5-10% of skin T cells express FoxP3 and are able to suppress T cell proliferation in vitro[147]. Both, epidermal Langerhans cells and dermal DCs, might be able to induce Tregs in the periphery, through production of TGF-β and presentation of antigens via MHC II[15]. Increased numbers of Tregs have been reported in cell carcinomas[155, 156] of the skin, primary melanoma and metastasizing forms of skin cancer. Interestingly, the majority of FoxP3^{+} Tregs from human peripheral blood bear skin-homing receptors, like CLA, the chemokine receptor CCR4 or CCR6[157]. Further, leasonal skin of psoriatic patients contains Tregs with reduced suppressive capacity[158], which suggests a major role of Tregs in maintaining skin immune homeostasis[159].

2.3.5   Skin-derived progenitor cells and their immunomodulatory potential

Two types of progenitor cells have been described in human skin. Skin-derived precursor cells (SKPs) are neural crest-related progenitor cells identified in rodent[160] and human skin[161, 162], which posses multipotency and show remarkable self-renewing capacities. SKPs are isolated by culturing of dissociated skin with epidermal and fibroblast growth factors, which results in the formation of spheres that can be transferred into new culture flasks and subsequently expanded[160], while remaining their differentiation capacities[162]. SKPs express markers specific of embryonic neural crest[163] and Nestin^{+} cells were shown to differentiate in vitro into neural cell types, expressing neuronal markers like β-III-tubulin, neurofilament-M, neuron-specific enolase and markers specific for the peripheral nervous system, like CD271[164] and CD56. Also glial markers, like the glial fibrillary acidic protein (GFAP) and CNPase could be detected, but resulted from differentiation of distinct SKP subpopulations[160]. Additional clonal analysis of diverse SKPs identified the individual potential of different clones to differentiate into neuronal and glial cells, but also into cells of the mesenchymal lineage, like α-SMA-expressing cells or adipocytes. SKPs were found to be situated in a distinct dermal niche, within the hair papillae[165] and whisker follicles[163]. This distincts SKPs from dermis-derived MSCs that are predominantly isolated from glabrous skin, like foreskin[161]. These progenitor cells might occupy a perivascular niche, known already from BM-MSCs, or reside in the interfollicular dermis[166] and can be isolated via sphere formation[161], described above, or removal of the epidermis, subsequent enzymatic digestion of apical dermis and selection for plastic adherence[148, 167]. MSC-like cells were described to be present in variable numbers within different skin donors[167] as just some cells within the dermal cell pool were able to differentiate into adipocytes, osteoblasts and chrondrocytes[167]. Further, dermal MSCs have been reported to differentiate in vitro into neurons, glia, smooth muscle cells and cells of the peripheral nervous system as well[161].

Investigations of the immunomodulatory potential revealed that dermal MSCs are functionally comparable to BM-MSCs[148], for instance they are capable to restore the microenvironment in bone marrow, through the maintenance HSC proliferation, engraftment and survival in vivo, at least in animals[168]. Further, human dermal MSCs have been reported to induce DC maturation[149], to suppress the proliferation of allogeneic T cells and PBMCs[167] in vitro via similar mechanisms, although reversible, modulate the cytokine expression pattern of T cells [148], cause cell-cycle arrest in PBMCs[167] and prevent apoptosis. Additional in vitro models of human graft-versus-host disease showed that after exposure of T cells with dermal MSCs, the reactions were at least dampened slightly[148]. This enhances the idea of an alternative MSC source that is easily accessible and could be used for cellular therapies.

3   Objective of the thesis

Mesenchymal stem cells are a very heterogeneous population of adult stem cells, resident in various tissues. We have previously shown that the human dermis harbors different MSC subsets. To better understand the localization and potential role of tissue-resident MSCs for the maintenance of skin immune homeostasis, it was the aim of this thesis to:

i)   localize dermal MSCs via immunofluorescence and to allocate them into a dermal MSC-niche in situ, through analysis of the microenvironment

ii)   visualize the morphology of adherent dermal cells in vitro via immunofluorescence

iii)   investigate the immunosuppressive potential of dermal MSC subsets via coculture assays with T cells and naive helper T cells and to elucidate the mechanism(s) that drive this immunosuppression

4   Materials & Methods

4.1   Apparatuses, instruments and software

1450 Microbeta liquid scintillation counter	PerkinElmer, Waltham, MA, USA
Cell separator (MiniMACS)	Miltenyi Biotech, Bergisch-Gladbach, GER
Centrifuge 5415 R	Eppendorf, Hamburg, GER
Compound microscope (Eclipse 80)	Nikon, Tokyo, JP
Confocal laser scanning microscope 510	Zeiss, Jena, GER
CO_2 incubator, humified	Heraeus, Vienna, AUT
Cooling centrifuges	Heraeus
Counting chamber	Neubauer improved, Laboroptik, GER
Cryo 1°C freezing container „Mr. Frosty"	Nalgene/NUNC, Rochester, NY, USA
EasySep®	Stemcell Technologies, Grenoble, F
FloJo Software	Tree Star Inc., Ashland, OR, USA
Flow cytometer (LSR II)	Becton Dickinson, San Jose, CA, USA
Forceps	
Freezers (-20°C, -80°C)	
Fridges	
Irradiator IBL 437C	CIS bio international, Gif sur Yvette, FR
JungCM1800 Cryostat	Leica Microsystems, Wetzlar, GER
Laminar flow	Holten, Allerod, DK
LSM image browser	Zeiss
Microcentrifuges	Eppendorf
Nikon Coolpix 995 digital camera	Nikon, Tokyo, JP
Optical microscope Nikon eclipse 80i	Nikon
Pipet	Gilson, Middleton, MI, USA
Pipetman (1-50 ml)	Hirschmann, Eberstadt, GER
Prism 5 for Windows	GraphPad Software, Inc., La Jolla, CA, USA
Scale	Sartorius, Vienna, AUT
Scalpels	
Scissors	
Stainless steel metal mesh	
Vortex Genie 2	Lactan, Graz, AUT
Water bath	GFL, Burgwedel, GER

4.2   Consumables

Bottle-top filters (0.2 and 0.4 µm)	Cornig, Amsterdam, NL
Cell separation columns (MS, LS)	Miltenyi Biotech
Cell strainer (40 and 70 µm)	Falcon, Lincoln Park, New Jersey, USA
Culture flasks	Cornig
Eppendorf tubes (1.5 ml, 2 ml)	Eppendorf
Falcon tubes (15 ml, 50 ml)	Becton Dickinson Bioscience
Gloves	Sempermed, Vienna, AUT
Lab-Tek™ II – CC^2™ chamber slide™(8-well)	Nalgene/NUNC
Microscope glass cover slips (24x40mm)	Marienfeld, Lauda-Königshofen, GER
Microscope slides	Marienfeld
Microtubes for flow cytometry	Micronic, Lelystad, NL
Parafilm	Brand, Wertheim, GER
Petri dishes for tissue culture (100x20mm)	Cornig
Pipettes (2 ml, 5 ml, 10 ml, 25 ml, 50 ml)	Cornig
REAL™ capillary gap microscope slides	Dako, Glostrup, DK
Round-bottom 96-well-plates	Cornig
Sterile tips (1-100 and 200-1000 µl)	Cornig

4.3   Chemicals, reagents, buffers and media

3-isobutyl-1-methylxanthine	Sigma-Aldrich, St. Louis, MO, USA
7-AAD	Sigma-Aldrich
Acetone (p.a.)	Merck
Alizarin Red	Sigma-Aldrich
Alpha-MEM	Gibco, Invitrogen, Carlsbad, CA, USA
Ascorbic acid	Sigma-Aldrich
Antibodies	see **Table 4|**
Betaisodona	Mundipharma, Vienna, AUT
β-mercaptoethanol	Gibco
BSA	Sigma-Aldrich
CFSE	Molecular probes, Eugene, Oregon, USA
Cytofix/Cytoperm solution	Becton Dickinson Bioscience
Dexamethasone	Sigma-Aldrich
Dispase II (neutral protease, grade II)	Roche Applied Science, Basel, CH
DMEM	Gibco
DMSO	Serva, Heidelberg, GER

Dynabeads	Invitrogen
Elite mouse IgG Vectastain Kit	Vector Laboratories, Burlinghame, CA, USA
FACS Sheath	Becton Dickinson Bioscience
Fetal calf serum (heat-inactivated)	PromoCell, Heidelberg, GER
Ficoll™Hypaque™PLUS	Amersham Bioscience, Buckinghamshire, UK
Gentamicin	PAA, Pasching AUT
Giemsa's Azure Eosin Methylene Blue	Merck
Glycerol-2-phosphate	Sigma-Aldrich
$[^3H]$-Thymidine	Hartmann Analytic, Göttingen, GER
Hematoxiline monohydrate	Merck
Heparin	Biochrom AG, Berlin, GER
HPL	Dr. Dirk Strunk, Med. Univ. of Graz, AUT
Hydrogen peroxide (30%)	Merck, Darmstadt, GER
Indomethacine	Sigma-Aldrich
Insulin (human)	Sigma-Aldrich
Isopropanol	Merck
L-glutamine	Gibco
Liberase Blendzyme 3	Roche Applied Science
May-Grünwald's eosin methylene blue sol.	Merck
MEM Alpha Medium + Glutamase – I (1x)	Invitrogen
Methanol	Merck
Microbeads (anti-biotin, -PE, -APC)	Miltenyi Biotec
Mounting medium for immunofluorescence	Vector Laboratories
Mounting medium for immunohistochemistry	Aquatex, Merck, Darmstadt, GER
Non-essential amino acids	Gibco
O.C.T.	Tissue-Tek, Sakura Finetek, Zoeterwoude, NL
PBS	Gibco
PenStrep	Gibco
PFA	Merck
RPMI 1640	Gibco
Saponin	Sigma-Aldrich
Sodium pyruvate	Gibco
Trypan blue (0.4%)	Sigma-Aldrich
Trypsin-EDTA solution	Gibco
(1x; 0.05% Trypsin, 1 mM EDTA)	

4.4 Buffers and solutions

4.4.1 Magnetic cell sorting (MACS) buffer
1x PBS

2 mM EDTA (for cell culture, autoclaved)

0.5% BSA

4.4.2 Dynabead buffer
1x PBS

0.1% BSA

2 mM EDTA (pH 7.4)

4.4.3 Buffers, fixatives and Ab diluents for immunofluorescence (IF) and immunohistochemistry (IHC)

Wash buffer for IF and IHC staining (1x)

10x PBS

aqua bidest

Ab diluent (2% BSA-PBS)

1x PBS

BSA (v/v 2%)

4.4.4 Buffers for flow cytometry

FACS buffer (FACS-Flow + 1% FCS)

For one liter of FACS buffer a sterile bottle was filled up with FACS-Flow and heat-inactivated FCS (see section culture media) was added in the appropriate amount to get a 1% concentration of FCS in the whole volume.

FACS washing buffer I (1x PBS + 5% FCS)

For each staining the buffer solution was freshly prepared [can be stored at 4°C for a maximum of 1 week, otherwise conservatives (acid) have to be added].

FACS permeabilisation buffer (1x PBS + 0.1% saponin)

The permeabilisation buffer was either freshly prepared (can be stored for up to one week), or a higher concentrated stock solution (10% saponin) was made that can be stored longer, and diluted to the adequate concentration before usage.

FACS washing buffer II (1x PBS + 0.1% saponin + 5% FCS)

FCS was added in the adequate concentration to the permeabilisation buffer.

4.4.5 Paraformaldehyde (PFA)

The 8% stock solution was stored at -20°C. The fixation reagent was diluted with 1x PBS to get a 4% solution. This was stored for up to 2 weeks in the fridge.

4.4.6 Carboxyfluorescein succinimidyl ester (CFSE) stock-solution

First, a stock solution was prepared with DMSO to get a final concentration of 5 µM (molar mass of CFSE = 557.47g/mol). Aliquots of 100 µl were stored at -20°C for several months.

4.5 Cell culture media

All media were always freshly prepared.

4.5.1 Heat inactivation of FCS

Frozen FCS was thawed o/n at 4°C and subsequently heat inactivated (56°C for 30 min) in a prewarmed waterbath. The serum was left to cool down for 30 min and 50 ml aliquots were prepared and immediately stored at -20°C.

4.5.2 NCM (Normal conditioned medium)

500 ml RPMI 1640

10% FCS

10 µg/ml gentamycin

2 mM L-glutamine

0.1 mM non-essential amino acids

1 mM sodium pyruvate

50 M β-mercaptoethanol, 1% PenStrep

4.5.3 α-MEM$_{DERM}$

500 ml MEM Alpha

10% FCS

1% PenStrep

4.5.4 α-MEM$_{BM}$

500 ml MEM Alpha

10% FCS

4.5.5 Expansion medium$_{BM}$

For expansion of bone marrow-derived cells, we used human platelet lysate (HPL) instead of FCS, as it has been reported by Schallmoser et al.[169] that the mean population doublings are significantly higher, which means that they expand more rapidly with addition of HPL.

Aliquots of 50 ml were centrifuged at 3000 rpm and the supernatant (around 40 ml) was used as supplement.

500 ml MEM Alpha
8-10% HPL
2 IU/ml Heparin

4.5.6 HaCaT & HEK 293 medium
500 ml DMEM
10 % FCS
1 % Penicillin/Streptomycin

4.5.7 Adipo$_{IND}$ medium
α-MEM$_{DERM}$
0.2 mM indomethacine
1 µM dexamethasone
0.5 mM 3-isobutyl-1-methylxanthine
10 µg/ml recombinant human insulin

4.5.8 Osteo$_{IND}$ medium
α-MEM$_{DERM}$
1 µM dexamethasone
50 µg/ml ascorbic acid
10 mM glycerol 2-phosphate

4.6 Kits

4.6.1 Pan T cell isolation kit II
Biotin-conjugated mAbs against CD14, CD16, CD19, CD36, CD56, CD123, and CD235a/Glycophorin A. Microbeads conjugated to a monoclonal anti-biotin Ab (isotype: mouse IgG1; Miltenyi Biotec).

4.6.2 Naive T cell isolation kit
Biotin-conjugated mAbs against CD8, CD14, CD15, CD16, CD19, CD25, CD34, CD36, CD45RO, CD56, CD123, TCR$\gamma\delta$, HLA-DR, and CD235a. Microbeads conjugated to a monoclonal anti-biotin Ab (isotype: mouse IgG1; Miltenyi Biotec).

4.7 Isolation of dermal cells

Non-inflamed juvenile human foreskin, undergoing routine circumcision, was obtained as discarded material. The study was approved by the ethics committee of the Medical University of Vienna in accordance with the Declaration of Helsinki Principles and parents gave their written informed consent. Until further processing, skin was stored (4°C in 1x PBS) for a maximum of 24 hours. The subcutis was scraped off with a sterile scalpel, before the skin was incubated for 5-10 min in undiluted Betaisodona at RT. Excess Betaisodona was flushed away with 70% ethanol. The disinfected skin was rinsed with 1x PBS and cut immediately into small pieces (4x2 mm), which were placed dermal side down on a 25% dispase solution (in 1x PBS) and incubated o/n at 4°C. On the next day, the epidermis was separated manually from the dermis with two forceps. The dermis was sheared with a scalpel and incubated for 90 min in 2x Liberase (equals 9.88 Wünsch units) + 10 ml 1x PBS (total collagenase concentration in dissociation solution: 0.18 mg/ml) at 37°C in a waterbath, shaken constantly to digest the tissue. To obtain single cells, the suspension was first sieved through a steel mesh to get rid of the undigested parts and thereupon filtered through a 70 µm cell strainer. Cells were washed with 30 ml NCM and centrifuged at 1400 rpm for 7 min at RT to collect the cells. The pellet was resuspended in medium and stored at 4°C until further processing.

4.8 Isolation of peripheral blood mononuclear cells (PBMCs)

Human PBMCs were isolated from purchased buffy coats of healthy adult volunteers that donated blood at the local transfusion service (Rotes Kreuz, Vienna, AUT).

4.8.1 Ficoll-Paque™PLUS density gradient centrifugation for isolating PBMCs

1.) Bring all involved reagents at RT.
2.) Blood samples are taken into heparinized tubes (Vacuette, 9 ml draw capacity).
3.) Invert the tubes several times to avoid coaggulation.
4.) Transfer the blood into 50 ml Falcon tubes and dilute 1:1 with 1x PBS.
5.) Add 9 ml of Ficoll-Paque PLUS™ (specific density 1.077 g/ml) by pipeting it slowly under the PBS-blood-mixture.
6.) Centrifuge for 25 min at 1300 rcf without brake.
7.) Pipett off the cloudy interface, which contains the mononuclear cells.
8.) Wash for at least 2 times with 1x PBS or NCM before follow up experiments.

4.9 Cell separation with MACS®

In general this cell separation technology is based on the detection of cell surface molecules by Abs, which are either covalently linked to a superparamagnetic nanoparticle[170] (direct

labeling) or function as primary Abs that are unconjugated, biotinylated or fluorochrome-conjugated. When using the indirect labeling method, the magnetic labeling is performed in a second-step procedure by using anti-immunoglobulin, anti-biotin, streptavidin or anti-fluorochrome microbeads. By placing the column into the separator, a high-gradient magnetic field is induced in the column matrix, which retains labeled cells with a high efficiency (*positive selection*). In case that untouched cells are needed, a mix of Abs can label all redundant cells and retard them in the column, while the desired fraction can pass unhampered (*negative selection*, see following section).

For cell separation, different isolation strategies were used. To enrich dermal subpopulations positive selection with direct magnetic labeling or via biotinylated Ab was used. The enriched cell suspension was called "positive fraction", or $CDxy^+$, the flow-through cells were termed "negative fraction" (or $CDxy^-$). $CD3^+CD4^+CD25RA^+CD25^-$ cells were isolated by initial depletion of $CD25^+$ cells, followed by the usage of the isolation kit for naive T_h cells, where untouched cell suspensions could be obtained. In brief, $CD25^+$ cells were labeled indirectly with an anti-CD25-mAb that was covalently linked to the fluorochrome APC. Anti-APC microbeads targeted the labeled cells for retention in the column. The flow-through cells were termed "CD25 negative" ($CD25^-$) and used for the subsequent isolation of untouched naive T_h cells.

4.9.1   Depletion of $CD25^+$ cells

Ice-cold MACS buffer was used and working steps were performed as fast as possible.

1.) Resuspend PBMCs in 1 ml of MACS buffer.

2.) Take approximately 10 µl for flow cytometry.

3.) Add 20 µl of Ab per $1x10^8$ cells and mix well.

4.) Incubate at 4°C for 30 min.

5.) Wash with MACS Buffer (↻ 6 min, 1400 rpm).

6.) Resuspend pellet in 500 µl MACS buffer.

7.) Add the microbeads (at least twice the amount of the Ab).

8.) Incubate for 20 min at 4°C.

9.) Wash with MACS buffer.

10.) Resuspend in 2 ml of buffer and put the cell suspension on the washed column.

11.) Collect the $CD25^-$ fraction for further enrichment.

12.) Elute the $CD25^+$ cells with 2 ml MACS buffer.

13.) Keep from every fraction at least 10 µl for purity control by flow cytometry.

14.) Wash the cell suspension with 1x PBS or NCM and keep cool until further handling.

4.9.2   Enrichment of untouched naive T_h cells

The protocol was adapted from Miltenyi Biotec

1.) Wash cells with MACS buffer.

2.) ↻ 5 min, 1400 rpm.

3.) Discard supernatant and resuspend the pellet with 1 ml MACS buffer.

4.) Determine cell number with trypan blue.

5.) Wash again with MACS buffer (5-10 ml; ↻ 5 min, 1400 rpm).

6.) Take 10-20 µl for flow cytometry analysis.

7.) Cell number $\leq$ $1x10^7$ → 40 µl MACS buffer

    $\geq$ $1x10^7$ → 70 µl MACS buffer

8.) Add 10 µl of the Ab cocktail per $1x10^7$ cells and incubate for 10 min at 4°C in the dark.

9.) Add 40 µl MACS buffer and 20 µl anti-biotin microbeads for $1x10^7$ cells and incubate (4°C, 20 min)

10.) Wash cells with 5-10 ml MACS buffer.

11.) Place the appropriate column in the magnetic field of the according separator (see **Table 2|**) and wet the column with 1 ml MACS buffer.

12.) Resuspend the pellet in 500 µl buffer and apply cell suspension onto the column.

13.) Collect flow-through cells, containing unlabeled naive T_h cells.

14.) Elute the negative fraction with 1 ml MACS buffer.

15.) Take from every fraction aliquots for flow cytometric examination of purity.

16.) Wash cells with 1x PBS or NCM and use immediately for downstream applications or refrigerate (for a maximum of 2 hours)

Table 2| Parameters for cell separation column decision

Column	Max. number of labeled cells	Max. number of total cells	Separator
MS	10^7	$2x10^8$	MiniMACS
LS	10^8	$2x10^9$	MidiMACS

(adopted from Miltenyi Biotec)

4.9.3   Positive selection of dermal subpopulations expressing MSC markers

1.) Wash the freshly prepared single cell solution with MACS buffer (↻ 7 min, 1400 rpm).

2.) Resuspend in 1 ml MACS buffer and add the appropriate volume of Ab (see **Table 3|**)

3.) Gently resuspend several times and incubate at 4°C for 45 min.

4.) Wash with 5 ml MACS buffer (↻ 5 min, 1400 rpm).

5.) Resuspend the pellet in 100 µl MACS buffer.

6.) Add 50 µl anti-PE, anti-APC or anti-biotin microbeads and incubate for 15 min at 4°C.

7.) Wash with MACS buffer (↻ 5 min, 1400 rpm)

8.) Resuspend the pellet in 500 µl MACS buffer.

9.) Place a MS column in the separator and wash it with 500 µl buffer before loading the cell suspension.

10.) Collect the flow-through and combine it with the retarded positive fraction by elution with 1 ml of MACS buffer.

11.) Proceed once again as stated in point 9.) with a new column.

12.) Collect the flow-through, which we call "negative fraction" (CDxy⁻)[a]

13.) Wash the column 2 times with buffer.

14.) Elute the "positive fraction" (CDxy⁺) with 1 ml MACS buffer.

15.) Take from every fraction 5-10 µl for flow cytometry analysis of purity.

16.) Wash both fractions and whole dermal cells with medium and store them at 4°C unless otherwise processed.

Table 3| Abs and dilutions for enrichment of dermal subtypes

Ab specifity	Clone	Ig Class	Working dilution	Source	Conjugate
CD271	ME20.4-1.H4	mouse IgG1	1:20	Miltenyi, BD	APC, Biotin
CD73	AD2	mouse IgG1	1:20	BD	PE
CD90	5E10	mouse IgG1	1:20	BD	PE

4.10 Expansion and culture of plastic-adherent bone marrow cells, umbilical cord blood cells and dermal cells

Cryopreserved, unpassaged adherent bone marrow cells from a healthy adult male volunteer and umbilical cord blood cells (a kind gift from PD Dr.med. Dirk Strunk, Div. of Hematology, Medical University of Graz) were quickly thawed at 37°C and washed immediately with 50 ml NCM (↻ 7 min, 1,400 rpm). The pellet was resuspended in expansion medium, cells were plated in 4 vented culture flasks (2.5×10^5 cells/225 cm^3) and expanded for 8-12 days in a humified atmosphere containing 95% air and 5% CO_2. Medium was changed every 2-3 days. When almost confluent, the medium was aspirated off and the cell layer was washed gently with prewarmed 1x PBS. Cells were harvested by detaching them with prewarmed trypsin-EDTA for 3-4 min at 37°C (frequently controlled under the microscope), flushing them down the culture flask by repeated pipetting 5-10 ml of NCM over the plastic surface and collecting by centrifuging. The pellet was resuspended in culture medium, counted and frozen in aliquots (1st passage). For in vitro experiments these aliquots were thawed as described before and cultured under normal conditions with α-MEM$_{BM}$.

Dermal cells were expanded and maintained in α-MEM$_{DERM}$ at 37°C and 5% CO_2. For expansion, cells were plated at a density of 1.5×10^4 viable cells/cm^2 in plastic petri dishes (id = 9 cm) for 5-10 days, with medium changed every 2-3 days. Once 80-90% confluency was reached, cells were trypsinized, as described above, and stored in aliquots in liquid nitrogen for future experiments.

---

[a] Although called "negative fraction", a varying percentage of cells expressing the "depletion antigen" was still present (5-40%, depending on the marker).

For analysis of phenotypical and morphological appearance of dermal and bone marrow cells, they were cultured in 8-well chamber slides (2-3x10^4 cells/cm^2) in their respective culture medium (250 µl/well). After 1-2 days, cells were about 80% confluent and ready for immunohistochemistry or visualization by immunofluorescence.

As bone marrow cells were found to be plastic-adherent, expressed all markers necessary for defining MSCs and showed the potential to differentiate into the three main mesenchymal lineages (chondro-, adipocytes, osteoblast), which was shown by C. Vaculik from our laboratory, they were termed BM-MSCs in upcoming experiments.

4.11   Expansion and culture of HaCaT and HEK 293 cells

Cryopreserved HaCaT[b] and HEK 293[c] were quickly thawed at 37°C and transferred into 225 cm^3 culture flasks with 30 ml of HaCaT & HEK 293 medium and left to adhere o/n. On the next day, medium was changed and cells were expanded for up to 2 weeks with medium changed every 2-3 days. When cells were around 80% confluent, cells were splitted 1:2 for HaCaT or 1:3 for HEK 293 by detaching them with trypsin-EDTA (0.5%) as described above. After sufficient expansion, cells were detached, one part used for experiments and the other part frozen and stored in liquid nitrogen (see **4.13**).

4.12   Cell counting

The cell pellet was resuspended in the appropriate medium (volume according to pellet size), 10 µl were mixed with an equal volume of 0.1% trypan blue (in 1x PBS) and incubated for several min at RT. Stained cells (10 µl) were loaded into a counting chamber (**Fig 3|**), viable cells were counted in all four quadrants (grey) and the concentration was calculated according the following principle:

Formula:

$$\frac{\text{counted cell number}}{\text{enumerated area (mm}^2\text{) x depth of chamber (mm)} \atop \text{x dilution}} = \text{cells per µl}$$
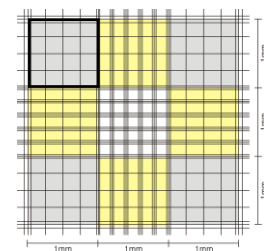
Fig. 3| Quadrants of counting chamber

4.13   Cryopreservation of dermal and bone marrow cells

The cell number of freshly prepared or expanded cells was estimated as described above and the concentration was adjusted to $1x10^6$ cells/ml with the appropriate culture medium. Aliquots of 900 µl were pipetted into cryopreservation vials, mixed with 100 µl DMSO (10% v/v) and placed immediately into an isopropanol bath (freezing container that cools 1°C/min) that was subsequently cooled in a -80°C freezer. In case, the freezing container was not available, the vials were placed into a polystyrene rack, which was put into a polystyrene box and thereupon deep frozen at -80°C. Within the next few days, the cells were transferred into the liquid nitrogen tank for final storage.

4.14   Chamber slides

At about 80% confluency of dermal and bone marrow cells, the medium was discarded and media chambers were detached from the glass slide via the separator (**Fig. 4|**). The slides were washed in 1x PBS for a few min and cells were fixed and permeabilized with methanol absolute for 5 min at RT. After rehydration in 1x PBS and drying of the spaces between the culture-wells with cotton swabs (**Fig. 4|**, white arrow), cells were covered with Ab solutions for visualization assays (see **4.16**).

Fig. 4| Chamber slides with gasket removal supply. We used 8-well chamber slides to culture and directly stain isolated single cells. The picture illustrates the removal of the media chambers that allows subsequent fixation and direct staining of adherent cells on the remaining microscope slide. The arrow depicts the gaps between the culture chambers. (picture adopted from Nalgene/NUNC[174])

4.15   Preparation of skin cryosections

After excision of the subcutis, skin was cut into small pieces (~ 3x10 mm) and embedded in O.C.T tissue-tec. These specimens were snap-frozen in liquid nitrogen and stored short time at -20°C or for longer periods at -80°C. For sectioning, blocks were affixed to the designated device on the cryostat, sections (5-7µm) were cut and adhered on capillary gap microscope slides, air-dried and fixed for 10 min in ice-cold acetone (-20°C). Slides were either used immediately or stored for future experiments. Before staining procedures, excess tissue-tec was scraped off and sections were encircled with a delimiting pen that provides a water repellent barrier for liquids. Before incubation with mAbs, the sections were rehydrated a few min in 1x PBS.

4.16　Immunofluorescence

Skin cryosections or single cells fixed on chamber slides, were incubated for 2 hours at RT or o/n at 4°C with primary mAbs in a humified staining box in the dark. MAbs were diluted in 2% BSA-PBS according to **Table 4|**, 50 µl were added to cells and/or tissues. For single staining with direct-conjugated mAbs, slides were washed three times in 1x PBS (in the dark) after the incubation step and mounted with a 1:6 dilution of Vectashield with DAPI (to visualize nuclei) and straight Vectashield mounting medium for fluorescence. Purified mAbs and those, who emitted only low intensity signals due to low marker expression on cells, were incubated at RT for up to one hour with a second-step (detecting/enhancing) Ab (AF$_{488}$, AF$_{546}$, AF$_{647}$), following the primary incubation and washing steps. In this case, a blocking step had to be included for double and triple staining, if the primary, secondary or tertiary mAb derived from the same species (like mouse anti-human). This was performed with 10% normal mouse serum (diluted in 1x PBS) or 10% normal goat serum for 30-60 min at RT. After blocking, the secondary and/or tertiary mAbs were pipetted onto the skin sections or cells without an additional washing step in-between and incubated for 2 hours at RT or o/n at 4°C. Afterwards, the slides were washed 3 times for 5 min and mounted with a DAPI-dilution. Isotype-matched controls from the same subclass, species and fluorochrome were treated exactly the same way like the specific mAbs. Pictures were captured with a confocal laser scanning microscope (CLSM) or a compound microscope (Nikon).

4.17　Immunohistochemistry

Primary mAbs and isotype-matched controls were diluted with 2% BSA-PBS according to the specifications in **Table 4|**. Fifty µl were pipetted onto the skin sections and incubated o/n at 4°C in a moisture chamber. The next day, slides were washed at least 2 times with 1x PBS for 5 min, incubated for 10 min with 1% hydrogen peroxide (30% H_2O_2 diluted in MetOH abs.) at RT to quench the endogenous peroxidase, washed again in 1x PBS and incubated for 1 hour at RT with the detecting second-step reagent that is covalently linked to a horseradish peroxidase. After an additional washing step, one drop of the substrate chromogen (AEC+) was placed on the section, which is metabolized in an enzymatic reaction into a red end product. The sections were mounted with an aqueous mounting solution (Aqua-mount). For enhancement of this staining procedure an intermediate step was included, to amplify the signal. A biotinylated IgG and IgM goat anti-mouse Ab was used for detection of the primary mouse anti-human mAb and incubated for 1 hour at RT. Meanwhile 20 µl of each, solution A and B (from the Vectastain-Kit for IHC), were mixed, diluted with 1.25 ml of 2% BSA-PBS and incubated for 45 min in the dark at RT. The slides were washed 2 times for 5 min in 1x PBS, 50 µl of the complex-solution was pipetted onto the sections and incubated for 45 min at RT in a humified box. After 2 washing steps, the chromogen solution was dropped onto

the slides and the production of the colorimetric end product was controlled under an inverted light microscope. After washing, the nuclei were stained with pure hematoxilin for a maximum of 1 min when indicated, the slides were washed again and mounted with Aqua-mount. Pictures were captured and analyzed with a compound microscope.

4.18   Dermal sheets

Subcutis from foreskin was gently scraped off with a scalpel. Then the skin was cut (~ 2x10 mm rectangles) and placed dermal side down on 3.8% ammoniumthiocyanate (in 1x PBS) for 1 hour at RT. The epidermis was separated from the dermis with 2 forceps and discarded, while the dermis was washed in 1x PBS for several min. To enhance the effectivity of the fixation, the tissue was cut into smaller pieces and thereafter incubated for 30 min in 2% PFA at RT. The fixed sheets were washed for 5 min in 1x PBS, incubated for 10 min in 2% BSA-PBS and placed into an Eppendorf tube containing the primary Ab in 100 µl BSA-PBS, o/n at 4°C. On the next day, sheets were washed 3 times for 5 min in 1x PBS, spread on a microscope slide and mounted with Vectastain for immunofluorescence. Specifity was confirmed with isotype-matched control mAbs and the dermal sheets were captured and analyzed with a CLSM.

4.19   Adipogenesis assay

To test the differentiation capacity of bone marrow and dermal cells into adipocytes, cells (1×10^4/500 µl) were seeded into 48-well plates and cultured for approximately one week with α-MEM$_{DERM}$ until confluency was reached. To differentiate the cells, Adipo$_{IND}$ medium was added to the cell layer and the induction medium was exchanged every 2-3 days for a total of 3 weeks. To visualize adipocytes, medium was discarded and cells were fixed with 4% PFA for 45 min at RT. Thereafter, cells were washed 3 times for 5 min with 1x PBS and 2 times with aqua bidest. The Oil Red O stock solution (3 mg/ml in isopropanol) was diluted 3:2 in aqua bidest, filtered and fixed cells were overlaid with the solution for 50 min at RT. Afterwards, the cells were washed for 3-4 times with aqua bidest to remove the staining solution, covered with water and stored at 4°C until analysis with a compound microscope.

4.20   Osteogenesis assay

To evaluate the differentiation capacity of dermal cells into osteoblasts, dermal cells (4×10^3cells/250µl) were cultivated in chamber slides. After 2 days, dead cells and debris were removed by aspiration of the medium, fresh culture medium (α-MEM$_{DERM}$) was added and the adherent cells were cultured for another 2 days, before the differentiation was initiated with freshly prepared Osteo$_{IND}$ medium. Every 2-3 days the complete medium was

changed for 3 weeks in total. The negative control was cultured in α-MEM$_{DERM}$. Osteogenesis was detected by staining calcific depositions in cells with Alizarin Red. In brief, the medium was discarded, cells were fixed for 5 min with 4% formalin in 70% EtOH (v:v = 1:1, mixed at 4°C) at RT, afterwards incubated with an Alizarin Red solution for 10 min at RT and gently washed in tap water until excess dye was removed. The slides were dried and pictures were captured with a compound microscope.

4.21 Differentiation potential of cryopreserved, plastic-adherent dermal cells

The multilineage differentiation potential is an important criterion to characterize MSCs. Christine Vaculik from our laboratory showed that freshly isolated dermal cells can differentiate into the three main lineages, namely adipocytes, osteoblasts and chondrocytes (manuscript in preparation). As cells can be altered by cryopreservation and storage for longer periods in liquid nitrogen, we tested the differentiation capacity of cryopreserved plastic-adherent total dermal cells into osteocalcin-producing or fat droplet-containing cells. In brief, cells were thawed and cultured for 21 days with supplemented media to induce the differentiation from uncommitted cells into osteoblasts or adipocytes that were stained with alizarin red and Oil Red O, respectively. Indeed, we found strong staining of calcific depositions throughout the culture (**Fig. 5| A|**, left), whereas staining was not observed in undifferentiated cells, which served as negative controls (**Fig. 5| A|**, right). Within the uniform alizarin red staining strong calcified nodules can be seen, that appear dark red (arrows). Single cells of plastic-adherent dermal cells showed the potential to build fat depositions upon induction (**Fig. 5| B|**, left). As cryopreservation does not interfere with the differentiation capacity of plastic-adherent dermal cells and it was shown for BM-MSCs that freezing does not affect the functionality[175], it can be assumed that the cells can be stably stored without loss of function.
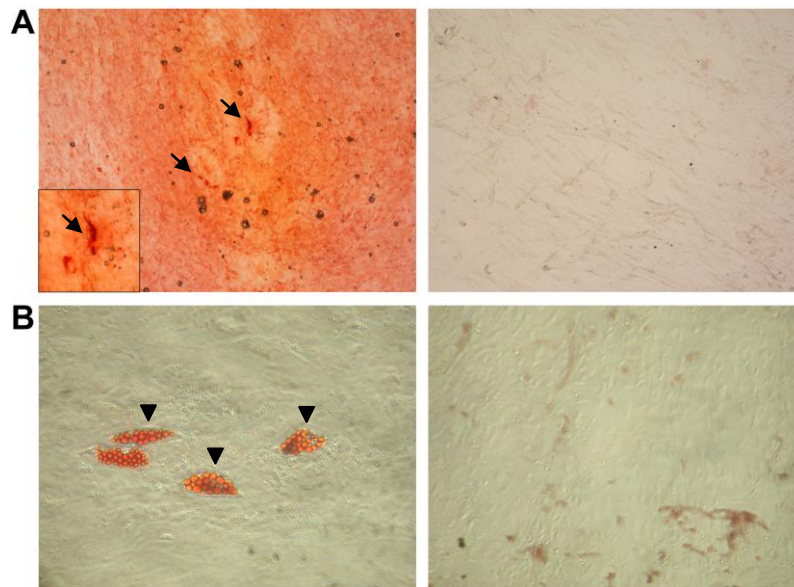
Fig. 5| Osteogenesis and adipogenesis of cryopreserved plastic-adherent dermal cells isolated. Cryopreserved, plastic-adherent dermal cells from infant foreskin were thawed and seeded into 48-well plates ($1x10^4$ cells/well), cultured till confluency and then incubated with appropriate induction media. After 21 days in culture with, the cell-layer was stained with alizarin red for detection of osteoblasts or Oil Red O to identify adipocytes. Pictures were captured with a light microscope, magnification x20, inset magnification x40. **A|** Arrows denote nodules with strong mineral deposition and arrowheads depict adipocytes in **B|** (negative controls on the right).

4.22   Flow cytometry

4.22.1   Extracellular staining protocol

For the analysis of cell surface antigens, single cell suspensions were washed, subsequently resuspended with FACS buffer and $1x10^6$ cells/100 µl were transferred into U-bottom tubes. Fluorochrome-conjugated mAbs were added, tubes were vortexed and incubated on ice for 30 min in the dark. After a washing step with 1 ml of FACS buffer and centrifugation for 5 min at 2,500 rpm, the supernatant was discarded by gently inverting the tubes, the pellets were resuspended in the remaining buffer (~100 µl) and kept on ice till analysis. Isotype-matched control mAbs were used to determine the specifity, dead cells were excluded by examining the uptake of 7-amino-actinomycin D (7-AAD).

4.22.2   Intracellular staining protocol

Bring all buffers and PFA to RT before usage.

1.) Wash cells with 1 ml of 1x PBS, centrifuge (5 min, 2,500 rpm) and resuspend the pellet with FACS washing buffer I.

2.) Transfer $1x10^6$ cells/100 µl to a FACS tube.

3.) For double staining with mAbs that are directed against extracellular molecules, add now the mAb (or the isotype control), vortex and incubate on ice in darkness.

4.) Wash once again with 1 ml FACS washing buffer I and pipet off the supernatant completely.

5.) Resuspend with 100 µl of 4% PFA and incubate at RT for 15 min (darkness).

6.) Wash twice with 1 ml FACS washing buffer I.

7.) Resuspend the pellet in 100 µl FACS permeabilisation buffer and incubate for 15 min in the dark at RT.

8.) Wash once with 1 ml FACS washing buffer II and resuspend the pellet with 50-100 µl of the same buffer.

9.) Add the specific mAb or the isotype control, vortex and incubate for 20 min at RT, protected from light.

10.) Wash the cells 2 times with 1 ml FACS washing buffer II

11.) Resuspend the pellet in FACS buffer and keep cells on ice till flow cytometric analysis.

Flow cytometry was performed using a LSR II (running FACS Diva) and analyzed with FlowJo V 8.8.6 for Macintosh or FlowJo V 7.2.5 for Windows.

4.23   Proliferation assay with CFSE

CFSE is a fluorophore derivative of fluorescein that is able to diffuse passively into cells and bind covalently to free amines inside the cytoplasma[176]. Unattached molecules exit the cell by the same mechanism as they enter and can be washed away. Once bound, CFSE is accessible for endogenous esterases that cleave its acetate groups, producing a molecule that is capable of emitting light in the visible spectrum (**Fig. 6| A|**). The molecule is excited at 492 nm and emits green light with a wavelength of 517 nm. Hence, it allows the simultaneous staining of cells with Abs conjugated to other fluorophores, as PE (emits yellow/orange light, at 578 nm) or APC (emits dark red light around 661 nm; compare with the spectrum in **Fig. 6| B|**).
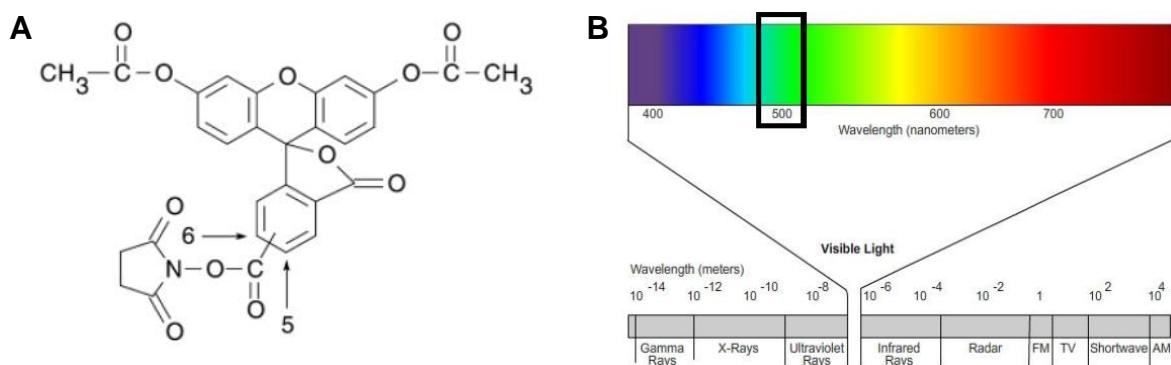
Fig. 6| Molecular structure of CFSE and its spectral working area. A| CFSE in its inactive, colorless form. After cleavage of the acetate groups, the molecule is able to perform its fluorescent activities. (Adopted from Molecular Probes, Invitrogen[177]). **B|** Visible Spectrum. Surrounded nanometer area equates to the spectral band occupied by CFSE. (Adopted from Emory University[178]).

There is a great variety of applications[179, 180] for fluorescent cell division markers, such as CFSE. Well established are isotype switch analyses of B cells following stimulation under

certain conditions[181, 182]. But also other lymphocytes, like T cells, are subject to investigation with CFSE as they constitute a clearly defined population in peripheral blood that highly improves peak resolution as has been reported previously[183]. As a result of the cytoplasmatic segregation during cell division, the intracellularily bound CFSE is partitioned equally among daughter cells, therefore they emit with halved fluorescence intensity (**Fig. 7|**).
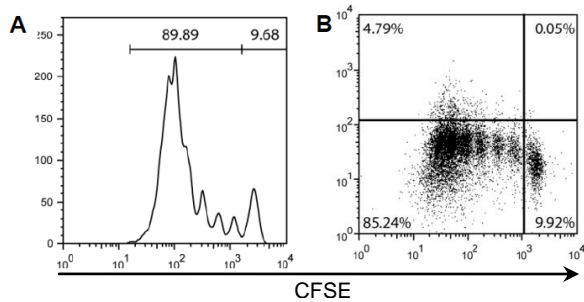

Fig. 7| Typical cell division profile for CFSE-stained PBMCs. Human PBMCs were incubated with CFSE (0.5µM) and then stimulated with mAbs against CD3 (1 µg/ml, plate-bound) and CD28 (1 µg/ml, soluble) at a cell density of 5×10^4 cells/well in a 96-well round-bottom plate. After 5 days of culture, cells were harvested and analyzed by flow cytometry. In **A|** data are expressed as a histogram, in **B|** as dot plot with counterstaining and 10,000 living cells were recorded.

This method allows us to monitor and measure the mitotic activity by successive twofold reduction in fluorescence intensity and the definition of dividing cells proportional to undivided ones[184]. Further, the relationship between proliferation and differentiation can be assessed in one single experiment[182], as it is additionally possible to investigate the expression of other extracellular markers or cytokine expression by flow cytometry[185].

4.23.1 CFSE staining protocol

1.) Wash PBMCs with 1x PBS.

2.) Centrifuge at 1400 rpm for 5 min.

3.) Meanwhile thaw an aliquot of the 5 mM CFSE-stock solution in your hand (to fasten the process).

4.) Add 10 µl of the CFSE-solution to 990 µl PBS, the stock should be refrozen immediately.

5.) Resuspend the pellet in 990 µl of PBS and add 10 µl of the 1:100 CFSE-dilution and mix well.

6.) Incubate the cells for 10 min at 37°C, protected from light.

7.) Wash at least once with ice-cold NCM (use at least 10 times of the staining volume).

8.) Resuspend the pellet in NCM and immediately use cells for proliferation assays or keep refrigerated.

4.23.2 Coating of plates with αCD3 mAbs

For coating of round-bottom 96-well plates, frozen aliquots of a mouse anti-human CD3 mAb were thawed, diluted with 1x PBS to obtain a concentration of 1 µg/ml, unless otherwise noted. Fifty µl of this Ab dilution were pipetted in each well, incubated for 2 hours at 37°C (humified incubator) or o/n at 4°C, washed at least 4 times with 150-200 µl of prewarmed

1x PBS and used immediately or stored for up to 2 hours in the fridge, covered with 1x PBS to avoid drying-out.

4.23.3   Experimental set up

Frozen aliquots of bone marrow and dermal cells (all passage 1) were thawed quickly in a 37°C waterbath, washed with medium and seeded in 225 cm^3 culture flasks, at approximately 1x10^6 cells per flask in 20-30 ml of corresponding medium. After culturing o/n at 37°C with 5% CO$_2$, cells were trypsinized like described before, washed with the appropriate medium and centrifuged (7 min, 1400 rpm). The pellet was resuspended in 1-5 ml medium (depending on the size) and put on ice immediately. Cells were irradiated [1x30 Gray (Gy)] and viable cells were pipetted in each well of an αCD3-coated round-bottom 96-well microtiter plate in a total volume of 100 µl, unless stated otherwise. Cells were allowed to adhere o/n at 37°C, humified. On the next day, freshly isolated PBMCs were depleted of CD25$^+$ cells, and/or enriched for CD3$^+$CD4$^+$CD45RA$^+$ or used as whole fraction, stained with CFSE and 5x10^4 cells (in a volume of 100 µl NCM) were seeded into each well of the microtiter plates, with or without a soluble αCD28 mAb (1 µg/ml).

For analysis of soluble factors that might be involved in immunomodulation, the supernatant was transferred into αCD3-coated wells after the o/n culture, the remaining cells were covered with fresh medium, other fractions were left with the supernatant for direct comparison.

To exclude false inhibitory results, created by sterical hindrance, HEK 293 and/or HaCaT cells were used as control cells and were handled the same way. Further, αCD3/CD28-coated Dynabeads (**Fig. 8|**) were used for stimulation of T cells in coculture with bone marrow and dermal cells to exclude a "nonspecific" blocking of the αCD3 mAb by adherent cells. In brief, beads were resuspended in the original vial carefully before usage, the appropriate amount was taken and washed with an equal amount (or at least 1 ml) of Dynabead buffer by resupending the beads several times. The tube was placed into a magnet (EasySep) for 1 min and the supernatant was discarded by quickly inverting the tube (with the magnet). The tube was removed from the magnet and the beads were resuspended in the same volume of medium as the initial volume, taken from the vial. Cell proliferation was stimulated by adding 25 µl Dynabead suspension to 1x10^6 cells to obtain a bead-to-cell ratio of 1:1, resuspended and 5x10^4 cells/well were seeded in round-bottom 96-well plates (total volume 100 µl), incubated for 4 or 5 days, harvested and analyzed by flow cytometry.
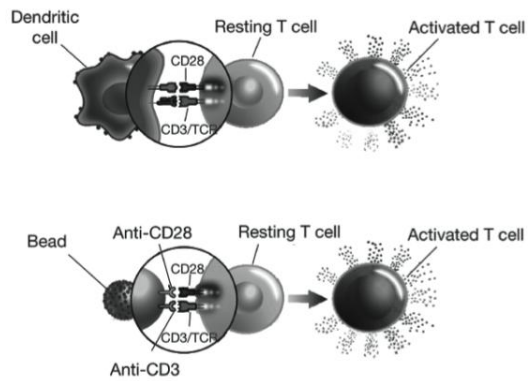
Fig. 8| Principle of T cell stimulation with Dyna-beads. Dynabeads are small super-paramagnetic polymer particles that mimic APCs by stimulating proliferation of T cells giving both, the primary signal (CD3 ε chain of the TCR) and the secondary signal (costimulation by binding the cell surface molecule CD28). (adopted from Invitrogen[186])

In addition, the following negative controls were included in the assays. T cells were cultivated without stimulation and without MSCs. Further, the influence of MSCs without stimulation (αCD3 with or without αCD28) was investigated. MSCs were cultured without T cells to exclude debris in flow cytometric analysis and the proliferation profile of stimulated and non-stimulated T cells without MSCs was examined. To estimate the autofluorescence of PBMCs they were also used unstained with or without stimulation. For each assay, irradiated bone marrow and dermal cells were stained with CFSE and analysed for successful inhibition of proliferation by flow cytometry.

4.24 Proliferation assay with [^{3}H]-thymidine (TdR)

To investigate the proliferation kinetics of naive T_h cells, T cells (5×10^4/200 µl NCM) were seeded in αCD3-coated 96-well round-bottom microtiter plates and costimulated with soluble αCD28 mAb (1 µg/ml). Additionally, negative fractions were included into the experiment, which consisted of utterly unstimulated cells or provision of only one stimulatory or costimulatory signal. Proliferation was measured using an 18-hour pulse of 37 kBq/well [^{3}H]-TdR on days 2, 3 and 4. Microtiter plates with radioactive labeled cells were stored at -20°C until further processing. For cell harvesting, mictotiter plates with labeled cells were thawed and the amount of radioisotope incorporation was determined with a 1450 Microbeta liquid scintillation counter.

For comparison of different lymphocyte subpopulations, whole PBMCs were enriched for CD25$^+$ cells. The negative (CD25-depleted) fraction was further enriched for naive T_h cells by negative selection. From each fraction, 5×10^4 cells were seeded into a 96-well plate with or without bone marrow cells, stimulated with αCD3/CD28-coated beads and incubated for 4 days until radioactive labeling and measurement of [^{3}H]-TdR uptake.

4.25   Statistical analysis

Data analysis was performed in GraphPad Prism5. For a minimum, triplicates were analyzed by the Mann Whitney test and P > 0.05 was considered as significant. For evaluation of standard errors (SED) or standard deviations (SD), data were imported in Prism and analyzed via the column statistics program. Data are expressed as mean expression in %±SED (or mean%±SD, when indicated).

Table 4│ mAbs & 2nd step reagents

Ab specifity	Clone	Ig class	Working dilution	Source	Conjugate
Flow Cytometry					
CD3	SK7	mouse IgG1	1:50	BD Pharmingen	APC, FITC
CD4	M-T466	mouse IgG1	1:50	Miltenyi Biotec	PE
CD25	4E3	mouse IgG2b	1:20	Miltenyi Biotec	APC, Biotin
CD26	M-A261	mouse IgG1, κ	1:100	BD Pharmingen	PE
CD31	WM59	mouse IgG1	1:50	Serotec	FITC
CD34	AC136	mouse IgG1, κ	1:100	Miltenyi Biotec	FITC
CD45RA	T6D11	mouse IgG2b	1:200	Miltenyi Biotec	FITC
CD73	AD2	mouse IgG1, κ	1:50	BD Pharmingen	purified, PE
CD80	L307.4	mouse IgG1, κ	1:20	BD Pharmingen	FITC
CD86	2331 (FUN-1)	mouse IgG1, κ	1:20	BD Pharmingen	FITC
CD90	F15-42-1	mouse IgG1, κ	1:100	AbD Serotec	purified
CD90	5E10	mouse IgG1, κ	1:200	BD Pharmingen	PE
CD105	166707	mouse IgG1	1:50	R&D	FITC
CD271	C40-1457	mouse IgG1, κ	1:50	BD Pharmingen	PE, purified
CD271	ME20.4-1.H4	mouse IgG1	1:50	Miltenyi	APC
FoxP3	259D/C7	mouse IgG1	1:5	BD Pharmingen	AF$_{647}$
HLA-A,B,C	G46-2.6	mouse IgG1, κ	1:50	BD Pharmingen	FITC
HLA-DR	L243	mouse IgG2a	1:500	BD Pharmingen	APC, FITC
Immunofluorescence & Immunohistochemistry					
α-SMA	1A4	mouse IgG2a	1:50	Sigma	FITC
β-III-tubulin	TU-20	mouse IgG1	1:50	Chemicon	
CD10	SS2/36	mouse IgG1, κ	1:50	Dako	FITC
CD34	AC136	mouse IgG1, κ	1:100	Miltenyi Biotec	FITC
CD45RA	T6D11	mouse IgG2b	1:200	Miltenyi Biotec	FITC
CD56	Leu-19	mouse IgG1	1:10	BD Pharmingen	purified
CD73	AD2	mouse IgG1, κ	1:50	BD Pharmingen	PE
CD90	5E10	mouse IgG1, κ	1:100	AbD Serotec	PE
CD105	166707	mouse IgG1	1:50	R&D	FITC
CD271	C40-1457	mouse IgG1, κ	1:100	BD Pharmingen	APC, PE
Col-IV	MAB1430	mouse IgG1	1:250	Chemicon	purified
GFAP	6F2	mouse IgG1	1:50	Dako	FITC
Oct-4	Poly6319	rabbit IgG	1:50	Biolegend	purified
2nd step reagents					
α–mouse	F(ab')$_2$ fragment		1:250	Invitrogen	AF$_{488}$
α–mouse	F(ab')$_2$ fragment		1:500	Invitrogen	AF$_{546}$
α–mouse	F(ab')$_2$ fragment		1:500	Invitrogen	AF$_{647}$
Nucleic acid staining					
7-AAD			1:400	Sigma	PerCP
DAPI			1:3	Sigma Vectashield	UV detection
Sytox			$1:1 \times 10^6$	Molecular Probes	Orange
T cell stimulation					
CD3	UCHT-1	mouse IgG1	1:200	Beckman Coulter	purified
CD28	L293	mouse IgG1, κ	1:500	BD Pharmingen	purified

AbD Serotec, Düsseldorf, GER; **Beckman Coulter**, Brea, CA, USA; **Biolegend**, San Diego, CA, USA; **BD Pharmingen**, San Jose, CA, USA; **Chemicon**, Billerica, MA, USA; **Dako**, Golstrup, DK; **Invitrogen**, Carlsbad, CA, USA; **Miltenyi**, Bergisch Gladbach, GER; **Molecular Probes** , Eugene, OR, USA; **R&D**, Minneapolis, MN, USA; **Sigma Vectashield**, Burlingame, CA, USA.

5   Results

5.1   In situ characterization of MSC subsets in human dermis

Because most of the studies have only characterized culture expanded MSCs, isolated from diverse tissues, the equivalent cells have not been identified in vivo and little is known about their exact tissue location. Encouraged by our in vitro findings that phenotypically-defined MSC subsets can be isolated from human dermis, markers known to be expressed on BM-MSCs, such as CD73, CD90, CD105 and CD271 were used to visualize these cells in juvenile foreskin. $CD73^+$ cells were mostly found in the upper dermis, close to the epidermal/dermal junction (**Fig. 9|**). $CD90^+$ and $CD105^+$ cells were present in the upper and lower part of the dermis (**Fig. 9|**). The mAb against CD271 stained fine nerve endings close to the epidermis (not shown) and huge, bulky formations in the middle and deep dermis (**Fig. 9|**).
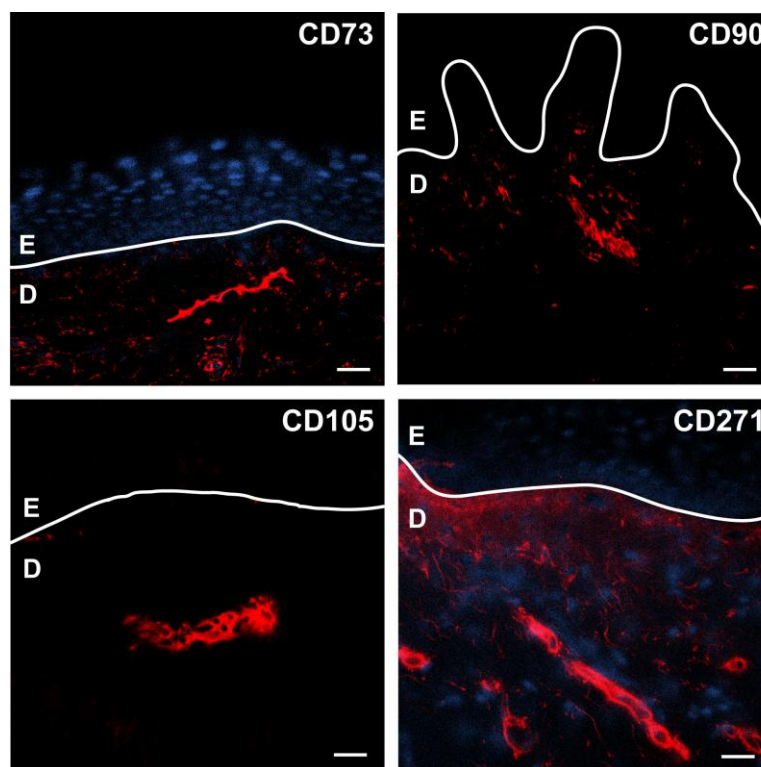

Fig. 9| Localizing cells expressing MSC markers in human foreskin. Immunofluorescence analysis of the indicated markers on cryostat sections from juvenile donors (aged between 2-13 years). PE emission was enhanced with $AlexaFluor_{546}$, nuclei were stained with DAPI and specifity was confirmed with isotype-matched controls. Pictures were captured with a CLSM. E = epidermis, D = dermis, scale bars = 20 µm

For the identification of MSCs, it is crucial that a combination of certain surface molecules is co-expressed. As shown in **Fig. 10|** around halve of the cells expressing CD271 are positive for CD90 in the upper and deep dermis. These findings nicely correlate with flow cytometric data of plastic-adherent total dermal cells (C. Vaculik et al., manuscript in preparation).
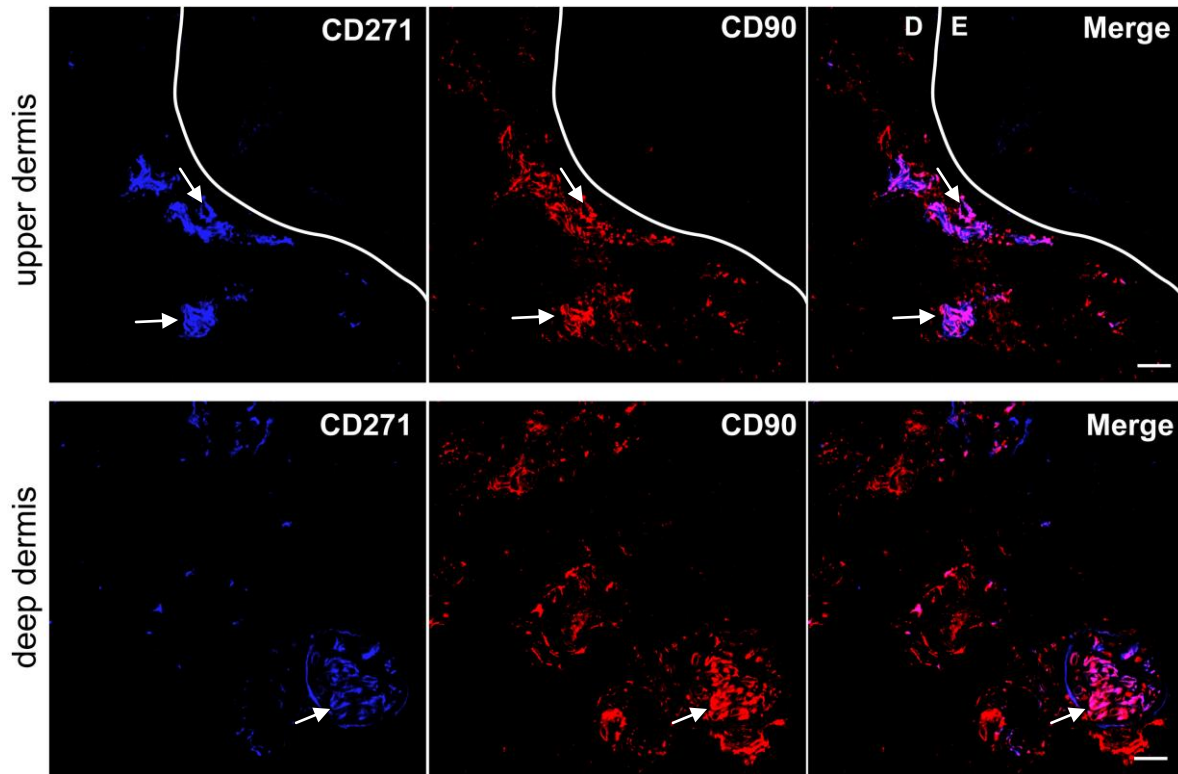

Fig. 10| Around 50% of the cells positive for CD271 coexpress CD90. This representative immunofluorescence double labeling was performed on cryosections of a 4-year-old donor and analyzed with CLSM. Arrows denote CD271$^+$CD90$^+$ double positive cells detected in close proximity to the epidermis (upper panel) or in deeper dermal layers (lower panel). Specifity was confirmed with isotype-matched controls. E = epidermis, D = dermis, scale bars = 20 μm

To further characterize the nature of CD90$^+$CD271$^+$ cells, we performed triple staining including the MSC marker CD73. Indeed, few CD73$^+$CD90$^+$CD271$^+$ cells could be located in the upper-mid-dermis (**Fig. 11|**, arrows) and the deep dermis (**Fig. 12|**, arrows). The majority of cells, however, was only double positive for CD73 and CD90 (over 90%). It is noticeable that all CD271$^+$ cells expressed CD73 and that most of these cells also expressed CD90 in three donors investigated.
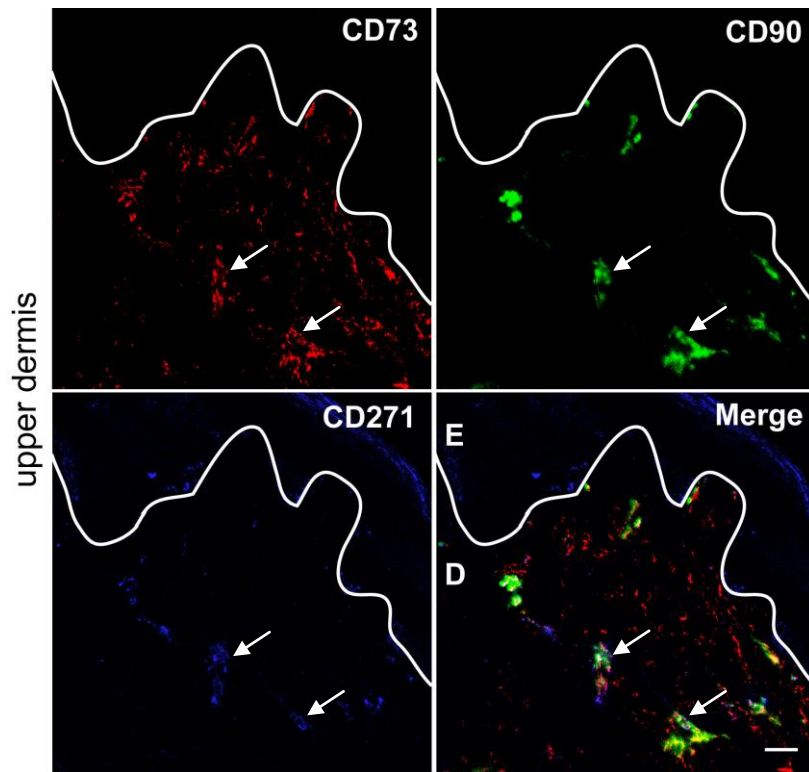
Fig. 11| CD73+CD90+CD271+ cells are present in the upper, papillary dermis of. Close to the epidermis of juvenile foreskin few cells were positive for all three markers, while many cells expressed CD73 and CD90. Arrows indicate CD73+CD90+CD271+ cells. CD73-PE was enhanced with AF_{546} and pictures were captured with a CLSM (n=3, aged between 2-10 years). E = epidermis, D = dermis, scale bar = 20 µm
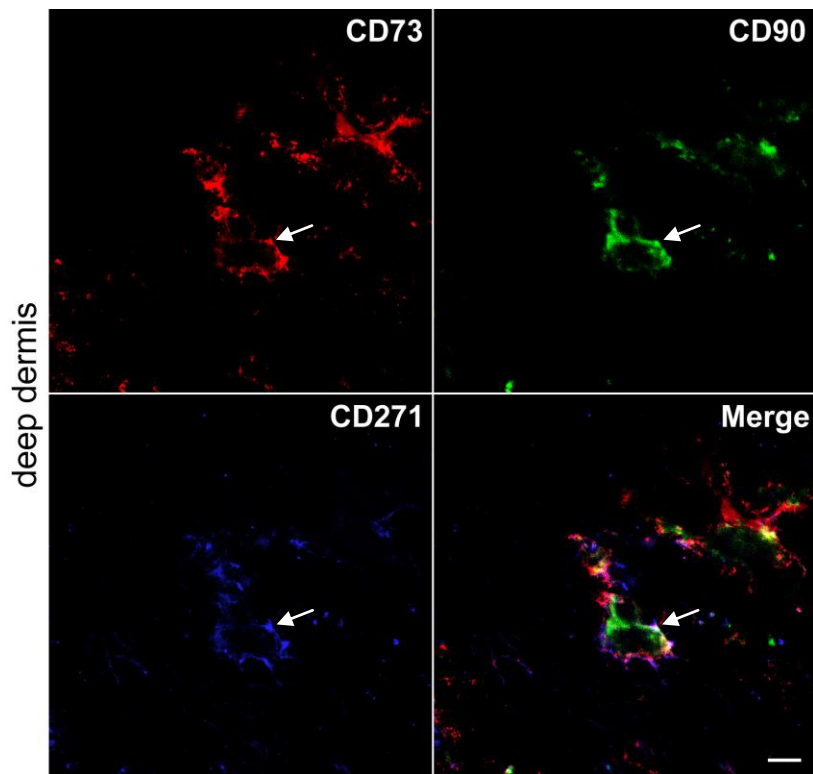

Fig. 12| CD73+CD90+CD271+ cells can be localized in the deep dermis. Triple labeling identified few CD73+CD90+CD271+ cells (arrows) and many CD73+CD90+271- cells. Scale bar = 20 µm

5.1.1 CD271$^+$ cells do not coexpress CD34 but are localized in close association with cells expressing this antigen

Based on the elongated structures formed by CD271$^+$ and CD90$^+$ cells found in all investigated skin donors, we decided to proceed with double and triple staining including mAbs directed against CD34[d] and type IV collagen[e] (Col-IV) to further unravel the nature of CD271$^+$ cells. Double labeling of CD34 and CD271 in cryosections showed ambiguous staining results. On the one hand, many longitudinal structures could be identified with cells that seemed to be double positive for CD34 and CD271 in the upper dermis (**Fig. 13|**, arrows) and single CD271$^+$ cells in-between. On the other hand, we found many circular structures in the deep dermis, which were CD271$^+$CD34$^-$ (**Fig. 13|**).
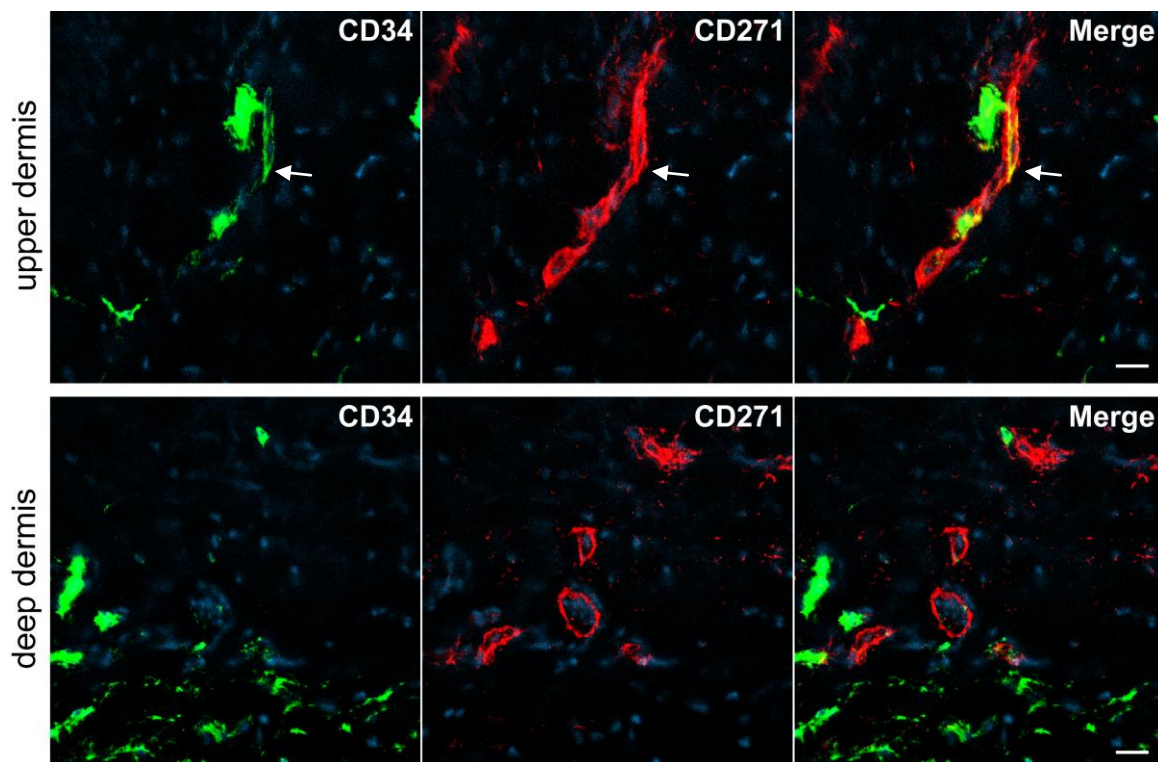

Fig. 13| CD271$^+$CD34$^+$ cells as well as CD271$^+$CD34$^-$ cells are present in the dermis. Arrows denote CD271$^+$CD34$^+$ cells in the subepidermal papillary dermis. Pictures are representative of at least two different experiments. Nuclei were stained with DAPI. Scale bars = 20 µm

Because vertical tissue staining could not clarify, whether CD271$^+$ cells indeed coexpress CD34, we employed another strategy to address this question. Using CLSM, dermal sheets allow the imaging of cell networks with all their complexity and topological relationship to other tissue components within whole tissue. **Fig. 14|** clearly shows, that CD271 is never coexpressed with CD34, though often colocalized (arrows). Both build discrete exceeding

---

[d] Besides its expression in HSCs, CD34 is known to be expressed on endothelial cells of blood vessels and lymphatics, perivascular stroma[187] and a small proportion of BM-MSC progenitors[188].
[e] This marker is expressed primarily in basement membranes, more precisely the lamina densa of its basal lamina, surrounding mostly blood vessels and lymphatics, but also in all epithelia and the nervous system[189, 190].

networks throughout the dermis. This confirms the independent existence of CD271^{+} cells from vascular bundles in human skin.
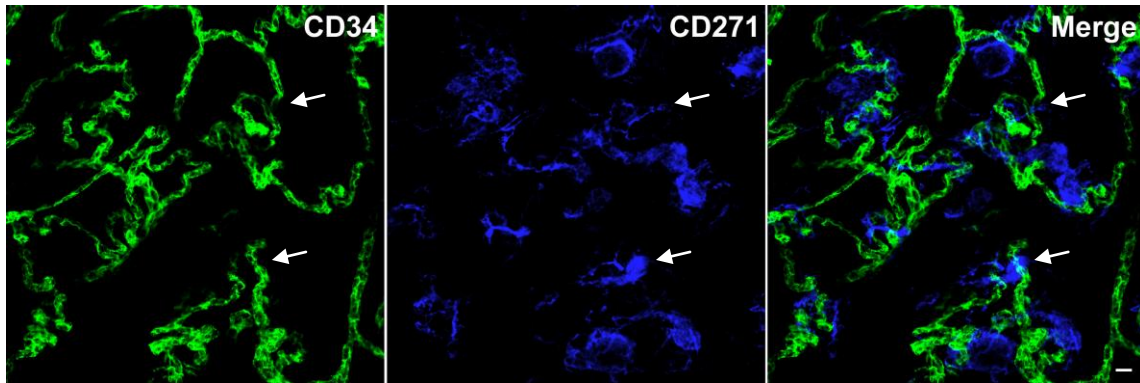

Fig. 14| Immunofluorescence double labeling confirmed autonomy of CD271^{+} cells by three-dimensional illustration of the dermis. Foreskin was incubated on ammoniumthiocyanate solution and after one hour, the epidermis was removed from the dermis, which was fixed with PFA, permeabilized with Triton-X and stained with the indicated mAbs or the respective isotype control. Dermal sheets were analyzed by CLSM. Arrows denote sites of colocalization of CD271^{+} and CD34^{+} cells. Scale bar = 10 µm

Interestingly, the inclusion of a mAb against Col-IV revealed that several CD271^{+} cells coexpress this marker in the subepidermal papillary, mid- and deep dermis (**Figs. 15|-17|**, arrowheads). Some cells expressing CD271 only, could be found in the deep dermis (**Fig. 16|**, arrows and **Fig. 17| A|**), along with cells that were assembled into big rounded structures in the deep dermis, which coexpressed Col-IV (**Fig. 17| B|**, arrowheads). In contrast, CD34^{+}CD271^{+}Col-IV^{+} cells were hardly detectable (**Fig. 17| A|**, asterisks), whereas CD34^{+} cells were almost invariably surrounded by Col-IV^{+} cells (**Figs. 15|-17|**). Remarkable is the finding that CD271^{+} cells always formed circular structures in the deep dermis, often colocalized with Col-IV (**Fig. 17| B|**). Due to their shape, these structures could represent cross-sections of vessels, peripheral nerve bundles, but also sebaceous and sweat glands, since expression of CD271 has been reported for all of these skin components[164].
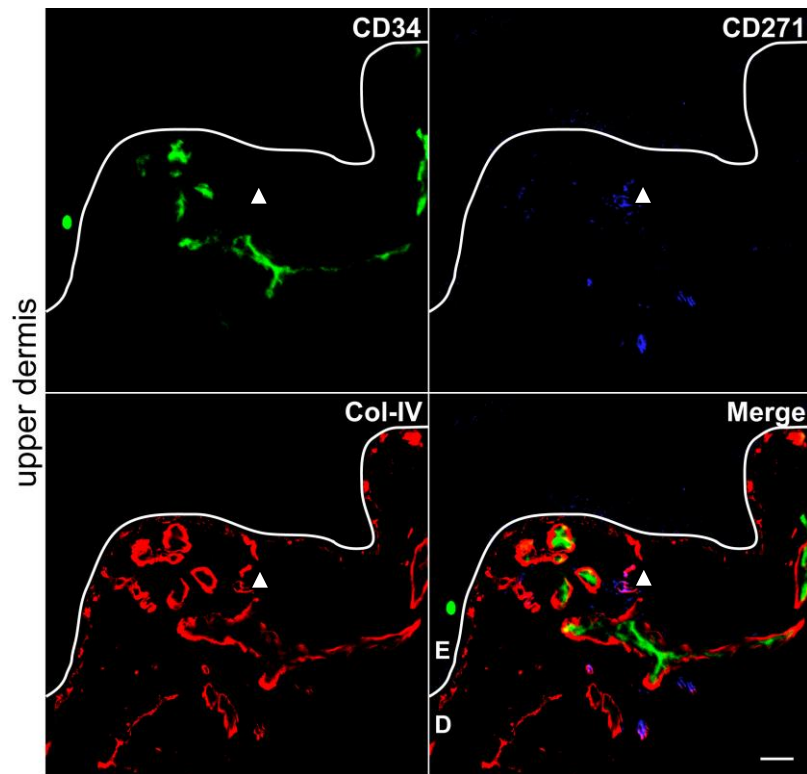
Fig. 15| **Close to the epidermis CD271$^+$ cells express extracellular matrix receptors.** Immunofluorescence staining of foreskin with mAbs directed against CD34, CD271 and Col-IV identified several double positive cells for CD271 and Col-IV (arrowheads), but rarely coexpression with CD34. E = epidermis, D = dermis, scale bar = 20 µm
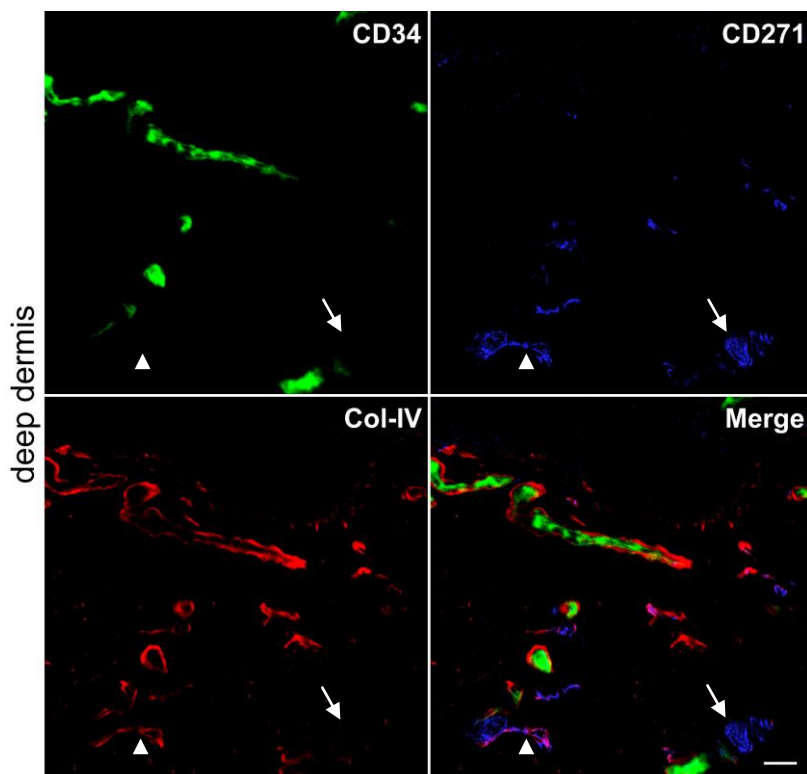
Fig. 16| **Human dermis harbors CD271$^+$Col-IV$^+$CD34$^-$ cells, but also single CD271$^+$ cells.** Cryosections of juvenile foreskins (aged between 2-13 years) were stained with mAbs directed against Col-IV, CD34 and CD271. Arrows denote CD271$^+$ cells, arrowheads CD271$^+$Col-IV$^+$ cells. Scale bar = 20 µm
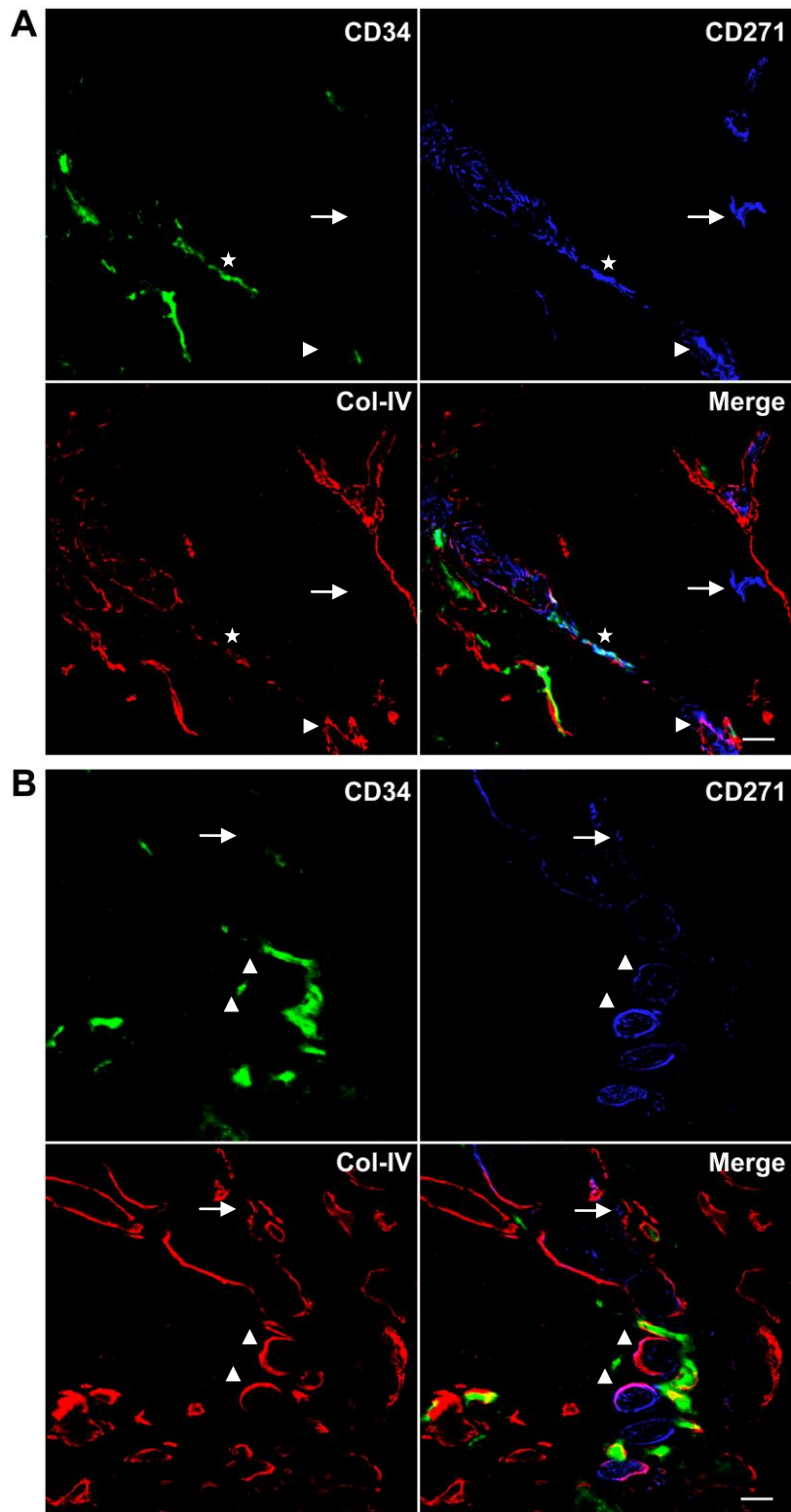
Fig. 17| CD271+Col-IV+CD34- cells colocalize with CD34+ cells in the deep dermis. Triple labeling of cryosections revealed cells double positive for CD271 and Col-IV (arrowheads in **A| B|**), colocalized with CD34+ cells. **A|** Triple positive cells are denoted with an asterisk, while arrows in **A| B|** point out CD271+ single positive cells. Scale bars = 20 µm

5.1.2 The morphology of dermal single cells in culture is mostly, but not entirely MSC alike

Due to our observations that plastic-adherent dermal cells share a lot of features and markers with MSCs from bone marrow, we selected key markers known to be expressed on BM-MSCs to further characterize the morphology of isolated dermal cells by immunofluorescence. To address this, adherent dermal cells (passage 2) were placed in chamber slides and incubated for 2-3 days, fixed, stained and then analyzed. Expanded cells stained with Mai-Grünwald/Giemsa illustrated a typical fibroblastoid appearance (**Fig. 18|**, upper panel, left) similar to that described for BM-MSCs and mesenchymal progenitor cells from other tissues[191]. Elongated spindle-shaped or rhomboid cells with a central nucleus were predominant. Almost all cells expressed CD73, CD90 and CD105 (**Fig. 18|**), confirming published data. Morphologically, the rhomboid shape with adherent pseudopods was most abundant. Arrowheads denote cell to cell junctions between CD105$^+$ cells. Few cells also expressed the mesenchymal marker α-SMA, which is an actin microfilament of smooth musculature, like heart. The transcription factor Oct-4, which is normally specific for undifferentiated ESCs, was also present in the nuclei of a few adherent dermal cells (**Fig. 18|**). Interestingly, CD271$^+$ cells appeared in two different morphologic shapes in vitro (**Fig. 18|**, lowest panel). Most of the cells revealed a MSC-like morphology (**Fig. 18|**, lowest panel, left picture). Some cells, however, had small cellular bodies with long, branched extensions, comparable with neuronal dendrites (**Fig. 18|**, middle and right picture). In summary, the visualization of single cells in culture revealed basically the expected morphology of MSCs, beside some sporadic CD271$^+$ cells resembling the morphology of neuronal cells.
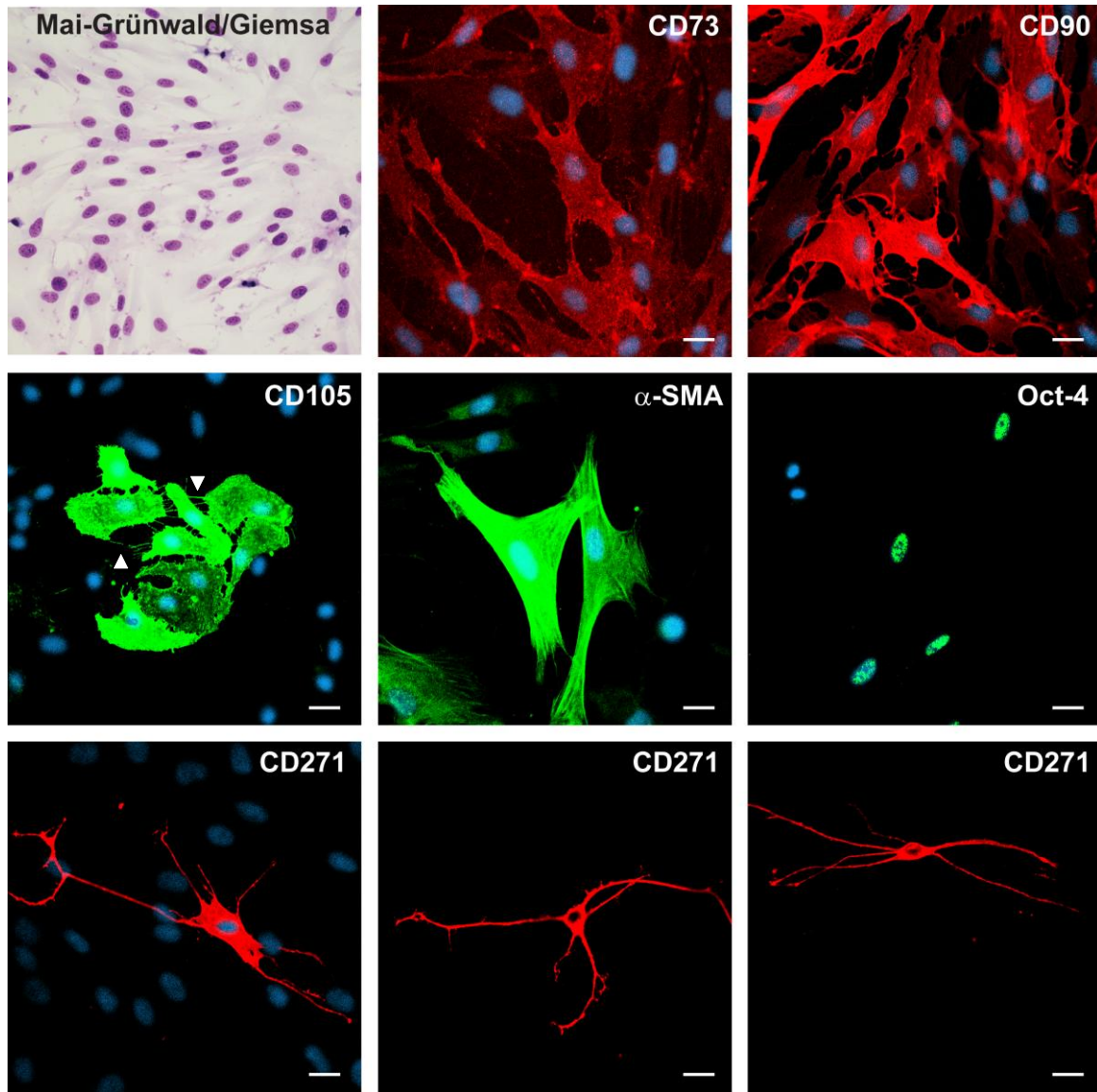
Fig. 18| Morphologic characterization of MSC subsets. Juvenile dermal cells from foreskin (passage 2) were seeded (3×10^4 cells/cm²) in chamber slides and expanded for 2-3 days. Cells were fixed with MetOH and subsequently stained with Mai-Grünwald/Giemsa (LM, magnification x20) or the indicated mAbs. For immunofluorescence analysis, nuclei were stained with DAPI and all signals were enhanced with Alexa Fluor (AF_{488} for FITC or AF_{546} for PE) and analyzed with a CLSM. Scale bars = 20 µm

5.1.4 The dermis harbors CD271⁺CD56⁺ and CD271⁺β-III-tubulin⁺ cells and cells single positive for CD271 in close association with cells expressing neuronal/glial markers

To further unravel the characteristics of CD271⁺ cells, we included NCAM (CD56) in our analysis and is known to be expressed on NK cells, neurons and glial cells. First, single staining on cryosections was performed to analyze the distribution of anti-CD56-reacting cells in foreskin. We found that the mAb marks certain cells and structures throughout the dermis (**Fig. 19|**). Close to the epidermal-dermal junction, many fine structures were found, possibly representing nerve endings (**Fig. 19| A|**). In the mid- and deep dermis (**Fig. 19| B|**) big, bulky structures that looked like multiple cell layers, could be found,

- 57 -

possibly representing cross-sections of peripheral nerves or mechanoreceptors of glabrous skin, such as Meissner's or Pacinian corpuscles, Merkel's discs[(145)] or Ruffini corpuscles.
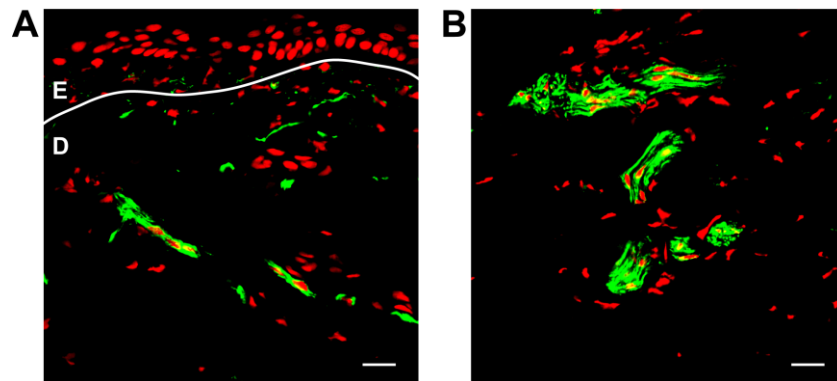
Fig. 19| **Dermal cells of the upper and deep dermis express CD56.** Cryosections from foreskin were incubated with a primary mAb against CD56 and visualized with goat-anti-mouse AF_{488}. Shown is one representative experiment of at least 4 independent experiments. Nuclei were stained with CytoxOrange and pictures were captured with a CLSM (**A|** upper dermis, **B|** lower dermis). Scale bars = 20 µm

Double staining confirmed our hypothesis about $CD271^+$ nerve endings in the papillary dermis, as we indeed identified $CD271^+CD56^+$ cells (**Fig. 20| A|**). In the deep dermis, $CD271^+$ cells mostly colocalized with cells expressing this glial/neuronal marker. $CD56^+$ structures/cells were always found to be surrounded by $CD271^+$ cells in the deep dermis (**Fig. 20| B|**). Very rarely, single cells positive for CD271 or $CD271^+CD56^+$ cells (**Fig. 20| B|**, asterisks) could be detected in dermal tissue.
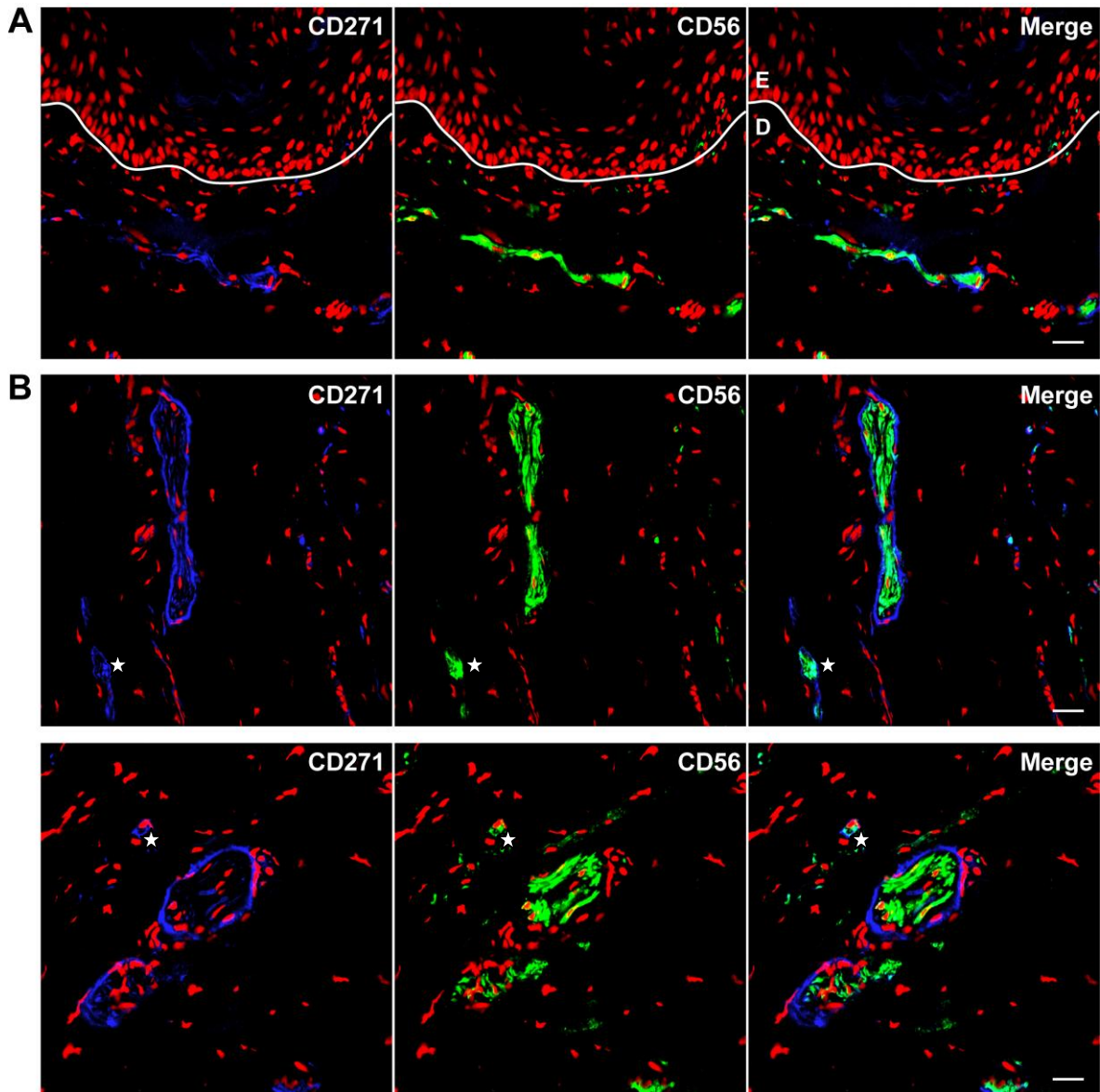
Fig. 20| **CD271⁺ cells colocalize with CD56⁺ cells in human dermis. A|** CD56$^+$ and CD271$^+$ cells colocalized in the upper dermis, **B|** as well as in the deep dermis (asterisks). Nuclei were stained with CytoxOrange and pictures were analyzed by CLSM. All pictures are representative of at least four different experiments with juvenile foreskin (aged between 2-13 years). E = epidermis, D = dermis, scale bars = 20 µm

Because CD56 is a neuronal and glial marker, further mAbs were introduced to discriminate neurons and glial cells. β-III-tubulin is a neuron-associated protein expressed in cells of the central as well as in the peripheral nervous system, but was believed not be expressed in healthy human skin[192]. Recent studies[193] and our findings, however, revealed that the mAb against β-III-tubulin stained similar cell aggregates in the deep dermis like the anti-CD56 mAb (**Fig. 21|**).
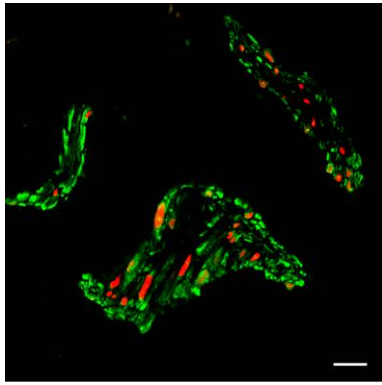
Fig. 21| **The distribution of β-III-tubulin⁺ dermal cells is similar to the staining pattern of CD56⁺ cells.** Cyrosections were stained with a FITC-conjugated mAb directed against the neuronal marker β-III-tubulin, nuclei were counterstained with CytoxOrange and pictures captured with a CLSM. Scale bar = 20 μm

Double staining with an anti-CD271 mAb showed the same occurrence in epidermal vicinity, as has been shown for CD56 (**Fig. 22|**). Cells positive for β-III-tubulin formed delicate, "capillary-like" structures in the upper dermis, surrounded by CD271⁺ cells, some single cells coexpressed CD271 (**Fig. 22| A|**, arrowheads). Again, rounded, bulky cell aggregates, also encapsulated by cells expressing CD271 (**B|**), including some CD271⁺β-III-tubulin⁺ cells (**Fig. 22| B|**, arrowheads), could be found in the deep dermis, whereas few cells were single positive for CD271 with no colocalisation (**Fig. 22| A| B|**, arrows).
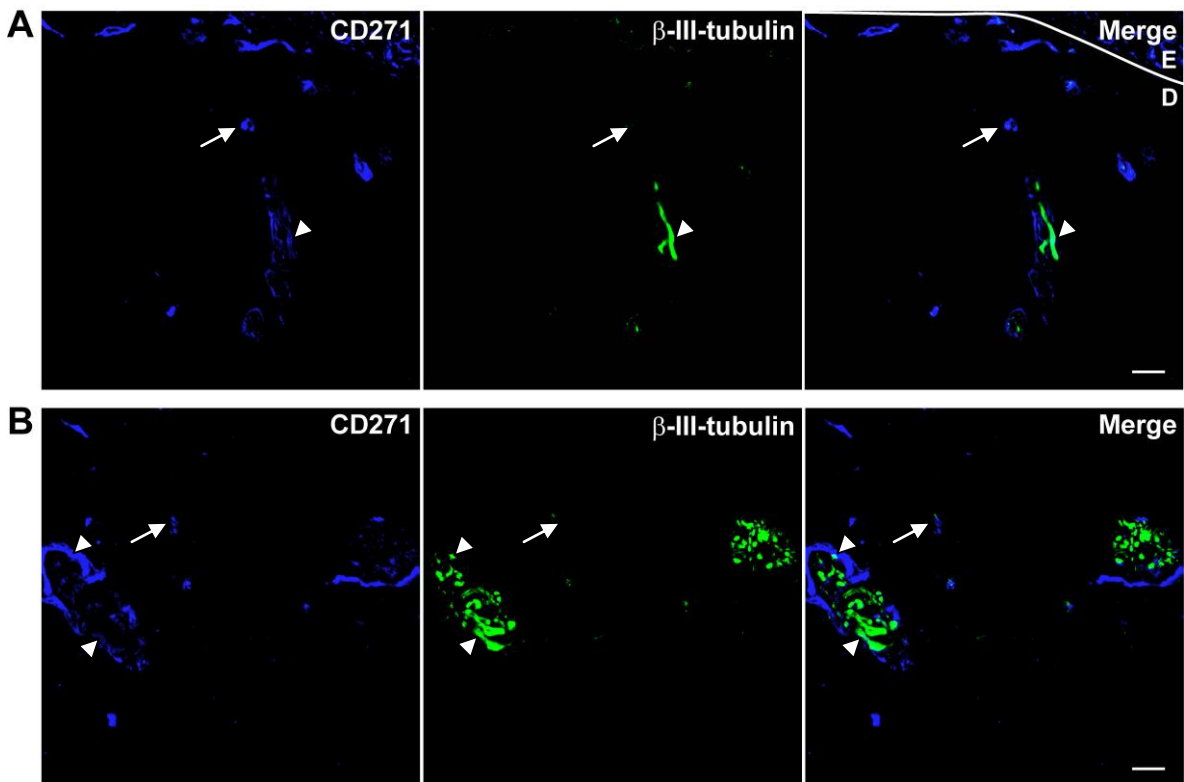
Fig. 22| **Double staining of CD271 and β-III-tubulin.** The apparent colocalisation of β-III-tubulin- and CD271-expressing cells in **A|** the upper and **B|** the deep dermis is almost equal to the staining pattern of CD56-expressing cells. Arrows denote CD271⁺ cells, whereas arrowheads depict CD271⁺β-III-tubulin⁺ cells. E = epidermis, D = dermis, scale bar = 20 μm

The protein GFAP is a member of the type III intermediate filaments and primarily expressed by cells of the central and peripheral nervous system, like Schwann cells and, in a small percentage, on BM-MSCs[194]. GFAP⁺ cells could be detected in the deep dermis, but with very low intensity. CD271⁺ cells colocalized with GFAP⁺ cell structures and infrequently CD271⁺GFAP⁺ cells could be detected that looked like cross-sectioned nerves (**Fig. 23|**), but the majority of CD271⁺ cells do not express GFAP and vice versa.
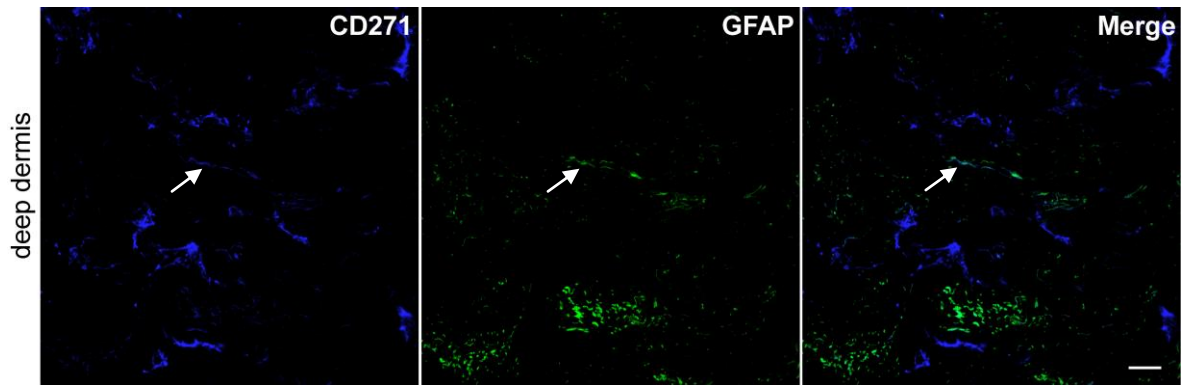
Fig. 23| Few CD271$^+$GFAP$^+$ cells are present in human dermis. Immunofluorescence double labeling of GFAP and CD271 showed a colocalization of cells expressing these markers throughout the dermis. Occasionally CD271$^+$GFAP$^+$ cells were found (arrows). Scale bar = 20 µm

5.2   Immunomodulatory potential of dermal MSC subsets

5.2.1   Phenotypic comparison of plastic-adherent bone marrow and dermal cells from different donors

According to the minimal criteria[85] to characterize multipotent MSCs, they are defined as plastic-adherent cells that express CD73, CD90 and CD105, but lack the expression of HLA-DR and several other surface proteins and can differentiate into adipocytes, chondrocytes and osteoblasts in vitro. In our lab, Dr. Christine Vaculik established methods for the prospective isolation and characterization of stem/progenitor cells in human dermis. She confirmed the existence of dermal cells, which fulfill these criteria (C. Vaculik, manuscript in preparation). **Fig. 24|** shows the flow cytometric comparison of BM-MSCs (**A|**) and primary dermal cells (**B|**), which were both preselected for plastic-adherence. The three major CD markers described for BM-MSCs are also present on adherent dermal cells in comparable percentages (**Fig. 24|**, black histograms). Over 90% of plastic-adherent dermal cells are strong positive for CD90, nearly 100% are positive for CD73 and CD105, but lack the expression for HLA-DR. This profile makes these cells perfect candidates for further immunomodulatory investigations.
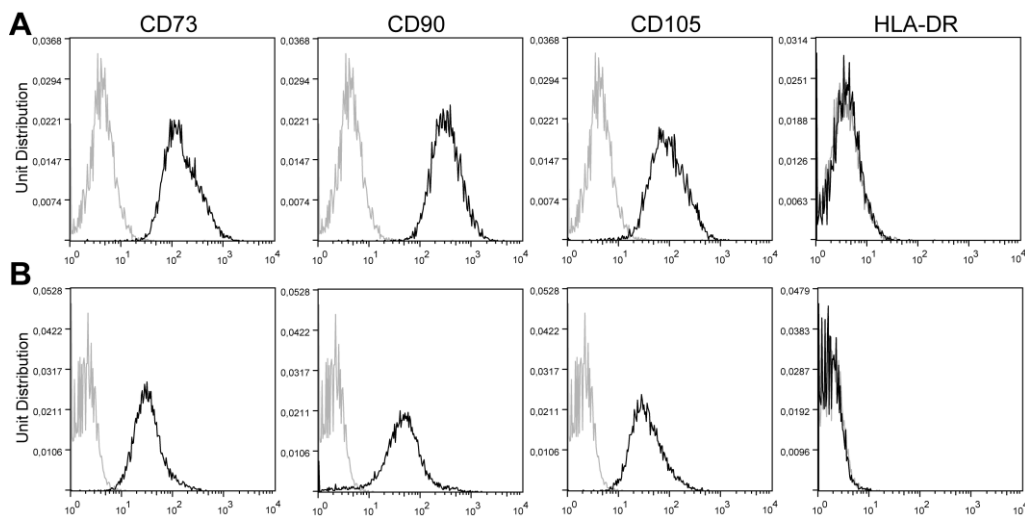
Fig. 24| Detection of MSC markers on plastic-adherent human dermal cells. Flow cytometry of plastic-adherent **A|** bone marrow cells and **B|** dermal cells (6 years, unpassaged) was performed by incubating single cell suspensions with the appropriate mAbs (black histograms) and isotype-matched controls (grey histograms). Dead cells were excluded with 7-AAD. Histograms are representative of at least 7 different experiments.

To further characterize the marker expression pattern of dermal cells, well-known markers described to be present and absent (CD80, CD86) on BM-MSCs were used. To delineate dermal MSCs, further markers were included such asCD31 and CD34. As CD271 is expressed on a small proportion of MSCs as well[195], we included this marker in our further experiments. **Table 5|** shows plastic-adherent dermal cells from seven individuals, uniformly expressing CD73, CD105 and HLA-A,B,C. This was comparable with the expression profile of bone marrow cells. Skin donors, however, were heterogeneous for CD26, CD90 and CD271, as demonstrated by high SED values. On both, dermal and bone marrow cells,

HLA-DR was minimally expressed and the CD28 ligands CD80 and CD86 were completely absent (**Fig. 25|**). Compared with bone marrow cells, the mean expression of CD271 in dermal cells was much higher, whereas CD90 was not uniformly expressed in dermal cells (about 10-15% lower than in bone marrow cells). These data demonstrate the similarity of adherent dermal cells to bone marrow cells, but also highlight some differences, especially for the marker CD90, which is one of the most prominent molecules to describe MSCs, and for CD271. The inhomogeneous marker expression in different donors makes it difficult to compare single individuals with each other, underlining the need of multiple donor comparisons.

Table 5| Marker expression of dermal and bone marrow cells

Markers	plastic-adherent	
	DERMAL CELLS	**BONE MARROW CELLS**
CD26	32.29±6.48	30.52±9.10
CD31	0.22	1.40
CD34	5.22	1.54±0.28
CD73	99.59±0.12	99.85±0.04
CD80	0.27±0.08	0.10±0.04
CD86	0.69±0.18	0.41±0.09
CD90	89.59±4.99	99.48±0.24
CD105	97.94±0.74	99.44±0.25
CD271	22.34±6.88	8.10±2.39
HLA-A,B,C	99.74±0.07	99.76±0.06
HLA-DR	1.70±0.32	1.21± 0.48

Whole dermal cells isolated from foreskin (n=7, aged between 2 and 9 years) and bone marrow cells (n=1) were expanded until 80-90% confluency, frozen and stored in liquid nitrogen until further processing. For analysis by flow cytometry, cells were thawed, cultured for 1-3 days and analyzed for marker expression as indicated. Single staining were made by incubation of $1x10^6$ cells with the indicated mAbs and at least 10,000 cells were recorded for every single sample. Isotype-matched controls were used to confirm specifity. Data are expressed as mean%±SED.

5.2.2   Phenotypic characterization of distinct MSC subsets in human dermis upon cryopreservation

Based on our previous observations, we analyzed distinct dermal subpopulations for their immunomodulatory potential. CD73$^+$ and CD90$^+$ dermal cells were selected due to their known capability to mediate leukocyte and lymphocyte adhesion to endothelium[97, 196-199], as we found that our cells of interest were prevalently located close to vascular cells. Further, it has been shown for BM-MSCs that the immunosuppressive capacity is lost with decreasing positivity for CD90[200]. Our finding that most of the CD271$^+$ dermal cells were also positive for CD73 and/or CD90 and that many CD271$^+$ cells colocalized with cells positive for Col-IV, a marker expressed in the basement membrane of lymphatic vessels, persuaded us to

include this cell subset into our experiments. Additionally, CD271 is a suitable marker to isolate MSCs from primary tissues as has been described previously[201]. In the first set of experiments, freshly isolated dermal cells were enriched for CD73-, CD90- and CD271-expressing cells with MACS columns (**Figs. 26|-28| A|**). Subsequently, positive and negative fractions[f], as well as total dermal cells were expanded in culture and cryopreserved until further investigations. For flow cytometric analysis and functional assays, cells were thawed and left to adhere o/n to tissue culture plates, trypsinized the next day and tested for marker expression, as shown in **Figs. 26|-28| B|**. Single staining were performed to detect and quantify CD80, CD86, HLA-A,B,C and HLA-DR, CD26, CD73, CD90, CD105 and CD271 expression in enriched and depleted cell suspensions compared with total dermal cells and, in certain experiments, bone marrow cells. Common in all experiments was the observation that total dermal cells did not express the costimulatory molecules CD80 and CD86 (**Fig. 25|**).
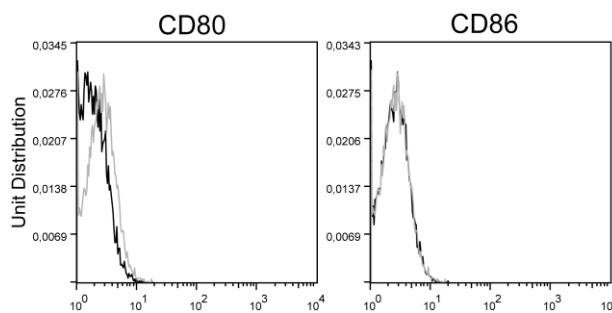

Fig. 25| Adherent dermal cells did not express the costimulatory molecules CD80 and CD86. Total dermal cells were isolated and cultured. Adherent cells were expanded and snap-frozen in liquid nitrogen. For flow cytometric analysis, cells were thawed, left to adhere o/n, detached via trypsinisation and subsequently analysed. Black profiles illustrate the reactivity of relevant mAbs, whereas grey profiles represent isotype-matched controls. Dead cells were excluded with 7-AAD and 10,000 living cells were recorded.

The expression profile of plastic-adherent CD73$^+$ cells after thawing and expansion did not vary greatly from CD73$^-$ cells and total dermal cells concerning the markers CD105, CD90, HLA-A,B,C and HLA-DR (**Fig. 26| B|** and data not shown). Surprisingly, the expression of the marker CD73 in positive and negative fractions was almost equal in all experiments performed, although they were initially highly purified, as can be seen by flow cytometric data acquired directly after the enrichment process, implying that CD73$^+$ cells proliferated better than CD73$^-$ cells before freezing (**Fig. 26| A|**). This hypothesis was confirmed by the observation that nearly 100% of plastic-adherent total dermal cells expressed CD73. Differences, however, were observed regarding the expression of CD26 and CD271. The percentage of CD26$^+$ dermal cells dropped after the enrichment procedure for CD73$^+$ and CD73$^-$ cells. Repeatedly, CD73$^-$ cells expressed marginally higher levels of CD26 than cells positive for CD73. This finding was more pronounced in experiments using other markers for enrichment (**Fig. 27|** and **Fig. 28|**). Further, we found that CD73$^+$ and CD73$^-$ cell fractions almost equally expressed CD271.

---

[f] To simplify matters, enriched fractions were called „positive", whereas depleted fractions were termed „negative", although both fractions could not be totally enriched or depleted for cells expressing the "one and only" marker with the methods used.

Fig. 26| Enrichment profile and marker analysis of whole dermal cells, enriched cells expressing CD73 and CD73-depleted cell populations upon cryopreservation. A| Freshly isolated primary dermal cells (6 year-old foreskin) were labeled with an αCD73 mAb, enriched with MACS columns and one part of cells was analyzed by flow cytometry as shown, the other part was expanded in culture. After expansion, cell fractions were stored in liquid nitrogen until further investigations. Upon thawing cells were expanded again and single staining with the indicated mAbs were made and examined by flow cytometry. **B|** Colored, open profiles represent the specific Ab expression. CD80/86 and HLA-DR expression is not shown, as no expression could be detected in all fractions. Specifity was controlled for every fluorochrome using isotype-matched controls (black, filled histograms). For overlays, y-axis were fixed to normalize the data. One representative of at least 3 different individual experiments, made with different skin donors, is shown. Dead cells were excluded with 7-AAD and 10,000 living cells were recorded for every fraction.

The comparison of CD90$^+$ and CD90$^-$ cells revealed no great marker variation with regard to CD73 (**Fig. 27| B|**). Surprisingly, CD90$^-$ cells showed a broader distribution of fluorescence emission, notably for CD105, but also for HLA-A,B,C, compared with the CD90$^+$ cell fraction. The depletion of CD90$^+$ cells, which coexpress high levels of CD105 and HLA-A,B,C, led to a left-over of heterogeneous cells in the CD90$^-$ cell fraction, with extremely diverse receptor density levels of these markers. In contrast to the enrichment with the αCD73 mAb, the

CD90$^+$ and CD90$^-$ cell fractions, showed remarkable differences concerning the expression of CD90 (**Fig. 27| A| B|**). Notable is further the almost entire depletion of CD26$^+$ cells within the CD90$^+$ cell fraction compared with CD90$^-$ or total dermal cells. CD271$^+$ cells were a priori almost completely absent in total dermal cells, which demonstrates again the individual differences between human donors concerning this marker.
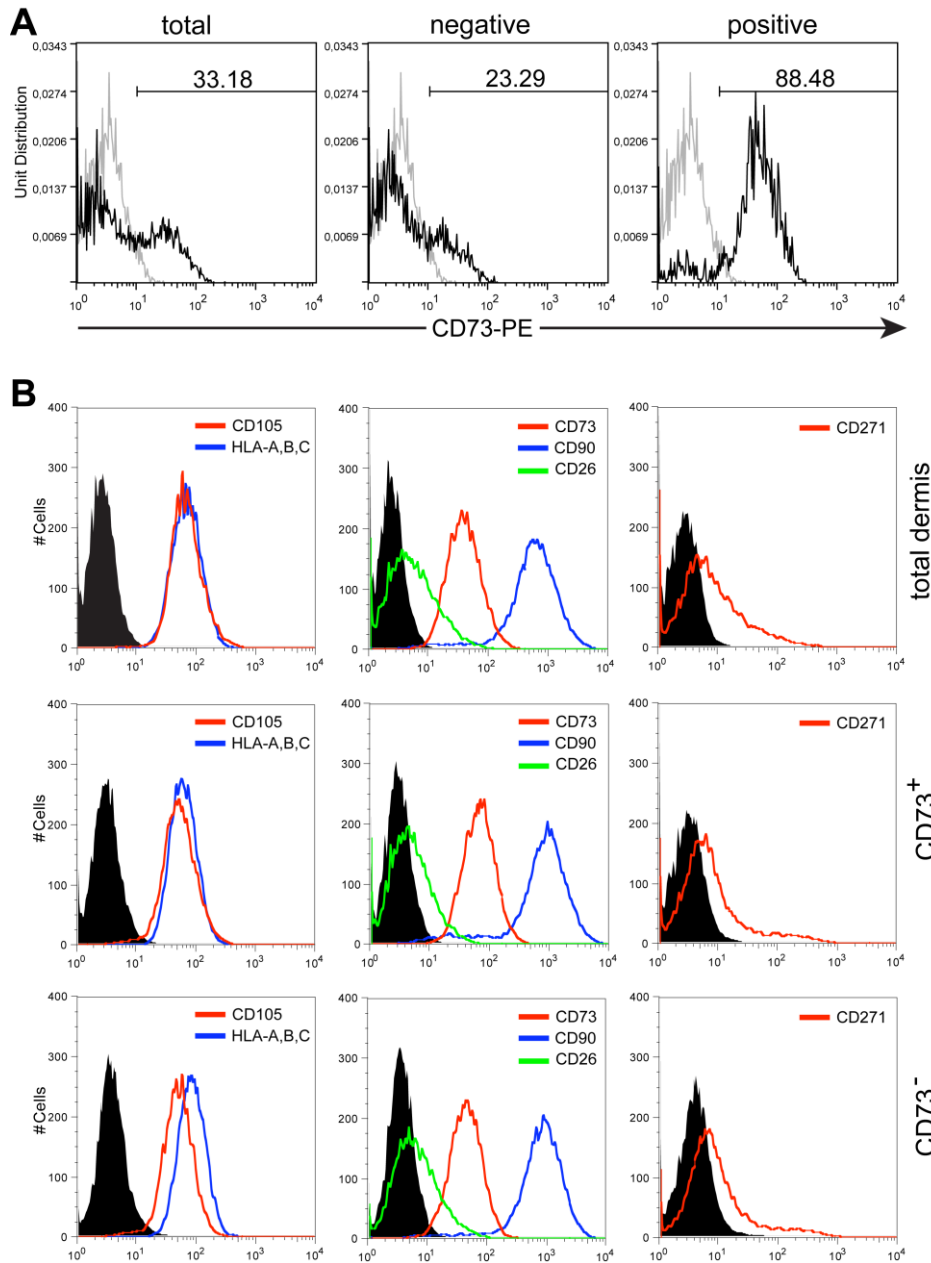

Fig. 27| **Enrichment profile and marker analysis of whole dermal cells, enriched cells expressing CD90 and CD90-depleted cell populations upon cryopreservation. A|** Freshly isolated primary dermal cells (6 year-old foreskin) were labeled with an αCD90 mAb, enriched with MACS columns and one part of cells was analyzed by flow cytometry as shown, the other part was expanded in culture. After expansion, cell fractions were stored in liquid nitrogen until further investigations. Upon thawing cells were expanded again and single staining with the indicated mAbs were made and examined by flow cytometry. **B|** Colored, open profiles represent the specific Ab expression. CD80/86 and HLA-DR expression is not shown, as no expression could be detected in all fractions. Specifity was controlled for every fluorochrome using isotype-matched controls (black, filled histograms). For overlays, y-axis were fixed to normalize the data. One representative of at least 3 different individual experiments, made with different skin donors, is shown. Dead cells were excluded with 7-AAD and 10,000 living cells were recorded for every fraction.

The phenotypic analysis of highly enriched, plastic-adherent, frozen-thawed CD271$^+$ or CD271$^-$ cells showed again no major differences between the expression of CD105, CD73 and HLA-A,B,C (**Fig. 28| B|**). The initial enrichment for CD271$^+$ cells lead to a definite increase of CD271$^+$ cells in the positive fraction, compared with the incomplete loss in the CD271$^-$ cell fraction (**Fig. 28| A|**). CD271$^+$ cells contained a marginally higher percentage of CD26$^+$ cells than total dermal cells, but almost halved levels compared with the depleted fraction. CD90 showed already in total dermis a remarkable bimodal distribution of CD90$^+$ and CD90$^-$ cells, which was enhanced with the enrichment of CD271$^+$ cells. In summary, approximately 50% of CD271$^+$ cells were CD90$^+$, while all cells negative for CD271 were positive for CD90.
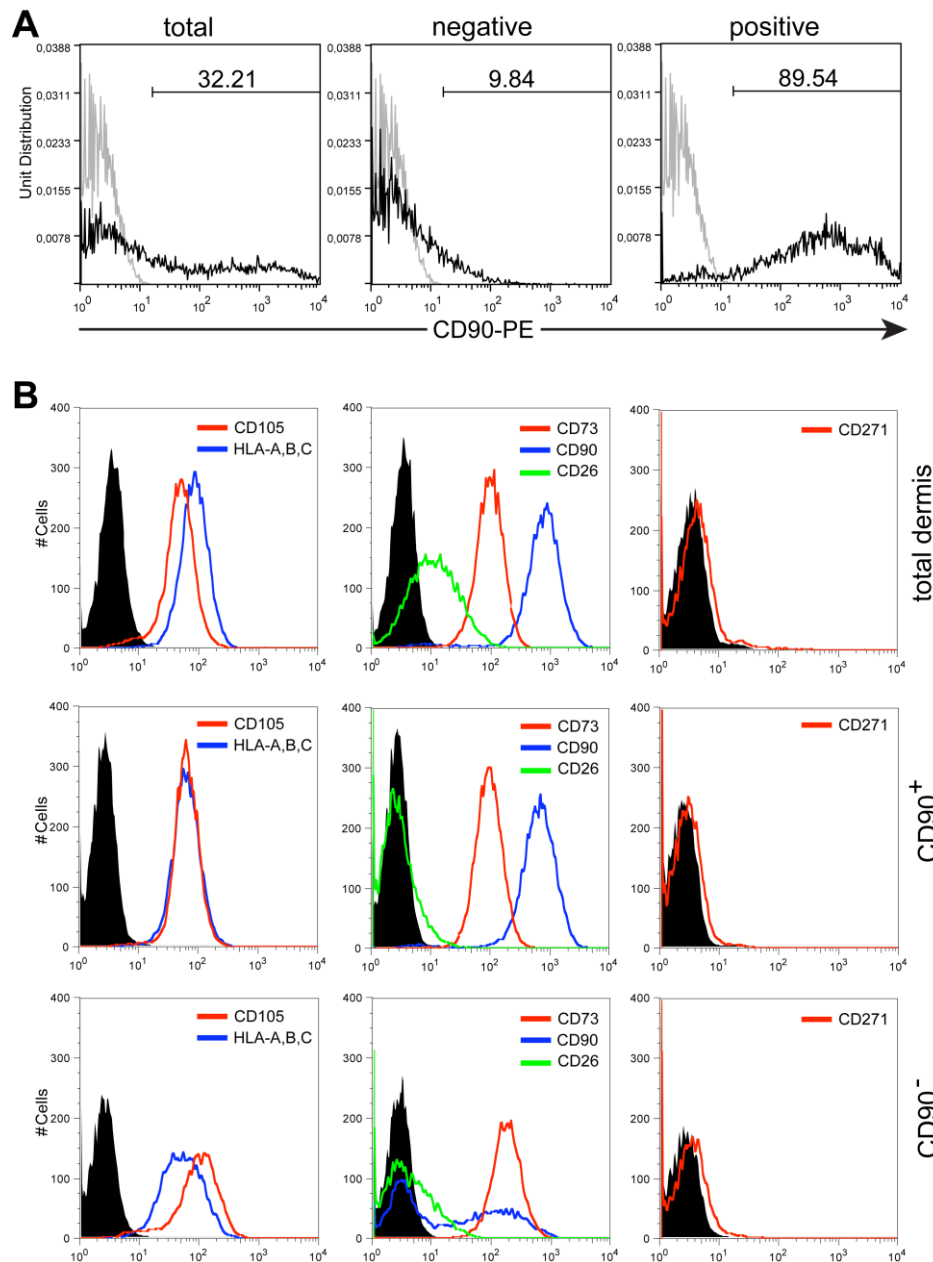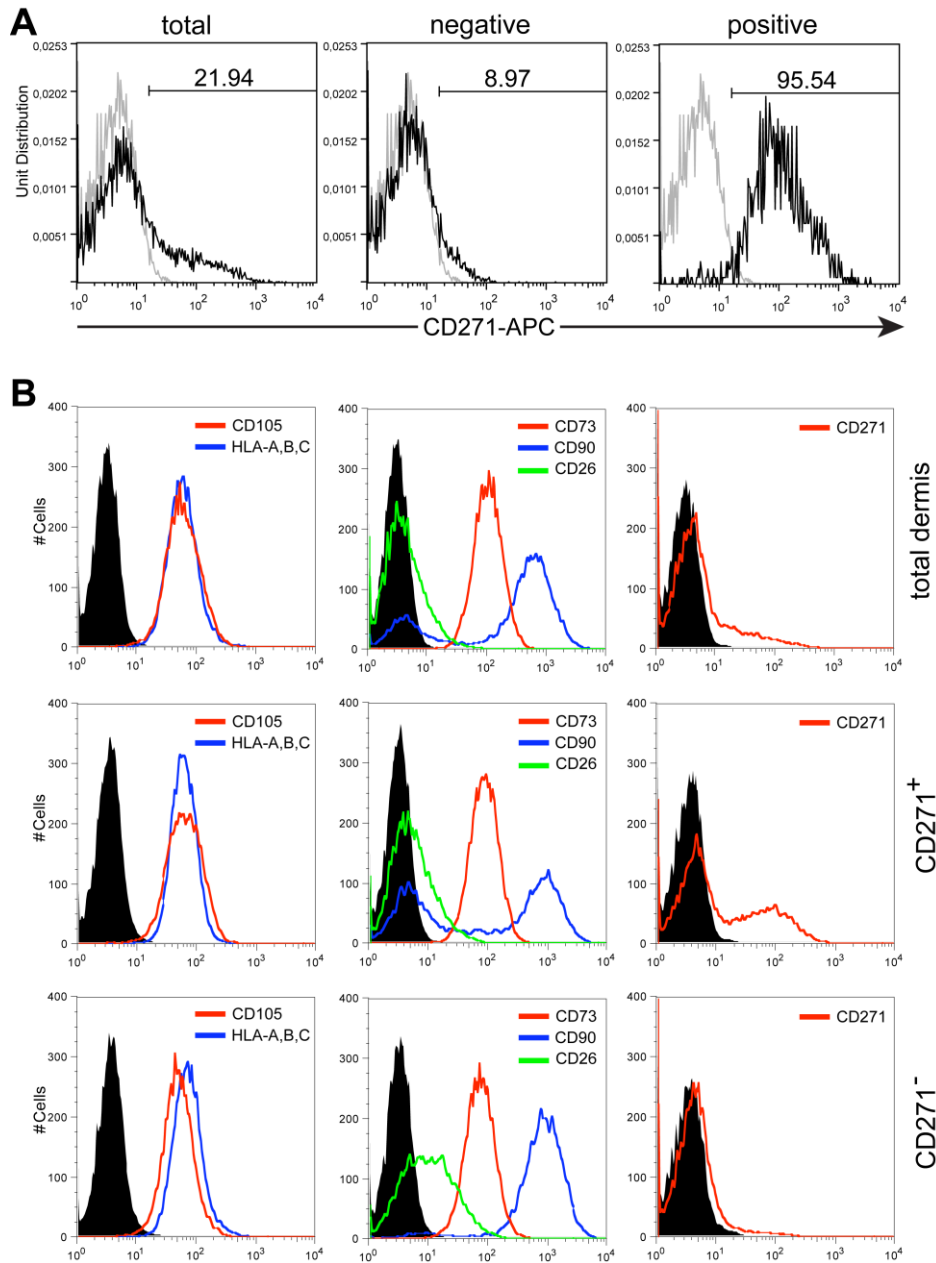
Fig. 28| **Enrichment profile and marker analysis of whole dermal cells, enriched cells expressing CD271 and CD271-depleted cell populations upon cryopreservation. A|** Freshly isolated primary dermal cells (6 year-old foreskin) were labeled with an αCD271 mAb, enriched with MACS columns and one part of cells was analyzed by flow cytometry as shown, the other part was expanded in culture. After expansion, cell fractions were stored in liquid nitrogen until further investigations. Upon thawing cells were expanded again and single staining with the indicated mAbs were made and examined by flow cytometry. **B|** Colored, open profiles represent the specific Ab expression. CD80/86 and HLA-DR expression is not shown, as no expression could be detected in all fractions. Specifity was controlled for every fluorochrome using isotype-matched controls (black, filled histograms). For overlays, y-axis were fixed to normalize the data. One representative of at least 3 different individual experiments, made with different skin donors, is shown. Dead cells were excluded with 7-AAD and 10,000 living cells were recorded for every fraction.

Altogether, the enrichment for CD90$^+$ and CD271$^+$ cells showed distinct expression patterns and were, thus, employed for a comparison of positive and depleted fractions in a coculture-based proliferation assay of lymphocytes. Regardless of a major lack of investigated differences, CD73$^+$ and CD73$^-$ cells were also included into further experiments.

5.2.3 Differences in the proliferation kinetics of PBMCs and naive T_h cells

The proliferative response is an essential feature of the adaptive immune response and it has been reported that MSCs from bone marrow and other tissues have the ability to modulate lymphocyte proliferation after stimulation with mitogens, allogens or direct engagement of the TCR complex and costimulatory molecules via Abs, such as αCD3 and αCD28, respectively. For our investigations, immobilized αCD3 and soluble αCD28 mAbs were used, as this type of stimulation is more physiological than mitogenic lectins[202].

Most studies investigating the immunomodulatory potential of MSCs used undefined PBMC-mixtures or pan T cells[203, 204]. To test, whether there are differences in the proliferative response of PBMCs and naive T_h cells, they were stimulated with αCD3 and/or αCD28 mAbs, labeled with [^{3}H]-TdR and harvested on days 3-6. PBMCs stimulated with αCD3/CD28 mAbs started to proliferate around day 3 (as inspected in wells), increased their proliferation till day 5 and decreased until day 6 (**Fig. 29| A|**). In contrast, naive T_h cells were initiated through αCD3/CD28 ligation to highly proliferate already before day 3 and appeared to have a steady proliferative response over almost 4 days, until proliferation decreased slowly around day 6 (**Fig. 29| B|**). Both lymphocyte fractions showed no response to αCD28 alone and did not proliferate without provision of external stimuli (**Fig. 29| A| B|**).
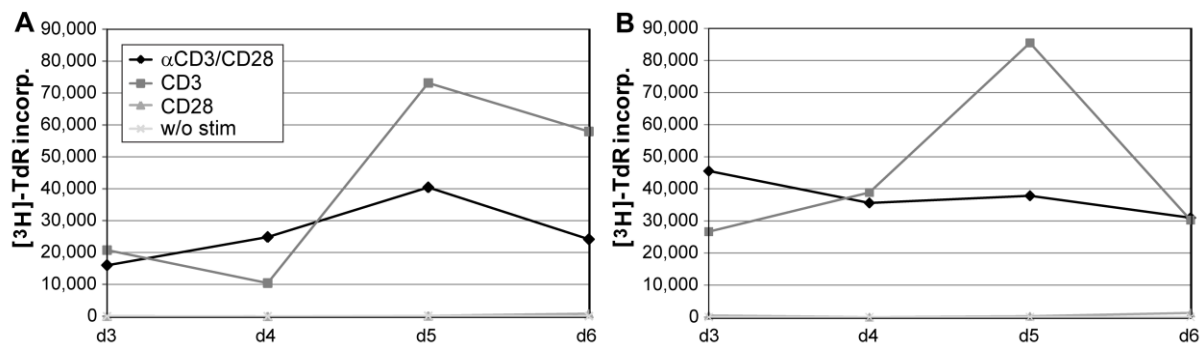
Fig. 29| Proliferation kinetics of PBMCs and CD4$^+$CD45RA$^+$ T cells with different stimuli. PBMCs and naive T_h cells (5x10^4/well in 200 µl NCM) were stimulated with plate-bound αCD3 (2 µg/ml) alone or in combination with soluble αCD28 (1 µg/ml) for 3-6 days in round-bottom 96-well plates. Cells were labeled with [^{3}H]-TdR for the last 18 hours of culture and harvested. **A|** PBMCs had a peak proliferative response at day 5, while **B|** CD4$^+$CD45RA$^+$ T cells proliferated almost equally until day 6, when stimulated with αCD3/CD28. d = day

The almost constant proliferation level over a long time period renders naive T_h cells highly suitable for investigations with CFSE, as this method allows the detection of time- or cell division-dependent influences by dermal MSC subtypes. In addition, a highly pre-sorted cell population is very advantageous for a CFSE-based cell division tracking system, as it improves peak resolution[183]. Furthermore, to our knowledge, few reports exist for human BM-MSCs and none with dermal MSCs studying their impact on naive T_h cells. Worth mentioning, is the delayed, but still strong stimulation of both responders with high concentrations of αCD3 alone. Therefore, we decided to use lower αCD3 concentrations for further experiments.

5.2.4 Establishment of a CFSE-based MSC – T cell coculture system

5.2.4.1 Adherent dermal cells inhibit the proliferation of αCD3/CD28-stimulated naive T_h cells

To elucidate the impact of dermal MSCs on naive T_h cells, a coculture system for a CFSE-based approach had to be developed. For this purpose, we used BM-MSCs as a positive control, as they are known to inhibit T cell proliferation. For the stimulation of naive T_h cells, αCD3-coated, round-bottom 96-well plates with/without a soluble αCD28 mAb were used. Different concentrations of BM-MSCs (5×10^3-1×10^5 cells/well) and dermal cells (5×10^3, 1×10^5 cells/well) were seeded and left to adhere o/n. On the next day, enriched naive T_h cells (**Fig. 30|**), were stained with CFSE, added to the wells (5×10^4 cells/well) and cultured for 5 days with/without BM-MSCs and dermal cells. Additionally, BM-MSCs and dermal cells were cocultured with naive T_h cells without stimulation to exclude allogeneic immune responses. Further, T cells and BM-MSCs were seeded alone with or without the indicated stimuli. Unstained T cells were used to estimate autofluorescence (data not shown).
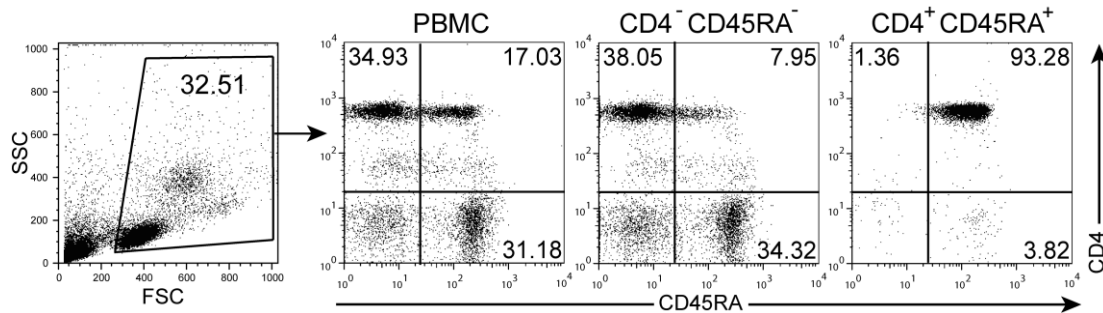
Fig. 30| Enrichment of naive T_h cells from total PBMCs. Lymphocytes and monocytes were separated from erythrocytes and neutrophils by density gradient centrifugation of buffy coats. The resulting PBMCs (FSC/SSC profile, left dot plot) were stained with a mAb mixture to retain unwanted cells in the magnetic columns (negative fraction, middle dot plot), while untouched naive T_h cells could pass (positive fraction, right dot plot). Enrichments were analyzed by flow cytometry by direct gating of PBMCs in the FSC/SSC profile and staining of CD4 and CD45RA. Purity was always between 93% and 99%.

No allogeneic stimulation could be detected, upon coculture of BM-MSCs with T_h cells without stimulation (**Fig. 31| A|**, upper panel, w/o stim) or dermal cells (see **5.2.5** and **5.2.11**). With increasing cell densities, BM-MSCs, as well as dermal cells, showed a remarkable inhibition of T cell proliferation, when stimulated with αCD3/CD28 mAbs (**Fig. 31| A| B|**). Interestingly, a small T cell population was proliferating even without costimulation, which was enhanced by low concentrations of BM-MSCs and dermal cells (**Fig. 31|**, CD3). This phenomenon could be seen with little variations in every experiment performed and could reflect costimulation with remaining APCs, as the percentage of proliferating cells decreased with increased T cell purity.
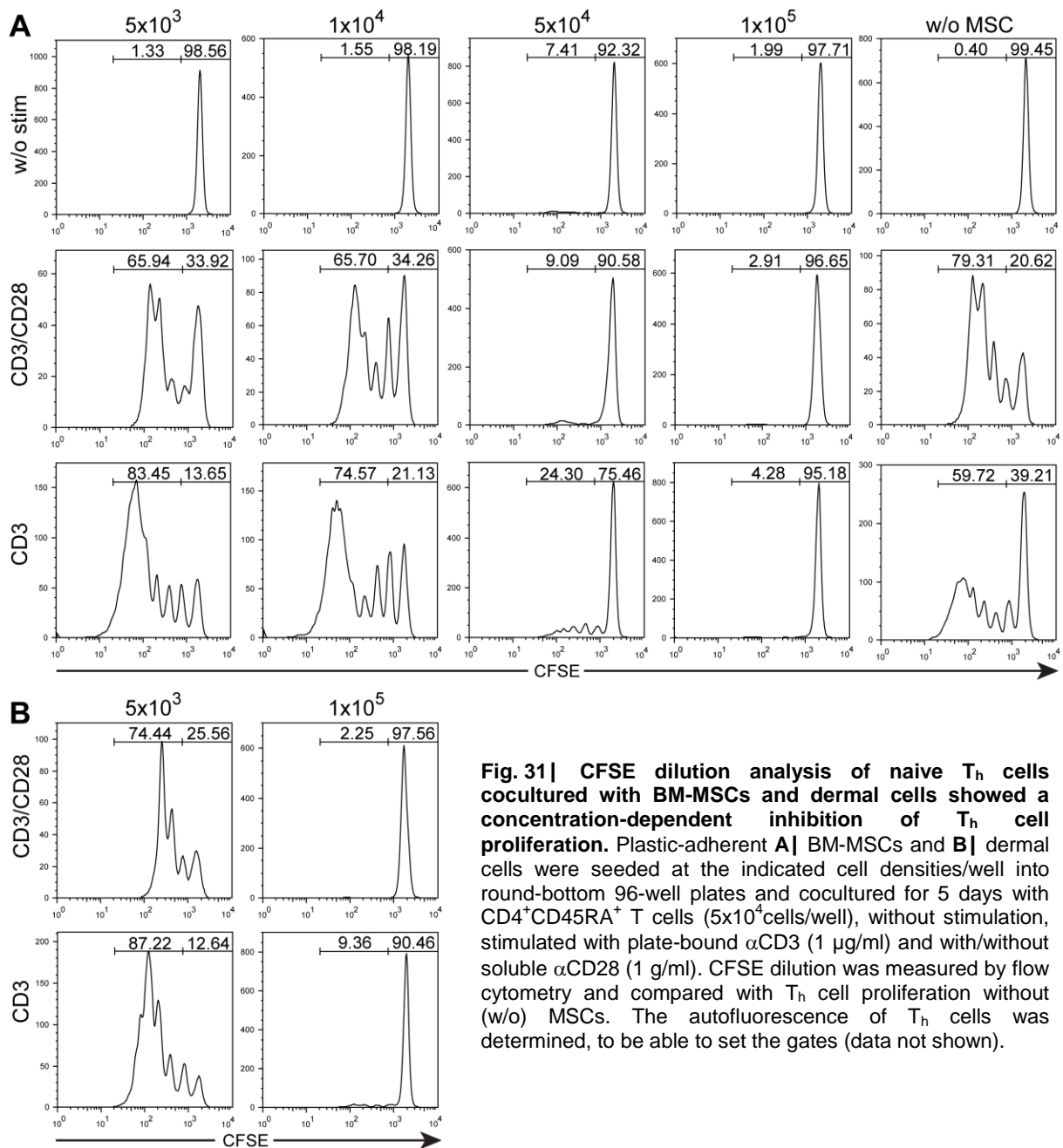
Fig. 31| **CFSE dilution analysis of naive T$_h$ cells cocultured with BM-MSCs and dermal cells showed a concentration-dependent inhibition of T$_h$ cell proliferation.** Plastic-adherent **A|** BM-MSCs and **B|** dermal cells were seeded at the indicated cell densities/well into round-bottom 96-well plates and cocultured for 5 days with CD4$^+$CD45RA$^+$ T cells (5x10^{4}cells/well), without stimulation, stimulated with plate-bound αCD3 (1 µg/ml) and with/without soluble αCD28 (1 g/ml). CFSE dilution was measured by flow cytometry and compared with T$_h$ cell proliferation without (w/o) MSCs. The autofluorescence of T$_h$ cells was determined, to be able to set the gates (data not shown).

5.2.4.2   High numbers of BM-MSCs inhibit the proliferation of αCD3/CD28-stimulated CD25-depleted naive T$_h$ cells

It has been reported that nTregs show increased proliferation upon coculture with BM-MSCs[128, 130, 205, 206]. As we were interested, whether the proliferation of defined naive T$_h$ cells could be altered by the addition of MSCs, we eliminated nTregs by depletion of CD25$^+$ cells from total PBMCs, before the enrichment of naive T$_h$ cells. T$_h$ cell proliferation increased strongly upon coculture with low numbers of BM-MSCs when stimulated with αCD3/CD28 and αCD3 alone (**Fig. 32|**, red histograms). With increasing BM-MSC densities the proliferation was clearly inhibited, as illustrated by a shift of the red histogram, which represents T cells from coculture, towards the unstimulated T cell fraction (single peak with highest fluorescence intensity). Interestingly, the proliferation of αCD3-stimulated T$_h$ cells

alone, was almost abolished (**Fig. 32|**), depending on the purity of CD25 depletion, which was verified in all experiments performed with different PBMC donors.
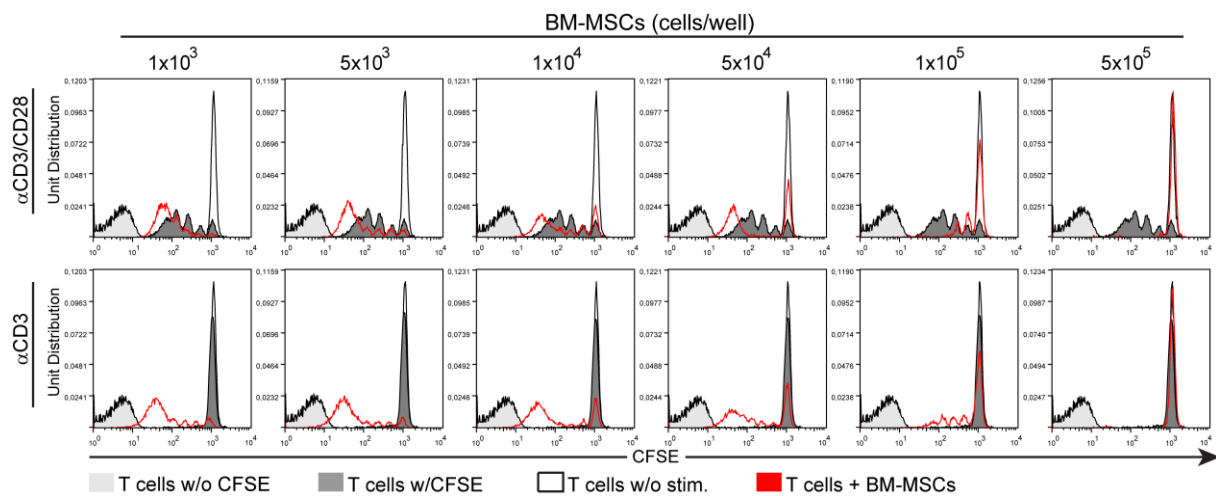

Fig. 32| Proliferation of CD4$^+$CD45RA$^+$CD25$^-$ T cells cocultured with BM-MSCs. Different concentrations of BM-MSCs were seeded into αCD3 (1µg/ml) precoated plates, left to adhere o/n and cocultured with CD25-depleted naive T$_h$ cells (5x10^4 cells/well) with or without an αCD28 mAbs (red histogram). After 5 days, cells were harvested, washed with FACS buffer and the CFSE dilution profile was assessed by flow cytometry. As negative control, unstimulated T cells were cocultured with MSCs (white peak). Stimulated T cells alone (dark grey histogram) served as positive proliferation control. Low numbers of BM-MSCs (1x10^{3}cells/well) seemed to have an enhancing effect on proliferation, while high numbers around 1x10^5/well completely abrogated the proliferation.

The dark grey histogram in the overlays resembles T$_h$ cells after 5 days culture and stimulation with the indicated Abs, whereas the light grey histogram results from autofluorescence of unstained T$_h$ cells.

5.2.4.3   HaCaT cells inhibit the proliferation of αCD3/CD28-stimulated CD25-depleted naive T$_h$ cells

The complete inhibition of T cell proliferation with MSC numbers around 1x10^5 cells/well or higher, lead us to critically assess the setup of this coculture system, as to our knowledge, all investigations of the inhibiting nature of MSCs reported by other groups showed a reduction of proliferation up to 90%, but never full inhibition[70, 207, 208]. One possible explanation could be a blocking of plate-bound αCD3 Abs by high densities of adherent MSCs. To test this hypothesis, we included HaCaT cells in our experiments, a nontumorigenic keratinocyte cell line that was reported to have no effect on T cell proliferation[148]. BM-MSCs and HaCaT cells (1x10^4 and 1x10^5 cells/well) were seeded into αCD3-coated 96-well plates and cultured o/n. At high BM-MSC densities (**Fig. 33| A|**, red histogram) we found nearly complete inhibition of T cell proliferation compared with the proliferation profile of αCD3/CD28-stimulated T cells alone (filled, dark grey histograms). Unexpectedly, also HaCaT cells massively inhibited T cell proliferation (**Fig. 33| B|**) implying that the inhibitory effect of the cells investigated is due to sterical hindrance by adherent cells. Thus, αCD3/CD28-coated beads were introduced for T cell stimulation to avoid this problem[8].
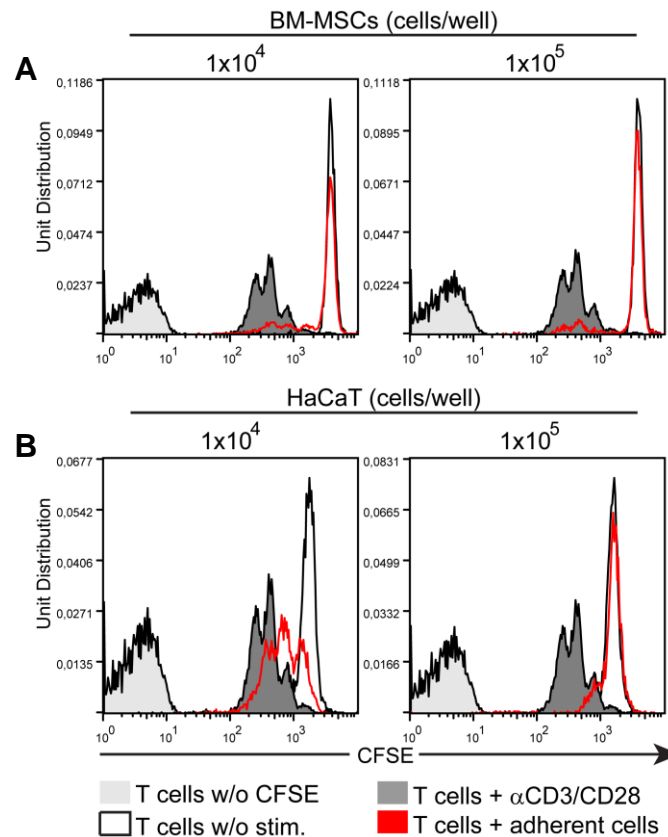
Fig. 33│ Analysis of possible sterical hindrance caused by adherent cells using HaCaT cells. High concentrations of **A│** BM-MSCs and **B│** HaCaT cells ($1x10^4$ and $1x10^5$ cells/well) were seeded into αCD3 precoated plates (1µg/ml) and cocultured with $CD4^+CD45RA^+CD25^-$ cells ($5x10^4$ cells/well) and a soluble αCD28 mAb, to test whether sterical hindrance by adherent cells is the inhibiting cause.

5.2.4.4 Establishment of the αCD3/CD28 bead-based stimulation

As adherent cells seemed to block plastic-bound Abs at high densities, we employed αCD3/CD28-coated beads in our experiments. First, the bead-cell ratio and the T cell concentration per well had to be determined. For this, the magnetic bead solution was resuspended, an aliquot was taken and washed according to the manufacturer's instructions. Isolated $CD25^-$, naive T_h cells were mixed with different amounts of the bead solution to obtain bead-cell ratios of 1:1, 2:1 and 3:1. The proliferation profile of T cells stimulated with the indicated bead concentrations appeared to have a similar number of division cycles (**Fig. 34│ A│**) as demonstrated by a histogram overlay (**Fig. 34│ B│**). Since CFSE is measured by flow cytometry and for this a certain cell number is indispensible, we compared different T cell numbers, to estimate the limit of cells/well for an optimal proliferative response. We found a T cell number-dependent decrease of T cell proliferation (**Fig. 34│ C│**).
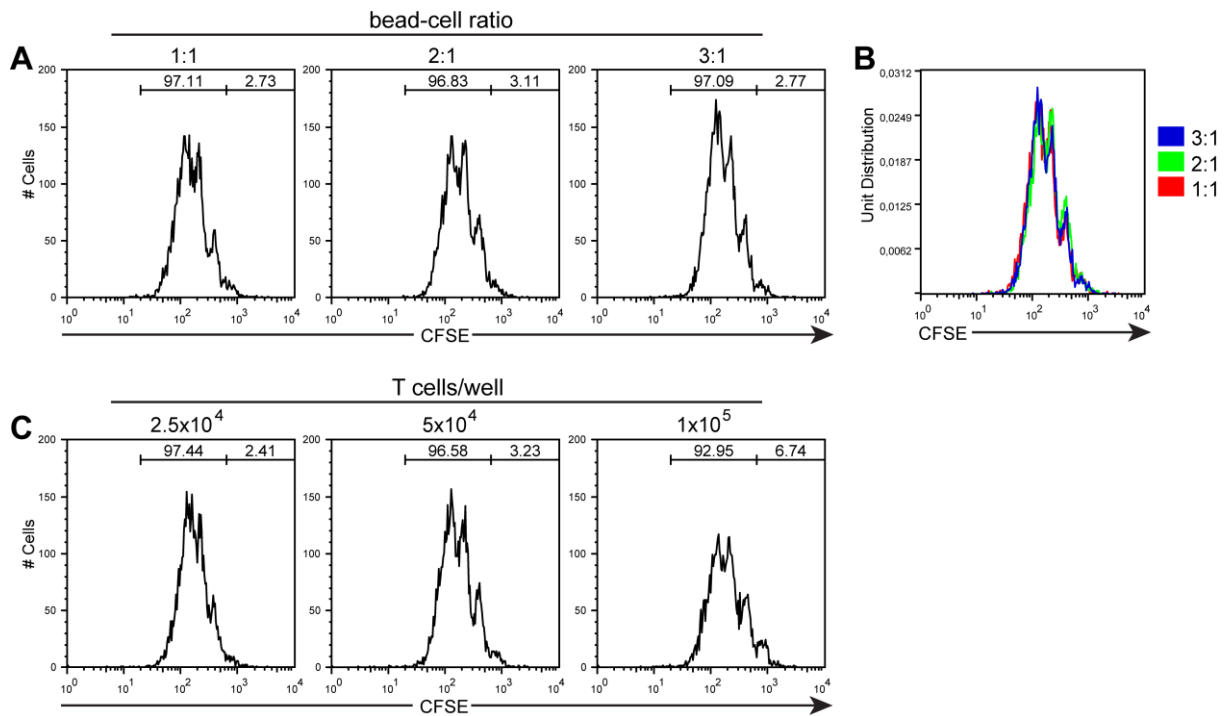
Fig. 34| Establishment of T cell stimulation with αCD3/CD28-coated beads. Plastic beads coated with αCD3/CD28 mAbs, mimicking APCs, were prepared according to the manufacturers protocol and used in different concentrations to stimulate CFSE-stained CD25-depleted naive T_h cells ($5x10^4$ cells/well; **A|** and overlay in **B|**) or **C|** with the recommended concentration (2:1), but varying seeding concentrations of T cells. Cells were stimulated for 4 days and proliferation was measured by CFSE dilution and flow cytometry.

The optimal T cell densities were further defined via measurement of T cell proliferation with [^{3}H]-TdR uptake[209]. There was an obvious difference between the T cell densities used differing in one order of magnitude (**Fig. 35|**). A higher number of T cells ($1x10^5$ cells/well) again seemed to inhibit itself, maybe due to shortage of space (cpm = 24,900), whereas $1x10^4$ cells/well showed a higher proliferative response, with cpm values around 35,000 (**Fig. 35|**). Based on these results we decided to use $5x10^4$ T cells/well in further experiments. Further, we decided to work with the lowest bead-cell ratio (1:1), as it showed optimal stimulation of T cell proliferation.
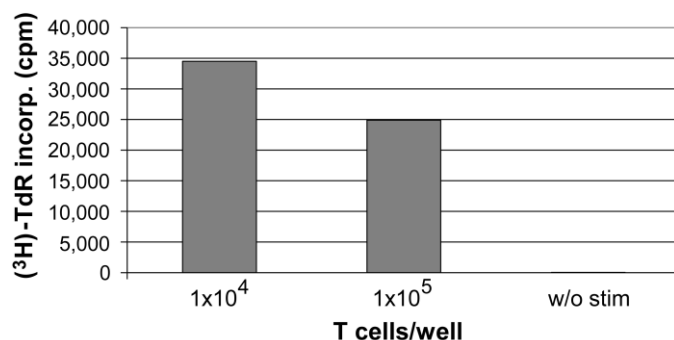
Fig. 35| The proliferative response is decreasing with higher T cell densities. Naive T_h cells ($1x10^4$ and $1x10^5$ cells/well) were seeded into round-bottom 96-well plates and stimulated with αCD3/CD28 mAbs (1µg/ml). Cells were labeled with [^{3}H]-TdR 18 hours before harvesting on day 3. Data represent the mean of triplicates.

5.2.5 Increasing numbers of plastic-adherent dermal cells inhibit the proliferation of pan T cells stimulated with αCD3/CD28-coated beads

Using our established parameters we next evaluated, whether they are applicable to verify already known data regarding the immunomodulatory potential of BM-MSCs. Further, we wanted to investigate the inhibitory potential of plastic-adherent dermal cells on pan T cell proliferation. Human embryonic kidney (HEK 293) cells served as a negative control, as they do not express HLA-DR or any costimulatory molecules (CD80, CD86) and express low levels of HLA-A,B,C (data not shown). For this purpose, cryopreserved dermal cells, BM-MSCs or HEK cells were thawed, seeded into round-bottom 96-well plates and left to adhere o/n. On the next day, freshly isolated pan T cells were stained with CFSE, added to the adherent cells and stimulated with αCD3/CD28-coated beads (adherent cell:T cell ratios = 1:50, 1:10 and 1:5). As controls, stimulated (**Fig. 36| A|**, filled, dark grey histograms) and unstimulated T cells were cultured alone and unstimulated T cells were cultured with plastic-adherent cells (**Fig. 36| A|**, single peaks at highest fluorescence intensities) and controls (HEK 293 cells). Unstained T cells (**Fig. 36| A|**, filled, light grey histograms) were cultured with and without stimulation and adherent cells and controls were cultured without T cells. To verify the reliability of the CFSE-based system, the same experiment was set up twice, one for CFSE tracking of cell division and another for an [^{3}H]-TdR-based approach (**Fig. 36| B|**). The CFSE proliferation profile of stimulated T cells from cocultures were plotted as red line in the overlays of **Fig. 36| A|**. The immunomodulatory potential of BM-MSCs (MSC:T cell ratio = 1:10) could be verified with the CFSE-based cell division tracing method, as the red histogram shifted towards the unstimulated cell fraction (**Fig. 36| A|**, left histogram). Low numbers of plastic-adherent total dermal cells (DERMAL CELL:T cell ratio = 1:50) did not alter the proliferative response, whereas increasing densities (ratio = 1:10 or 1:5) clearly inhibited pan T cell proliferation. As HEK 293 cells did not induce a shift of the red histogram towards the unstimulated cell fraction, we could prove that no sterical hindrance is responsible for the inhibition of T cell proliferation in this setting. Moreover, a similar inhibiting potential of BM-MSCs and dermal cells could be visualized by measuring the [^{3}H]-TdR uptake (**Fig. 36| B|**). BM-MSCs and dermal cells at equal cell numbers inhibited the T cell proliferation to a similar extent.
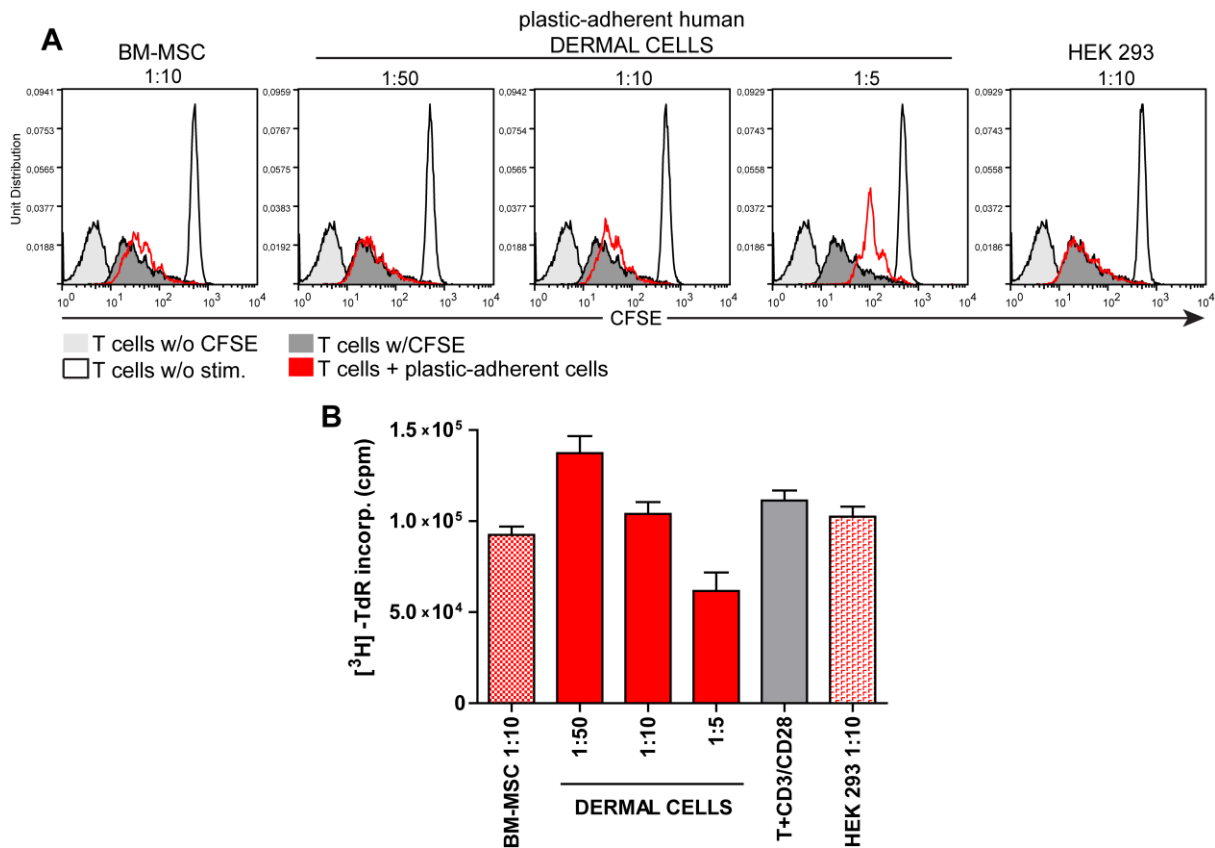
Fig. 36| Plastic-adherent dermal cells inhibit pan T cell proliferation in a cell density-dependent manner. Both, freshly isolated dermal single cells from juvenile foreskin and, as a positive control, BM-MSCs were expanded until passage 2 (P II) and stored in liquid nitrogen. Before coculture, cells were thawed, cultured for 2-3 days, trypsinized, seeded in different cell numbers into round-bottom 96-well plates [dermal cells (1×10^3, 5×10^3 and 1×10^4 cells/well) and BM-MSCs and HEK cells (5×10^3 cells/well)] and left to adhere o/n. On the next day, freshly isolated pan T cells (purity > 98%) were added to obtain cell ratios ranging from 1:50-1:5 (adherent cells:T cells) and stimulated with Dynabeads (cell-bead ratio = 1:1). BM-MSCs were used as a positive control and HEK cells served as negative control. **A|** CFSE-based approach. In each histogram, unstimulated T cells from coculture with the indicated plastic-adherent cells, are plotted (single peak at high CFSE intensities). The filled, light grey histograms show T cells without CFSE staining, whereas the dilution profiles in dark grey resulted from stimulated T cells alone. The red histogram displays the T cell division cycles after stimulation and 4 days of coculture with the mentioned cell types. **B|** [^{3}H]-TdR incorporation assay. The same experimental approach was pipetted a second time into another 96-well plate, labeled with [^{3}H]-TdR for the last 18 hours of culture and harvested on day 4. Shown is one representative experiment out of three.

5.2.6 Investigating the role of Tregs in MSC-induced T cell suppression

nTregs are known to suppress a great variety of pathological and physiological immune responses in vivo[210]. It has been suggested that the functional activity of this cell type is related to the expression of the transcription factor FoxP3. To test whether Tregs play a role in the decrease of pan T cell proliferation we observed upon coculture with plastic-adherent dermal cells, we counterstained CFSE-labeled T cells with an αFoxP3 mAb. Indeed, the percentage of FoxP3$^+$ cells strongly increased after coculture with BM-MSCs (15.81%), compared with αCD3/CD28-stimulated T cells alone (5.80%; **Fig. 37|**). This increase of cells with a regulatory phenotype support the concept of a Treg-driven immunosuppression, mediated via MSCs.
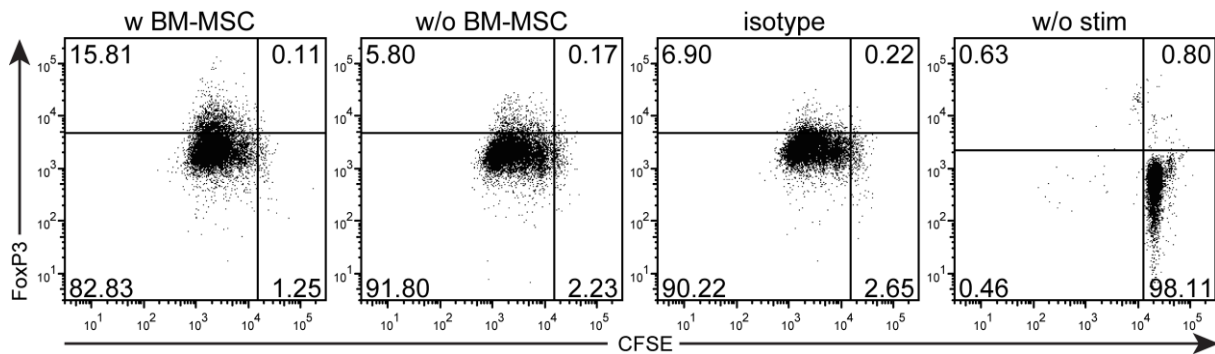
Fig. 37| The percentage of FoxP3$^+$ T cells increased after coculture with BM-MSCs. Pan T cells were enriched from PBMCs, stained with CFSE, stimulated with αCD3/CD28-coated beads and cultured (5×10^4 cells/well) with or without BM-MSCs (1×10^3 cells/well). After 4 days, cells were harvested, beads were removed by magnetic forces, T cells were fixed, permeabilized and stained with an AlexaFluor$_{647}$ labeled mAb directed against the intracellular marker FoxP3. Cells were immediately analyzed by flow cytometry and 10,000 cells were recorded for each setting. Shown is one representative experiment out of three.

5.2.7 High numbers of BM-MSCs and umbilical cord blood- (UCB-)MSCs suppress the proliferation of CD25-depleted T$_h$ cells stimulated with αCD3/CD28-coated beads

Most of the published data about the immunoregulatory potential of MSCs include the analysis of total PBMCs, pan T cells, CD4$^+$ or CD8$^+$ T cells[119, 211]. As our previous results indicated an MSC-induced increase of FoxP3$^+$ T cells, we were intrigued, whether MSCs could also inhibit the proliferation of naive T$_h$ cells, which were depleted of nTregs. To address this question, we decided to use MSCs from tissues that have been proven several times to have immunosuppressive activity, such as bone marrow and umbilical cord blood. Therefore, BM- and UCB-MSCs were cocultured at varying cell densities with CD25-depleted naive T$_h$ cells, which were stimulated with αCD3/CD28-coated beads (MSC:T cell ratios ranging from 1:50 to 1:0.5). After 4 days, the CFSE dilution profile was analyzed by flow cytometry. Low BM-MSC:T cell ratios (1:50) showed no inhibitory effect on T$_h$ cell proliferation (**Fig. 38| A|**, histogram on the left, red line) compared with cell division peaks of T cells alone (filled, grey histogram). The white peak on the right displays the unstimulated cell fraction. Beginning at MSC:T cell ratios from 1:5 (**Fig. 38| A|**, middle histogram) and higher (right histogram), the proliferation of T$_h$ cells was clearly inhibited by BM-MSCs as indicated by a shift of the red histogram towards the unstimulated cell peak. The inhibitory potential of UCB-MSCs was comparable to BM-MSCs, as low numbers did not alter the CFSE division profile or even enhanced the proliferative response to a very low extent, whereas increasing UCB-MSC densities showed a clear inhibition of T cell proliferation (**Fig. 38| B|**). The finding that MSCs from different sources have the potential to inhibit the proliferation of highly purified CD25$^-$ T$_h$ cells has, thus, been shown for the first time, to our knowledge. This would suggest that MSCs have a direct effect on T$_h$ cells without the interaction of lymphocytes, other than T cells.
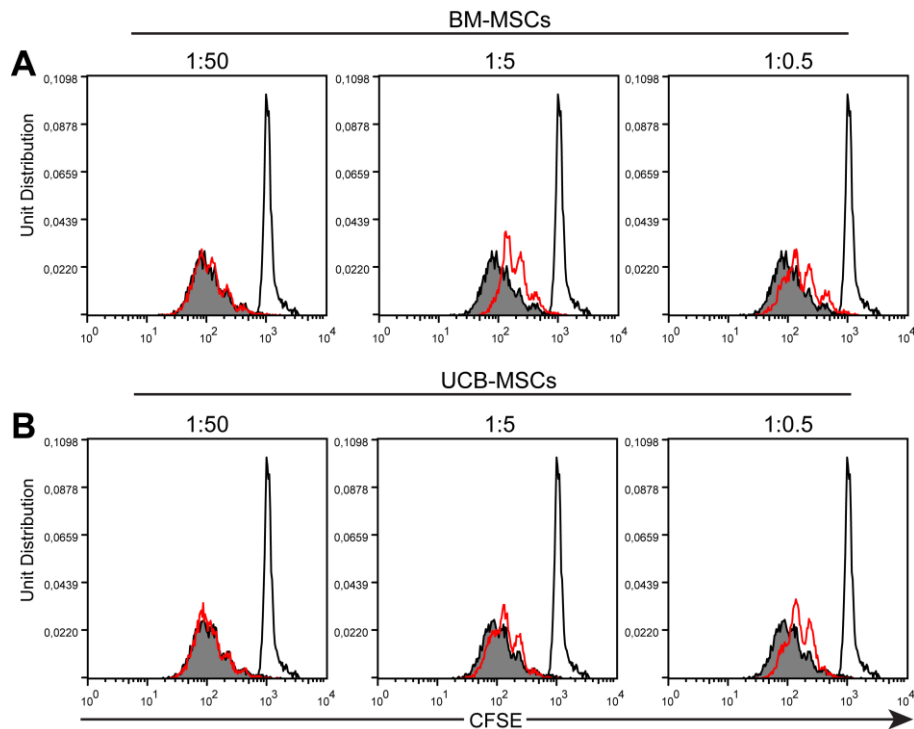
Fig. 38| **BM-MSCs and UCB-MSCs showed a cell density-dependent inhibition of T_h cell proliferation in a CFSE-based cell division tracking system.** CFSE-stained CD25-depleted naive T_h cells ($5x10^4$ cells/well; purity > 96%) were stimulated with αCD3/CD28-coated beads (bead-cell ratio = 1:1) and cultured with or without irradiated BM-MSCs and UCB-MSCs at different ratios (MSC:T cell ratios ranging from 1:50-1:0.5). Cells were harvested on day 4 and CFSE dilution was measured by flow cytometry. **A|** Low cell numbers of BM-MSCs did not alter the proliferation of T_h cells after stimulation (red histogram), compared with T_h cell proliferation without coculture (grey histogram), whereas increasing BM-MSC:T cell ratios resulted in a clear shift of the T_h cell division profile from coculture towards the unstimulated T_h cell fraction (black peak on the very right). **B|** UCB-MSCs showed a similar effect with increasing cell densities. Data are representative of two individual experiments performed with two different blood donors. Every setting was done in triplicates.

5.2.8   Supernatants from BM-MSC and UCB-MSC cultures do not inhibit T_h cell proliferation

In addition to coculture assays, supernatants were analyzed, to investigate a potential immunosuppressive role of soluble factors that are constitutively secreted by MSCs. For this purpose, supernatants from BM-MSCs and UCB-MSCs that were cultured at different cell densities in round-bottom 96-well plates, were harvested after 24 hours and transferred into a new mictotiter plate. CD25-depleted naive T_h cells were stained with CFSE, added ($5x10^4$ cells/well) to the supernatants, stimulated with αCD3/CD28-coated beads and cultured for 4 days. Again, proliferating T cells without supernatants were displayed as grey histograms, whereas red lines represent T cell proliferation with supernatants. The black peak on the very right shows unstimulated T cells. We found that supernatants from BM-MSCs and UCB-MSCs showed no or only marginal effects on T_h cell proliferation (**Fig. 39| A| B|**). This confirmed data published by other groups[128, 131, 212], that endorse the assumption that an interaction between T cells and MSCs is required for the secretion of soluble factors involved in T cell inhibition.
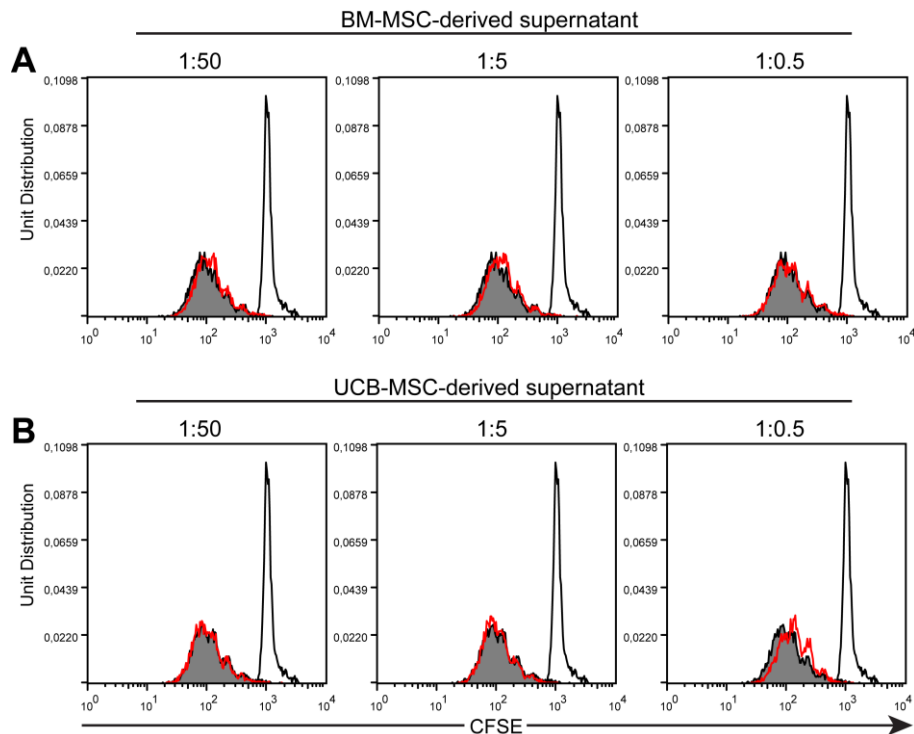
Fig. 39| **Soluble factors that might be involved in immunosuppression of T cell proliferation are not constitutively expressed by MSCs.** CFSE-stained, CD25-depleted, naive T_h cells were cultured with supernatants of **A|** BM-MSCs and **B|** UCB-MSCs (100 µl supernatant of $1x10^3$, $1x10^4$ and $1x10^5$ MSCs/well, harvested after 24 hours) and stimulated with αCD3/CD28-coated beads. After 4 days, T_h cells were harvested and analyzed by flow cytometry. Medium derived from any cell density of BM-MSCs and UCB-MSCs did not suppress T cell proliferation. Shown is one representative experiment out of two.

5.2.9 BM-MSCs increase the differentiation of CD25-depleted naive T_h cells into Tregs upon stimulation with αCD3/CD28-coated beads

Next we wanted to test, whether FoxP3$^+$ T cells are also induced when CD25$^+$ lymphocytes were depleted prior to the enrichment process. Highly purified, naive T_h cells were cultured with or without BM-MSCs and stimulated with αCD3/CD28-coated beads or left unstimulated for 4 days. After coculture with BM-MSCs, CD4$^+$FoxP3$^+$ T cells increased slightly compared with stimulated T_h cells alone (**Fig. 40|**). Surprisingly, stimulation of naive T_h cells with αCD3/CD28-coated beads induced the expression of FoxP3 confirming recently published results from other groups, concerning the development of nTregs in the thymus of rodents and humans[26]. Nevertheless, BM-MSCs were again able to marginally elevate the percentage of FoxP3$^+$CD4$^+$ T cells, though not significant, suggesting an enhanced differentiation towards the regulatory phenotype upon cell contact.
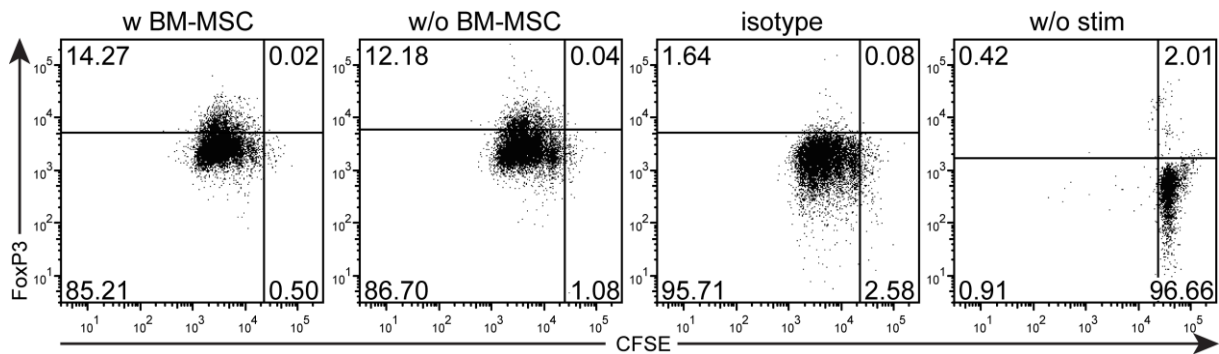
Fig. 40| BM-MSCs marginally increase the percentage of FoxP3$^+$ T cells in CD25-depleted naive T$_h$ cells. CFSE-stained CD25-depleted, naive T$_h$ cells (5x10^4 cells/well) were cultured with or without BM-MSCs (1x10^3 cells/well) and stimulated with αCD3/CD28-coated beads for 4 days. Compared with the isotype control, unstimulated T cells expressed almost no FoxP3, whereas stimulation of these cells enhanced the percentage of CD3$^+$CD4$^+$CD25$^+$FoxP3$^+$ cells. The percentage of these cells with a regulatory phenotype slightly, but not significantly, increased upon coculture with BM-MSCs. Shown is one representative experiment out of two.

5.2.10 Significant induction of FoxP3 expression in CD25-depleted naive T$_h$ cells upon coculture with plastic-adherent dermal cells and stimulation with αCD3/CD28-coated beads

As we found in previous experiments an inhibitory activity of plastic-adherent dermal cells on the proliferation of T cells, which was comparable with the activity of BM- and UCB-MSCs, we asked whether also dermal cells have the potential to enhance FoxP3 expression in naive CD25-depleted T$_h$ cells. For this purpose, total dermal cells from two donors were preselected for plastic-adherence, subsequently seeded at low cell densities (1x10^3 cells/well) and cocultured with CD25-depleted naive T$_h$ cells that were stimulated with αCD3/CD28-coated beads for 4 days. As negative control, we used HEK 293 cells. Dermal cells, but not HEK 293 cells, were able to significantly increase the percentage of FoxP3-expressing T$_h$ cells compared with stimulated T cells alone (**Fig. 41|**). Again, the simultaneous engagement of the TCR complex and CD28 lead to a more than 50% increase of FoxP3 in stimulated cells compared with T cells without stimulation. The elevated induction of FoxP3 by dermal cells was similar to BM-MSCs, favoring the idea of a related pathway.
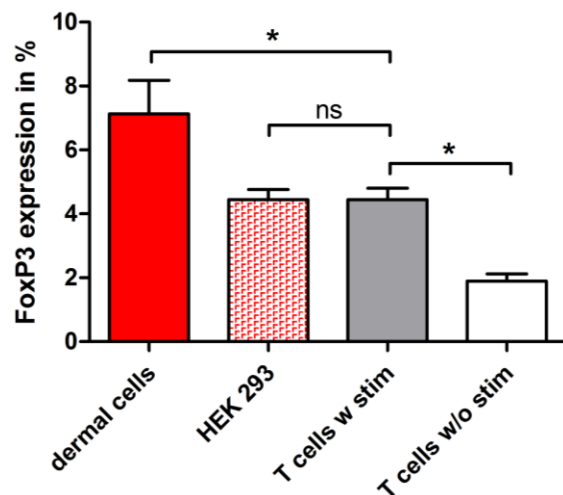
Fig. 41| Adherent dermal cells enhance the expression of FoxP3 in initially naive T$_h$ cells stimulated with αCD3/CD28-coated beads. Plastic-adherent total dermal cells from two different donors were cocultured with CFSE-stained, CD25-depleted naive T$_h$ cells at a ratio of 1:50. T cells were stimulated with αCD3/CD28-coated beads and analyzed on day 4 by flow cytometry. FoxP3 expression in percent was determined by counterstaining with an αFoxP3-AF$_{647}$ mAb and specificity was confirmed with an isotype matched control. Shown is the mean expression of triplicates from two skin donors.

5.2.11 Total dermal cells and different dermal MSC subsets are able to induce FoxP3 in naive T_h cells without activation of the CD28-driven costimulatory pathway

For a long time scientists are debating the need of the engagement of costimulatory receptors like CD28. While data have been shown suggesting that costimulation is just an enhancer of the TCR signal and does not activate an independent signal transduction cascade[7], other studies have reported that anergy or even apoptosis is induced in the absence of the CD28-mediated costimulatory signal[213, 214]. Further, it has been shown that CD28 ligation on naive T_h cells in vitro promotes the differentiation towards the T_h2 lineage[215, 216] and that the costimulatory signal is essential for the differentiation of Tregs from naive T_h cells in the thymus[217] and their survival and homeostasis in the periphery. To further investigate potential effects of dermal MSCs on the differentiation of naive T_h cells towards the regulatory phenotype, we stimulated isolated T_h cells without provision of a prominent costimulatory signal and thereby created an environment that is independent of well known costimulatory side-effects, as dermal cells and BM-MSCs lack the expression of CD80 or CD86. For this purpose, low numbers of irradiated total dermal cells, enriched dermal MSC subsets and, as a control, BM-MSCs were seeded into each well of αCD3-coated 96-well plates and cocultured with CFSE-stained, CD25$^-$ naive T_h cells for 5 days (MSC:T cell ratio = 1:50). In **Fig. 42|** one representative experiment is shown, where skin cells were enriched with regard to their expression of CD90, CD271 and CD73, to test whether different subsets may induce different percentages of FoxP3$^+$ T cells. First, it is important to mention that in all experiments performed, the depletion of CD25$^+$ cells was highly successful, with residual CD25$^+$ cell numbers below 0.7%. The lack of CD28 ligation led to a low proliferative response and minute numbers of FoxP3-expressing T cells. (**Fig. 42| B|**, T cells w/o stim). Coculture with BM-MSCs, dermal cells and dermal subtypes induced a proliferation of T cells, even though no costimulatory signals were provided. Total dermal cells were able to induce more than 18% FoxP3$^+$ T cells in initially naive T_h cells (**Fig. 42| A|**, upper left dot plot) compared with stimulated or unstimulated T cells alone (**Fig. 42| B|**). Unexpectedly, BM-MSCs were able to induce similar numbers of FoxP3$^+$ T cells (~18%). A comparison of the different dermal MSC subtypes revealed a tendency for CD90$^+$ dermal cells to induce more FoxP3$^+$ T cells than the CD90$^-$ cell fraction (**Fig. 42| A|**, 20.75% versus 9.74%). In contrast, a comparison of CD271$^+$ with CD271$^-$ dermal cells revealed that CD271$^-$ cells induced more FoxP3$^+$ T cells than the positive fraction (11.38% versus 8.11%). Evaluation of potential differences between CD73$^+$ and CD73$^-$ cells showed no trend as data varied among the different experiments performed (**Fig. 42| C|**). It is essential to mention that T_h cells from every coculture setting had the same number of division cycles (**Fig. 42| A| C|**, histogram overlays). This is one of the most important facts for the numerical comparison of changes in expression profiles.
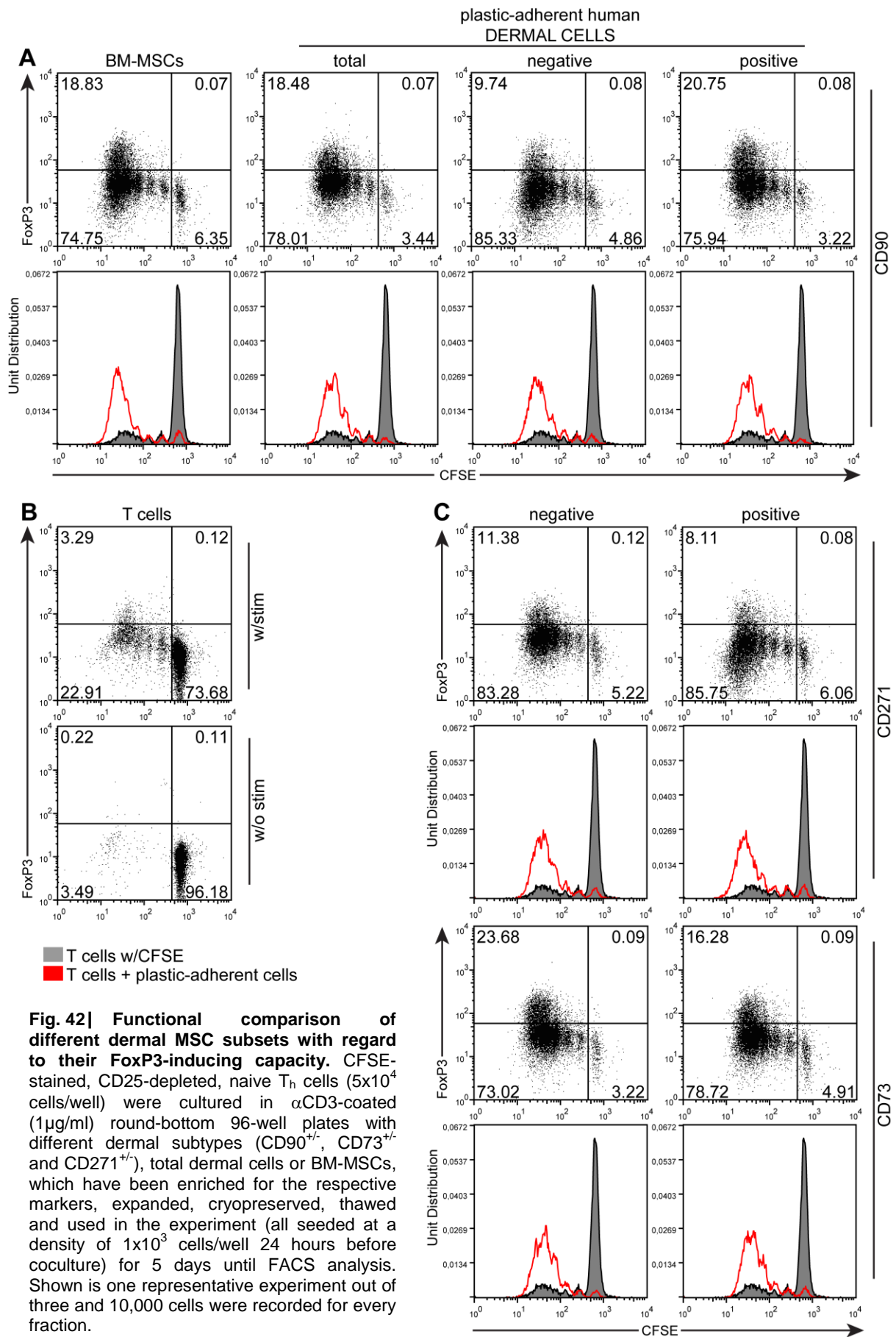
Fig. 42| Functional comparison of different dermal MSC subsets with regard to their FoxP3-inducing capacity. CFSE-stained, CD25-depleted, naive T_h cells (5×10^4 cells/well) were cultured in αCD3-coated (1μg/ml) round-bottom 96-well plates with different dermal subtypes (CD90$^{+/-}$, CD73$^{+/-}$ and CD271$^{+/-}$), total dermal cells or BM-MSCs, which have been enriched for the respective markers, expanded, cryopreserved, thawed and used in the experiment (all seeded at a density of 1×10^3 cells/well 24 hours before coculture) for 5 days until FACS analysis. Shown is one representative experiment out of three and 10,000 cells were recorded for every fraction.

Statistical analysis of all experiments performed, revealed that total dermal cells significantly increased FoxP3 expression from a value of 4.09%±1.26 in stimulated T cells alone, to 15.36%±1.81 after coculture (P<0.01, n=7; **Fig. 43|**), whereas BM-MSCs induced 10.98%±2.0 FoxP3$^+$ T cells (P<0.05, n=6). Moreover, we found that CD90$^+$ dermal cells were twice as potent to induce FoxP3 compared with CD90$^-$ cells (19.14%±4.02 vs. 8.11%±1.70, n=3). CD271$^-$ dermal cells, on the contrary, showed a higher, though not significant, FoxP3-inducing capacity than CD271$^+$ dermal cells (14.56%±2.54 vs. 9.62%±2.56, n=3). The comparison of the inducing capacity of CD73$^{+/-}$ cells showed a huge variability and no tendency was recognizable. With this data we could show for the first time that total dermal cells induce T cells with a regulatory phenotype, dependent on the phenotype of the MSC subset and independent of the external provision of αCD28. In preliminary experiments, we could eliminate possible sterical hindrance and validated the induction of FoxP3 through dermal cells in the absence of CD28-ligation, using αCD3-coated beads (data not shown).
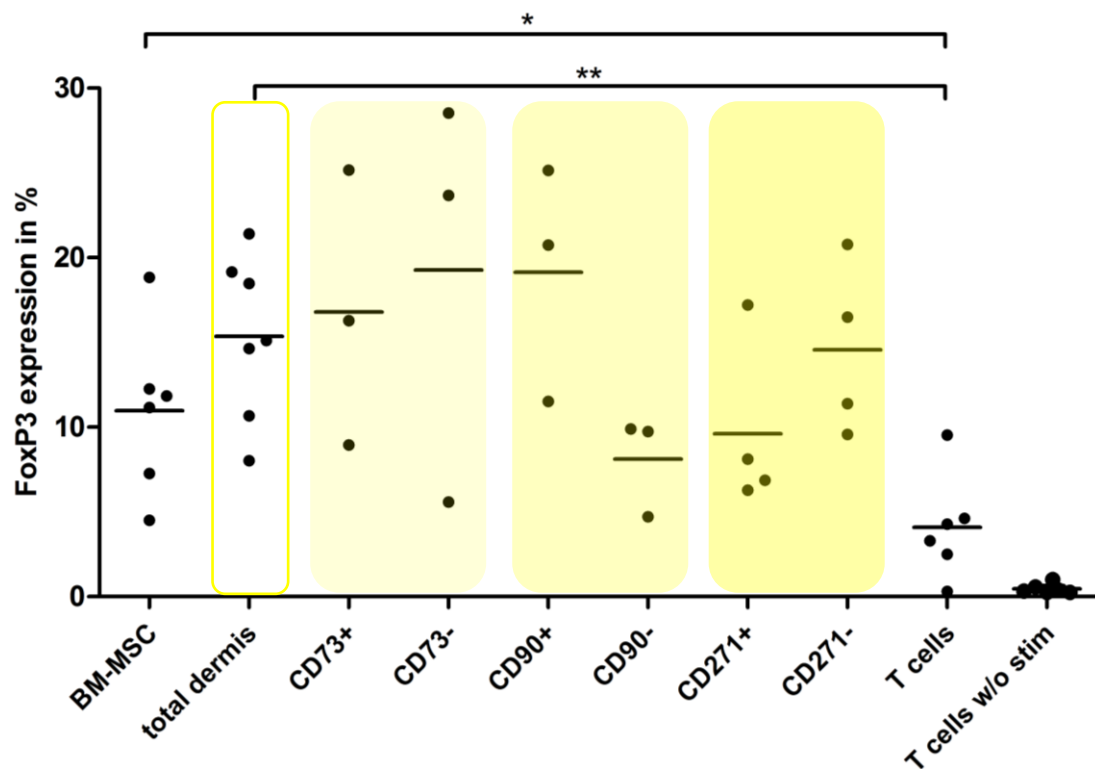
Fig. 43| **FoxP3-expressing capacity of total dermal cells, dermal MSC subsets and BM-MSCs.** Statistical analysis of individual experiments with different skin and T cell donors, revealed a high potency of total dermal cells to induce FoxP3 in initially naive T$_h$ cells without provision of costimulatory molecules. Comparisons of the different dermal subtypes showed a tendency for CD90$^+$ cells to induce more FoxP3 than CD90$^-$ cells and a higher percentage of FoxP3$^+$ T cells upon coculture with CD271$^-$ cells, compared with CD271$^+$ cells, though not significant. A Mann-Whitney-U test was used to evaluate significant differences between study and control groups. P<0.05 (*) was considered significant, whereas P<0.01 (**) was considered as highly significant.

6   Discussion

Undifferentiated stem cells in post-natal tissues are thought to be responsible for the regeneration of injured tissues and the replacement of damaged cells in adult organisms[81, 218]. Human skin, especially the dermis, has been reported to harbor a reservoir of resident MSCs, which possess the plasticity to differentiate towards several lineages[219] and express a comprehensive marker panel, similar to BM-MSCs. The fact that most studies investigated dermal MSCs, which were isolated from hair follicles and the dermal papilla, distincts our project, as our aim was the in situ localization and functional characterization of non-follicular dermal MSC subsets in glabrous skin.

Immunofluorescence in situ analysis of common MSC makers, like CD73, CD90, CD105 and CD271 demonstrated the dermal occurrence of cells expressing these markers. In human skin, an increase of CD271-expressing cells correlates with scar formation, which promotes the idea of a tissue-resident stem cell reservoir for tissue regeneration[220]. With immunofluorescence triple staining, we could verify flow cytometric data showing that (i) around 50% of CD271-expressing cells are positive for CD90, (ii) all CD271$^+$ cells are positive for CD73 and (iii) the majority of CD73$^+$ cells are CD90$^+$. Further, few cells triple positive for all three markers could be identified in the papillary dermis, as well as in the deep dermis, which endorses the hypothesis of a scattered distribution of dermal MSCs in adult tissues, like skin[221]. To better characterize the nature of CD271$^+$ cells, we performed triple staining including the markers CD34 and Col-IV. Although, it has been reported that some MSCs coexpress the HSC marker CD34, which also stains capillaries in adult dermis[187], no CD271$^+$CD34$^+$ cells were detected in dermal sheet preparations. CD271$^+$ cells seemed to preferentially colocalize with cells positive for CD34. Recently, it was found that human ESC-derived CD34$^+$ cells, can differentiate into cells displaying a MSC phenotype, with simultaneous downregulation of CD34[188]. This would suggest, that MSCs in human skin resemble a more terminally differentiated type of progenitor cell, which is also reflected by the passage-induced senescence of human MSCs after approximately 40 population doublings[222]. Interestingly, we could identify several CD271$^+$ cells that coexpressed Col-IV, which is known to specifically stain the basement membranes of blood vessels, lymphatics and the peripheral nervous system, and colocalized in deep dermis with cells expressing CD34. Few studies have reported the expression of Col-IV in MSCs[223, 224], all of them dealing with bone marrow-derived cells. Although Col-IV expression in healthy human skin and skin tumors has been already reported[189, 190], the presence of CD271$^+$Col-IV$^+$ cells in human skin, is novel to our knowledge. Our findings strongly suggest a perivascular location of dermal MSCs and support the hypothesis for BM-MSCs that have been found to form a unique perivascular niche[110, 138, 225] as well.

Investigating the morphology of plastic adherent dermal cells at the single-cell level, we found that they display a typical fibroblastoid appearance. They highly expressed CD73, CD90 and CD105, which confirmed previous flow cytometric data[219]. Few adherent cells also expressed α-SMA, an actin isoform typical for smooth muscle cells in vascular walls, especially in the cytoplasm of pericytes[226]. Evidence, however, has been provided that mesenchymal progenitor cells of different origins can also express this marker[227]. Surprisingly, the transcription factor Oct-4, the master regulator of self-renewal in undifferentiated ESCs[228], was also expressed in a few adherent dermal cells. Although the selected Ab stains both slicing products, namely Oct-4A, which is specific for ESCs and Oct-4B that is expressed in many other cells too, our data favor the existence of somatic multipotent progenitor cell populations within the skin. This hypothesis is supported by our observation that just the nuclei were positive for Oct-4, whereas the unspecific factor Oct-4B is mainly localized in the cytoplasm[229]. The two different morphologies of cultured CD271$^+$ cells, on the one hand fibroblastoid, but on the other hand almost neuronal/glial-like persuaded us to investigate in situ, possible correlations with neural crest-derived cells.

Double staining with a CD56 mAb confirmed the expression of CD271 and CD56 on peripheral nerve endings in the dermis[164, 230]. MSCs that express CD271 in combination with CD56 have also been found in human bone marrow and are thought to resemble a distinct subtype of MSCs with high clonogenicity[106, 201]. However, CD271 is also known to be a marker for migrating neural crest-derived Schwann cell progenitors and has been reported to be coexpressed with CD56 in early Schwann cell development during scar formation[220]. Together with the finding that Schwann cells can differentiate into α-SMA-expressing myofibroblasts, this allows the assumption that neural crest progenitors and MSCs from peripheral tissues share more features than initially thought. Further, BM-MSCs are believed to have a neural predisposition[194], and have been reported to express neuronal markers, like β-III-tubulin, which is mainly expressed in neurons of the peripheral and central nervous system, but was also found to be a general component of the mitotic spindle of various cell types[193], or glial markers, like GFAP. We showed the existence of CD271$^+\beta$-III-tubulin$^+$ cells and CD271$^+$GFAP$^+$ cells within the dermis, and a preferred colocalisation of CD271$^+$ cells to cells expressing these neuronal/glial markers. Thus, our data indicate that dermal MSC subtypes and pericytes are related cells[231]. The close association of dermal MSCs to skin vasculature, in combination with the expression of adhesion proteins, like CD90, which allow the interaction with endothelial cells[133], and the expression of the pericyte specific marker α-SMA, supports our hypothesis. The successful isolation of MSCs from the subendothelial area of the umbilical vein[232, 233], support our conclusion. The fact that both, pericytes[234] and BM-MSCs express CD271[231], strongly suggests that these cells derive from a common ancestor[231], maybe originating from the neural crest, which harbors migratory cells showing

multipotency before and after migration[235]. The close vicinity to endothelial cells also suggests a facilitated interaction of MSCs with circulating lymphocytes from the blood stream, with an enhanced probability of immunomodulatory activities in situ. The absence of HLA-DR expression and the lack of costimulatory molecules, like CD80/86, renders dermal MSCs hypo-immunogeneic.

Using a CFSE-based division tracing coculture system, which has been adapted for our experiments during this thesis, we were able to confirm the suppressive activity of plastic-adherent dermal cells[148, 167, 236] and allogeneic BM-MSCs on total T cell proliferation, stimulated via αCD3/CD28-coated beads. In accordance with other studies[148, 167], we found a cell density-dependent inhibition of T cell proliferation by plastic-adherent dermal cells, starting at ratios around 1:10 (dermal cell:T cell) and showing strong T cell inhibition at the ratio 1:5, which was comparable with BM-MSCs[111]. Interestingly, low numbers of dermal cells and BM-MSCs (ratio=1:50) seemed to have no effect on T cell proliferation and even had stimulating activity. This enhancement of lymphocyte proliferation with low numbers of BM-MSCs has been reported previously[204] for ratios lower than 1:10[236], in allogeneic, mitogenic or interleukin-induced proliferation models[211]. Regarding CD8$^+$ and CD4$^+$ T cells, low numbers of BM-MSCs (ratio=1:50) in combination with the addition of IL-2, IL-7 and IL-15 has been reported to significantly enhance lymphocyte proliferation. As IL-2, in combination with TCR complex stimulation, is known to be suitable for the efficient clonal expansion of Tregs[49] and IL-7 and IL-15 are also involved in the development and function of Tregs[49], the observed increase of lymphocyte proliferation might be based on proliferating Tregs. In line with this idea is the finding that human dermal fibroblasts promote the proliferation of FoxP3$^+$ Tregs upon addition of soluble IL-2 and IL-15[237]. Numerous studies, dealing with the effect of MSCs on Tregs, are enhancing the perception that MSCs from bone marrow and other tissues recruit, regulate and expand Tregs[128, 129]. We could show via analysis of the CFSE dilution profile and counterstaining of FoxP3 that FoxP3$^+$ T cells strongly increase upon coculture with BM-MSCs, which suggests a possible role of Tregs in T cell inhibition. With our data we confirmed the results from other groups, which used total PBMCs, total T cells, CD4$^+$ and CD8$^+$ T cells[129]. As we were interested whether nTregs are induced to multiply by MSCs or whether naive T_h cells are induced to differentiate towards a regulatory phenotype, highly enriched CD25-depleted, naive T_h cells were cocultured with BM- and UCB-MSCs. Even highly purified T cells were clearly inhibited in their proliferation upon coculture with BM- and UCB-MSCs. As we could not see any effect with conditioned media from cultured BM- or UCB-MSCs, we propose that the inhibition is based on a cross-talk between T cells and MSCs. Hence, possible soluble factors are not secreted constitutively. Analysis of the possible induction of FoxP3 revealed that stimulation with αCD3/CD28 alone induced the expression of FoxP3 in initially CD25-depleted naive T_h cells. Coculture with dermal cells or BM-MSCs, however, slightly but not significantly increased the percentage of

FoxP3$^+$ T cells. The role of CD28 signaling for the generation of nTregs in the thymus and for Treg survival and homeostasis in the periphery has been demonstrated for mice[217] and humans[238]. Although, CD28 ligation via CD80 or CD86 is not obligatory for the induction of effector T cell proliferation, it has been shown that additional costimulatory signals generally enhance and fasten T cell activation, proliferation, cytokine production, survival and up-regulate anti-apoptotic proteins, which leads to more vigorous T cell responses[239]. In contrast, it has been shown for Tregs to have different costimulatory requirements than effector T cells, as postthymic Tregs depend on signals induced by CD28 ligation to expand and maintain their function[238]. We could show that only low numbers of CD25-depleted naive T$_h$ cells enter the cell division cycle upon stimulation with αCD3 only, whereas the percentage of dividing cells decreased with increasing purity of naive T$_h$ cells. Interestingly, we found a strong induction of T cell proliferation upon coculture with total dermal cells, dermal subsets and BM-MSCs, although these cells lack the expression of CD80 and CD86. Using counterstaining of FoxP3 in CFSE-labeled initially FoxP3$^-$CD25$^-$CD4$^+$ T cells, we were able to visualize the induction of FoxP3 expression upon coculture with dermal cells and BM-MSCs. The finding that dermal cells had a higher inducing capacity than BM-MSCs, suggests an important role of dermal cells in the peripheral generation of iTregs. One of the most prominent candidates for the substitution of CD28 in the generation of Tregs, is TGF-β. It was shown in multiple in vitro experiments that TGF-β, together with a stimulus for the TCR complex, is a potent trigger for FoxP3-induction. For our in vitro system, we can exclude that dermal cells produce this growth factor, as we showed previously that TGF-β is primarily expressed in the epidermis and practically absent in human dermis[240]. Nevertheless, the induction of TGF-β expression in dermal cells upon coculture with T cells cannot be excluded, but signals induced through CD28-ligation are still vital for the survival and maintainance of Tregs[241]. Further, one can speculate that CD80 or CD86 expression could be induced upon coculture with T cells, which we were able to refute in preliminary experiments (data not shown). However, the question whether these FoxP3$^+$ T cells are functionally equivalent to nTregs remains and still has to be elucidated.

In summary, we showed the in vivo identity of dermal MSC subsets, preferentially located close to the skin vasculature, suggesting their homing in a perivascular niche. This would allow dermal MSCs to directly interact with lymphocytes. Moreover, we demonstrated new insights in peripheral Treg generation through dermal cells and could show a trend towards dermal subtypes, to induce more FoxP3 expression than others. This strongly suggests a homeostasis-driven proliferative response induced by the interaction of naive T$_h$ cell with self-peptide-presenting APCs in the periphery[242-245] with simultaneous induction of FoxP3 by local tissue MSCs for a rapid induction of Tregs, via bypassing the regulatory checkpoint of CD28 engagement or binding of CD28 through other ligands than CD80/CD86.

7   References

1.) Abul K.Abbas & Andrew H.Lichtman Cellular and Molecular Immunology. W.B. Saunders Company, 5th edition, 2005

2.) Janeway,C.A., Travers,P., Walport,M., & Shlomchik,M.J. Immunobiology. Garland Science Publishing, 6th edition, 2005

3.) Cronin,S.J. & Penninger,J.M. From T-cell activation signals to signaling control of anti-cancer immunity. *Immunol. Rev.* 220: 151-168, 2007

4.) Kabelitz,D. Effector functions and control of human gamma delta T-cell activation. *Microbes. Infect.* 1: 255-261, 1999

5.) Kabelitz,D., Wesch,D., & Hinz,T. Gamma delta T cells, their T cell receptor usage and role in human diseases. *Springer Semin. Immunopathol.* 21: 55-75, 1999

6.) Smith-Garvin,J.E., Koretzky,G.A., & Jordan,M.S. T cell activation. *Annu. Rev. Immunol.* 27: 591-619, 2009

7.) Acuto,O. & Michel,F. CD28-mediated co-stimulation: a quantitative support for TCR signalling. *Nat. Rev. Immunol.* 3: 939-951, 2003

8.) Trickett,A. & Kwan,Y.L. T cell stimulation and expansion using anti-CD3/CD28 beads. *J. Immunol. Methods* 275: 251-255, 2003

9.) Tchilian,E.Z. & Beverley,P.C. Altered CD45 expression and disease. *Trends Immunol.* 27: 146-153, 2006

10.) O'Shea,J.J. & Paul,W.E. Mechanisms underlying lineage commitment and plasticity of helper CD4+ T cells. *Science* 327: 1098-1102, 2010

11.) Mosmann,T.R., Cherwinski,H., Bond,M.W., Giedlin,M.A., & Coffman,R.L. Two types of murine helper T cell clone. I. Definition according to profiles of lymphokine activities and secreted proteins. *J. Immunol.* 136: 2348-2357, 1986

12.) Abbas,A.K., Murphy,K.M., & Sher,A. Functional diversity of helper T lymphocytes. *Nature* 383: 787-793, 1996

13.) Vignali,D.A., Collison,L.W., & Workman,C.J. How regulatory T cells work. *Nat. Rev. Immunol.* 8: 523-532, 2008

14.) Sakaguchi,S., Yamaguchi,T., Nomura,T., & Ono,M. Regulatory T cells and immune tolerance. *Cell* 133: 775-787, 2008

15.) Yamazaki,S. & Steinman,R.M. Dendritic cells as controllers of antigen-specific Foxp3^{+} regulatory T cells. *J. Dermatol. Sci.* 54: 69-75, 2009

16.) Peng,G. Characterization of regulatory T cells in tumor suppressive microenvironments. *Methods Mol. Biol.* 651: 31-48, 2010

17.) Suzuki,M., Konya,C., Goronzy,J.J., & Weyand,C.M. Inhibitory CD8^{+} T cells in autoimmune disease. *Hum. Immunol.* 69: 781-789, 2008

18.) Sakaguchi,S., Miyara,M., Costantino,C.M., & Hafler,D.A. FOXP3^{+} regulatory T cells in the human immune system. *Nat. Rev. Immunol.* 10: 490-500, 2010

19.) Sakaguchi,S. Regulatory T cells: key controllers of immunologic self-tolerance. *Cell* 101: 455-458, 2000

20.) Shevach,E.M. CD4^{+} CD25^{+} suppressor T cells: more questions than answers. *Nat. Rev. Immunol.* 2: 389-400, 2002

21.) Zhang,L. & Zhao,Y. The regulation of Foxp3 expression in regulatory CD4^{+}CD25^{+}T cells: multiple pathways on the road. *J. Cell Physiol* 211: 590-597, 2007

22.) Hori,S., Nomura,T., & Sakaguchi,S. Control of regulatory T cell development by the transcription factor Foxp3. *Science* 299: 1057-1061, 2003

23.) Lal,G. & Bromberg,J.S. Epigenetic mechanisms of regulation of Foxp3 expression. *Blood* 114: 3727-3735, 2009

24.) Kmieciak,M. *et al.* Human T cells express CD25 and Foxp3 upon activation and exhibit effector/memory phenotypes without any regulatory/suppressor function. *J. Transl. Med.* 7: 89, 2009

25.) Liu,W. *et al.* CD127 expression inversely correlates with FoxP3 and suppressive function of human CD4^{+} Treg cells. *J. Exp. Med.* 203: 1701-1711, 2006

26.) Allan,S.E. *et al.* Activation-induced FOXP3 in human T effector cells does not suppress proliferation or cytokine production. *Int. Immunol.* 19: 345-354, 2007

27.) Watanabe,N. *et al.* Hassall's corpuscles instruct dendritic cells to induce CD4^{+}CD25^{+} regulatory T cells in human thymus. *Nature* 436: 1181-1185, 2005

28.) Chen,W. *et al.* Conversion of peripheral CD4^{+}CD25^{-} naive T cells to CD4^{+}CD25^{+} regulatory T cells by TGF-beta induction of transcription factor Foxp3. *J. Exp. Med.* 198: 1875-1886, 2003

29.) Akbar,A.N., Taams,L.S., Salmon,M., & Vukmanovic-Stejic,M. The peripheral generation of CD4^{+} CD25^{+} regulatory T cells. *Immunology* 109: 319-325, 2003

30.) Bluestone,J.A. & Abbas,A.K. Natural versus adaptive regulatory T cells. *Nat. Rev. Immunol.* 3: 253-257, 2003

31.) Apostolou,I. & von,B.H. In vivo instruction of suppressor commitment in naive T cells. *J. Exp. Med.* 199: 1401-1408, 2004

32.) Kretschmer,K. *et al.* Inducing and expanding regulatory T cell populations by foreign antigen. *Nat. Immunol.* 6: 1219-1227, 2005

33.) Taams,L.S. & Akbar,A.N. Peripheral generation and function of CD4^{+}CD25^{+} regulatory T cells. *Curr. Top. Microbiol. Immunol.* 293: 115-131, 2005

34.) Lohr,J., Knoechel,B., & Abbas,A.K. Regulatory T cells in the periphery. *Immunol. Rev.* 212: 149-162, 2006

35.) Apostolou,I. *et al.* Peripherally induced Treg: mode, stability, and role in specific tolerance. *J. Clin. Immunol.* 28: 619-624, 2008

36.) Yamazaki,S. *et al.* Effective expansion of alloantigen-specific Foxp3^{+} CD25^{+} CD4^{+} regulatory T cells by dendritic cells during the mixed leukocyte reaction. *Proc. Natl. Acad. Sci. U. S. A* 103: 2758-2763, 2006

37.) Yamazaki,S. *et al.* Dendritic cells are specialized accessory cells along with TGF- for the differentiation of Foxp3^{+} CD4^{+} regulatory T cells from peripheral Foxp3 precursors. *Blood* 110: 4293-4302, 2007

38.) Curotto de Lafaille,M.A., Lino,A.C., Kutchukhidze,N., & Lafaille,J.J. CD25^{-} T cells generate CD25^{+}Foxp3^{+} regulatory T cells by peripheral expansion. *J. Immunol.* 173: 7259-7268, 2004

39.) Liang,S. *et al.* Conversion of CD4^{+} CD25^{-} cells into CD4^{+} CD25^{+} regulatory T cells in vivo requires B7 costimulation, but not the thymus. *J. Exp. Med.* 201: 127-137, 2005

40.) Walker,M.R., Carson,B.D., Nepom,G.T., Ziegler,S.F., & Buckner,J.H. De novo generation of antigen-specific CD4^{+}CD25^{+} regulatory T cells from human CD4^{+}. *Proc. Natl. Acad. Sci. U. S. A* 102: 4103-4108, 2005

41.) Furtado,G.C., Curotto de Lafaille,M.A., Kutchukhidze,N., & Lafaille,J.J. Interleukin 2 signaling is required for CD4^{+} regulatory T cell function. *J. Exp. Med.* 196: 851-857, 2002

42.) Fontenot,J.D., Rasmussen,J.P., Gavin,M.A., & Rudensky,A.Y. A function for interleukin 2 in Foxp3-expressing regulatory T cells. *Nat. Immunol.* 6: 1142-1151, 2005

43.) Setoguchi,R., Hori,S., Takahashi,T., & Sakaguchi,S. Homeostatic maintenance of natural Foxp3^{+} CD25^{+} CD4^{+} regulatory T cells by interleukin (IL)-2 and induction of autoimmune disease by IL-2 neutralization. *J. Exp. Med.* 201: 723-735, 2005

44.) Wolf,M., Schimpl,A., & Hunig,T. Control of T cell hyperactivation in IL-2-deficient mice by CD4^{+}CD25^{-} and CD4^{+}CD25^{+} T cells: evidence for two distinct regulatory mechanisms. *Eur. J. Immunol.* 31: 1637-1645, 2001

45.) Malek,T.R. & Bayer,A.L. Tolerance, not immunity, crucially depends on IL-2. *Nat. Rev. Immunol.* 4: 665-674, 2004

46.) Sakaguchi,S., Wing,K., & Miyara,M. Regulatory T cells - a brief history and perspective. *Eur. J. Immunol.* 37 Suppl 1: S116-S123, 2007

47.) Lin,S.J., Cheng,P.J., & Hsiao,S.S. Effect of interleukin-15 on effector and regulatory function of anti-CD3/anti-CD28-stimulated CD4^{+} T cells. *Bone Marrow Transplant.* 37: 881-887, 2006

48.) Imamichi,H., Sereti,I., & Lane,H.C. IL-15 acts as a potent inducer of CD4^{+}CD25^{hi} cells expressing FOXP3. *Eur. J. Immunol.* 38: 1621-1630, 2008

49.) Rochman,Y., Spolski,R., & Leonard,W.J. New insights into the regulation of T cells by gamma(c) family cytokines. *Nat. Rev. Immunol.* 9: 480-490, 2009

50.) Xia,J., Liu,W., Hu,B., Tian,Z., & Yang,Y. IL-15 promotes regulatory T cell function and protects against diabetes development in NK-depleted NOD mice. *Clin. Immunol.* 134: 130-139, 2010

51.) Jurgens,B., Hainz,U., Fuchs,D., Felzmann,T., & Heitger,A. Interferon-gamma-triggered indoleamine 2,3-dioxygenase competence in human monocyte-derived

dendritic cells induces regulatory activity in allogeneic T cells. *Blood* 114: 3235-3243, 2009

52.) Brenk,M. *et al.* Tryptophan deprivation induces inhibitory receptors ILT3 and ILT4 on dendritic cells favoring the induction of human CD4$^+$CD25$^+$ Foxp3$^+$ T regulatory cells. *J. Immunol.* 183: 145-154, 2009

53.) Housley,W.J. *et al.* PPARgamma regulates retinoic acid-mediated DC induction of Tregs. *J. Leukoc. Biol.* 86: 293-301, 2009

54.) Benson,M.J., Pino-Lagos,K., Rosemblatt,M., & Noelle,R.J. All-trans retinoic acid mediates enhanced Treg cell growth, differentiation, and gut homing in the face of high levels of co-stimulation. *J. Exp. Med.* 204: 1765-1774, 2007

55.) Mucida,D. *et al.* Reciprocal TH17 and regulatory T cell differentiation mediated by retinoic acid. *Science* 317: 256-260, 2007

56.) Sun,C.M. *et al.* Small intestine lamina propria dendritic cells promote de novo generation of Foxp3 T reg cells via retinoic acid. *J. Exp. Med.* 204: 1775-1785, 2007

57.) Coombes,J.L. *et al.* A functionally specialized population of mucosal CD103$^+$ DCs induces Foxp3$^+$ regulatory T cells via a TGF-beta and retinoic acid-dependent mechanism. *J. Exp. Med.* 204: 1757-1764, 2007

58.) Curotto de Lafaille,M.A. & Lafaille,J.J. Natural and adaptive Foxp3$^+$ regulatory T cells: more of the same or a division of labor? *Immunity.* 30: 626-635, 2009

59.) Ramalho-Santos,M. & Willenbring,H. On the origin of the term "stem cell". *Cell Stem Cell* 1: 35-38, 2007

60.) Majeti,R., Park,C.Y., & Weissman,I.L. Identification of a hierarchy of multipotent hematopoietic progenitors in human cord blood. *Cell Stem Cell* 1: 635-645, 2007

61.) NIH. NIH Stem Cell Information Home Page. 29-9-0010
HP: http://stemcells.nih.gov/index

62.) Robertson,J.A. Embryo stem cell research: ten years of controversy. *J. Law Med. Ethics* 38: 191-203, 2010

63.) Thomson,J.A. *et al.* Embryonic stem cell lines derived from human blastocysts. *Science* 282: 1145-1147, 1998

64.) Takahashi,K. *et al.* Induction of pluripotent stem cells from adult human fibroblasts by defined factors. *Cell* 131: 861-872, 2007

65.) Takahashi,K. & Yamanaka,S. Induction of pluripotent stem cells from mouse embryonic and adult fibroblast cultures by defined factors. *Cell* 126: 663-676, 2006

66.) Knoepfler,P.S. Deconstructing stem cell tumorigenicity: a roadmap to safe regenerative medicine. *Stem Cells* 27: 1050-1056, 2009

67.) Gutierrez-Aranda,I. *et al.* Human induced pluripotent stem cells develop teratoma more efficiently and faster than human embryonic stem cells regardless the site of injection. *Stem Cells* 28: 1568-1570, 2010

68.) Zwaka,T.P. Stem cells: Troublesome memories. *Nature* 467: 280-281, 2010

69.) Afanasyyev,B.V., Elstner,E.E., & Zander,A.R. A. J. Friedenstein, founder of the mesenchymal stem cell concept. *Cellular Therapy and Transplantation* 1: 35-38, 2009

70.) Ren,G. *et al.* Mesenchymal stem cell-mediated immunosuppression occurs via concerted action of chemokines and nitric oxide. *Cell Stem Cell* 2: 141-150, 2008

71.) Caplan,A.I. Mesenchymal stem cells. *J. Orthop. Res.* 9: 641-650, 1991

72.) Kopen,G.C., Prockop,D.J., & Phinney,D.G. Marrow stromal cells migrate throughout forebrain and cerebellum, and they differentiate into astrocytes after injection into neonatal mouse brains. *Proc. Natl. Acad. Sci. U. S. A* 96: 10711-10716, 1999

73.) Sanchez-Ramos,J. *et al.* Adult bone marrow stromal cells differentiate into neural cells in vitro. *Exp. Neurol.* 164: 247-256, 2000

74.) Lee,K.D. *et al.* In vitro hepatic differentiation of human mesenchymal stem cells. *Hepatology* 40: 1275-1284, 2004

75.) Young,H.E. *et al.* Mesenchymal stem cells reside within the connective tissues of many organs. *Dev. Dyn.* 202: 137-144, 1995

76.) da Silva,M.L., Chagastelles,P.C., & Nardi,N.B. Mesenchymal stem cells reside in virtually all post-natal organs and tissues. *J. Cell Sci.* 119: 2204-2213, 2006

77.) Krampera,M. *et al.* Induction of neural-like differentiation in human mesenchymal stem cells derived from bone marrow, fat, spleen and thymus. *Bone* 40: 382-390, 2007

78.) Gallo,R. *et al.* Generation and expansion of multipotent mesenchymal progenitor cells from cultured human pancreatic islets. *Cell Death. Differ.* 14: 1860-1871, 2007

79.) Chamberlain,G., Fox,J., Ashton,B., & Middleton,J. Concise review: mesenchymal stem cells: their phenotype, differentiation capacity, immunological features, and potential for homing. *Stem Cells* 25: 2739-2749, 2007

80.) Wang,X.Y. *et al.* Identification of mesenchymal stem cells in aorta-gonad-mesonephros and yolk sac of human embryos. *Blood* 111: 2436-2443, 2008

81.) Valtieri,M. & Sorrentino,A. The mesenchymal stromal cell contribution to homeostasis. *J. Cell Physiol* 217: 296-300, 2008

82.) Ponte,A.L. *et al.* The in vitro migration capacity of human bone marrow mesenchymal stem cells: comparison of chemokine and growth factor chemotactic activities. *Stem Cells* 25: 1737-1745, 2007

83.) Uccelli,A., Moretta,L., & Pistoia,V. Mesenchymal stem cells in health and disease. *Nat. Rev. Immunol.* 8: 726-736, 2008

84.) Dalberto,T.P., Nardi,N.B., & Camassola,M. Mesenchymal stem cells as a platform for gene therapy protocols. *Sci. Prog.* 93: 129-140, 2010

85.) Dominici,M. *et al.* Minimal criteria for defining multipotent mesenchymal stromal cells. The International Society for Cellular Therapy position statement. *Cytotherapy.* 8: 315-317, 2006

86.) Porada,C.D., Zanjani,E.D., & Almeida-Porad,G. Adult mesenchymal stem cells: a pluripotent population with multiple applications. *Curr. Stem Cell Res. Ther.* 1: 365-369, 2006

87.) Online Mendelian Inheritance in Man, OMIM (TM). 2010
HP: http://www.ncbi.nlm.nih.gov/omim/

88.) Pernick, N. PathologyOutlines.com, Inc. 14-9-2010
HP: http://pathologyoutlines.com/cdmarkers.html

89.) Deaglio,S. *et al.* Adenosine generation catalyzed by CD39 and CD73 expressed on regulatory T cells mediates immune suppression. *J. Exp. Med.* 204: 1257-1265, 2007

90.) Kobie,J.J. *et al.* T regulatory and primed uncommitted CD4 T cells express CD73, which suppresses effector CD4 T cells by converting 5'-adenosine monophosphate to adenosine. *J. Immunol.* 177: 6780-6786, 2006

91.) Halfon,S., Abramov,N., Grinblat,B., & Ginis,I. Markers distinguishing mesenchymal stem cells from fibroblasts are downregulated with passaging. *Stem Cells Dev.* 2010

92.) Pittenger,M.F. *et al.* Multilineage potential of adult human mesenchymal stem cells. *Science* 284: 143-147, 1999

93.) Mikhailov,A. *et al.* CD73 participates in cellular multiresistance program and protects against TRAIL-induced apoptosis. *J. Immunol.* 181: 464-475, 2008

94.) Jin,D. *et al.* CD73 on tumor cells impairs antitumor T-cell responses: a novel mechanism of tumor-induced immune suppression. *Cancer Res.* 70: 2245-2255, 2010

95.) Murray,L. *et al.* Enrichment of human hematopoietic stem cell activity in the CD34$^+$Thy-1$^+$Lin$^-$ subpopulation from mobilized peripheral blood. *Blood* 85: 368-378, 1995

96.) Nakamura,Y. *et al.* Expression of CD90 on keratinocyte stem/progenitor cells. *Br. J. Dermatol.* 154: 1062-1070, 2006

97.) Wetzel,A. *et al.* Human Thy-1 (CD90) on activated endothelial cells is a counterreceptor for the leukocyte integrin Mac-1 (CD11b/CD18). *J. Immunol.* 172: 3850-3859, 2004

98.) Rege,T.A. & Hagood,J.S. Thy-1 as a regulator of cell-cell and cell-matrix interactions in axon regeneration, apoptosis, adhesion, migration, cancer, and fibrosis. *FASEB J.* 20: 1045-1054, 2006

99.) Koumas,L., Smith,T.J., Feldon,S., Blumberg,N., & Phipps,R.P. Thy-1 expression in human fibroblast subsets defines myofibroblastic or lipofibroblastic phenotypes. *Am. J. Pathol.* 163: 1291-1300, 2003

100.) Sorrell,J.M. & Caplan,A.I. Fibroblasts-a diverse population at the center of it all. *Int. Rev. Cell Mol. Biol.* 276: 161-214, 2009

101.) Dallas,N.A. *et al.* Endoglin (CD105): a marker of tumor vasculature and potential target for therapy. *Clin. Cancer Res.* 14: 1931-1937, 2008

102.) Cheifetz,S. *et al.* Endoglin is a component of the transforming growth factor-beta receptor system in human endothelial cells. *J. Biol. Chem.* 267: 19027-19030, 1992

103.) Boiko,A.D. *et al.* Human melanoma-initiating cells express neural crest nerve growth factor receptor CD271. *Nature* 466: 133-137, 2010

104.) Morrison,S.J., White,P.M., Zock,C., & Anderson,D.J. Prospective identification, isolation by flow cytometry, and in vivo self-renewal of multipotent mammalian neural crest stem cells. *Cell* 96: 737-749, 1999

105.) Quirici,N. *et al.* Isolation of bone marrow mesenchymal stem cells by anti-nerve growth factor receptor antibodies. *Exp. Hematol.* 30: 783-791, 2002

106.) Buhring,H.J. *et al.* Novel markers for the prospective isolation of human MSC. *Ann. N. Y. Acad. Sci.* 1106: 262-271, 2007

107.) Battula,V.L. *et al.* Isolation of functionally distinct mesenchymal stem cell subsets using antibodies against CD56, CD271, and mesenchymal stem cell antigen-1. *Haematologica* 94: 173-184, 2009

108.) Nauta,A.J. & Fibbe,W.E. Immunomodulatory properties of mesenchymal stromal cells. *Blood* 110: 3499-3506, 2007

109.) Jones,B.J. & McTaggart,S.J. Immunosuppression by mesenchymal stromal cells: from culture to clinic. *Exp. Hematol.* 36: 733-741, 2008

110.) da Silva,M.L., Caplan,A.I., & Nardi,N.B. In search of the in vivo identity of mesenchymal stem cells. *Stem Cells* 26: 2287-2299, 2008

111.) Ramasamy,R., Tong,C.K., Seow,H.F., Vidyadaran,S., & Dazzi,F. The immunosuppressive effects of human bone marrow-derived mesenchymal stem cells target T cell proliferation but not its effector function. *Cell Immunol.* 251: 131-136, 2008

112.) Barry,F.P., Murphy,J.M., English,K., & Mahon,B.P. Immunogenicity of adult mesenchymal stem cells: lessons from the fetal allograft. *Stem Cells Dev.* 14: 252-265, 2005

113.) Momin,E.N., Vela,G., Zaidi,H.A., & Quinones-Hinojosa,A. The oncogenic potential of mesenchymal stem cells in the treatment of cancer: directions for future research. *Curr. Immunol. Rev.* 6: 137-148, 2010

114.) Lazarus,H.M. *et al.* Cotransplantation of HLA-identical sibling culture-expanded mesenchymal stem cells and hematopoietic stem cells in hematologic malignancy patients. *Biol. Blood Marrow Transplant.* 11: 389-398, 2005

115.) Le,B.K. *et al.* Transplantation of mesenchymal stem cells to enhance engraftment of hematopoietic stem cells. *Leukemia* 21: 1733-1738, 2007

116.) Meuleman,N. *et al.* Infusion of mesenchymal stromal cells can aid hematopoietic recovery following allogeneic hematopoietic stem cell myeloablative transplant: a pilot study. *Stem Cells Dev.* 18: 1247-1252, 2009

117.) Jiang,X.X. *et al.* Human mesenchymal stem cells inhibit differentiation and function of monocyte-derived dendritic cells. *Blood* 105: 4120-4126, 2005

118.) Nauta,A.J., Kruisselbrink,A.B., Lurvink,E., Willemze,R., & Fibbe,W.E. Mesenchymal stem cells inhibit generation and function of both CD34^{+}-derived and monocyte-derived dendritic cells. *J. Immunol.* 177: 2080-2087, 2006

119.) Beyth,S. *et al.* Human mesenchymal stem cells alter antigen-presenting cell maturation and induce T-cell unresponsiveness. *Blood* 105: 2214-2219, 2005

120.) Ramasamy,R. *et al.* Mesenchymal stem cells inhibit dendritic cell differentiation and function by preventing entry into the cell cycle. *Transplantation* 83: 71-76, 2007

121.) Aggarwal,S. & Pittenger,M.F. Human mesenchymal stem cells modulate allogeneic immune cell responses. *Blood* 105: 1815-1822, 2005

122.) Corcione,A. *et al.* Human mesenchymal stem cells modulate B-cell functions. *Blood* 107: 367-372, 2006

123.) Di,N.M. *et al.* Human bone marrow stromal cells suppress T-lymphocyte proliferation induced by cellular or nonspecific mitogenic stimuli. *Blood* 99: 3838-3843, 2002

124.) Bartholomew,A. *et al.* Mesenchymal stem cells suppress lymphocyte proliferation in vitro and prolong skin graft survival in vivo. *Exp. Hematol.* 30: 42-48, 2002

125.) Krampera,M. *et al.* Bone marrow mesenchymal stem cells inhibit the response of naive and memory antigen-specific T cells to their cognate peptide. *Blood* 101: 3722-3729, 2003

126.) Zappia,E. *et al.* Mesenchymal stem cells ameliorate experimental autoimmune encephalomyelitis inducing T-cell anergy. *Blood* 106: 1755-1761, 2005

127.) Benvenuto,F. *et al.* Human mesenchymal stem cells promote survival of T cells in a quiescent state. *Stem Cells* 25: 1753-1760, 2007

128.) Di,I.M. *et al.* Mesenchymal cells recruit and regulate T regulatory cells. *Exp. Hematol.* 36: 309-318, 2008

129.) Prevosto,C., Zancolli,M., Canevali,P., Zocchi,M.R., & Poggi,A. Generation of CD4^{+} or CD8^{+} regulatory T cells upon mesenchymal stem cell-lymphocyte interaction. *Haematologica* 92: 881-888, 2007

130.) Maccario,R. *et al.* Interaction of human mesenchymal stem cells with cells involved in alloantigen-specific immune response favors the differentiation of CD4^{+} T-cell subsets expressing a regulatory/suppressive phenotype. *Haematologica* 90: 516-525, 2005

131.) English,K. *et al.* Cell contact, prostaglandin E(2) and transforming growth factor beta 1 play non-redundant roles in human mesenchymal stem cell induction of CD4^{+}CD25[High] forkhead box P3^{+} regulatory T cells. *Clin. Exp. Immunol.* 156: 149-160, 2009

132.) Chabannes,D. *et al.* A role for heme oxygenase-1 in the immunosuppressive effect of adult rat and human mesenchymal stem cells. *Blood* 110: 3691-3694, 2007

133.) Stagg,J. Immune regulation by mesenchymal stem cells: two sides to the coin. *Tissue Antigens* 69: 1-9, 2007

134.) Schofield,R. The relationship between the spleen colony-forming cell and the haemopoietic stem cell. *Blood Cells* 4: 7-25, 1978

135.) Muguruma,Y. *et al.* Reconstitution of the functional human hematopoietic microenvironment derived from human mesenchymal stem cells in the murine bone marrow compartment. *Blood* 107: 1878-1887, 2006

136.) Calvi,L.M. *et al.* Osteoblastic cells regulate the haematopoietic stem cell niche. *Nature* 425: 841-846, 2003

137.) Maier,C.L., Shepherd,B.R., Yi,T., & Pober,J.S. Explant outgrowth, propagation and characterization of human pericytes. *Microcirculation.* 17: 367-380, 2010

138.) Mendez-Ferrer,S. *et al.* Mesenchymal and haematopoietic stem cells form a unique bone marrow niche. *Nature* 466: 829-834, 2010

139.) Weitz,B. Atlas der Anatomie. Weltbild Verlag, München, 1998

140.) Kanitakis,J. Anatomy, histology and immunohistochemistry of normal human skin. *Eur. J. Dermatol.* 12: 390-399, 2002

141.) Potten,C.S. & Booth,C. Keratinocyte stem cells: a commentary. *J. Invest Dermatol.* 119: 888-899, 2002

142.) Blanpain,C. & Fuchs,E. Epidermal homeostasis: a balancing act of stem cells in the skin. *Nat. Rev. Mol. Cell Biol.* 10: 207-217, 2009

143.) Costin,G.E. & Hearing,V.J. Human skin pigmentation: melanocytes modulate skin color in response to stress. *FASEB J.* 21: 976-994, 2007

144.) Kanitakis,J. Immunohistochemistry of normal human skin. *Eur. J. Dermatol.* 8: 539-547, 1998

145.) Winkelmann,R.K. & Breathnach,A.S. The Merkel cell. *J. Invest Dermatol.* 60: 2-15, 1973

146.) Johnson,K.O. The roles and functions of cutaneous mechanoreceptors. *Curr. Opin. Neurobiol.* 11: 455-461, 2001

147.) Clark,R.A. Skin-resident T cells: the ups and downs of on site immunity. *J. Invest Dermatol.* 130: 362-370, 2010

148.) Haniffa,M.A. *et al.* Adult human fibroblasts are potent immunoregulatory cells and functionally equivalent to mesenchymal stem cells. *J. Immunol.* 179: 1595-1604, 2007

149.) Saalbach,A. *et al.* Dermal fibroblasts induce maturation of dendritic cells. *J. Immunol.* 178: 4966-4974, 2007

150.) Nestle,F.O., Di,M.P., Qin,J.Z., & Nickoloff,B.J. Skin immune sentinels in health and disease. *Nat. Rev. Immunol.* 9: 679-691, 2009

151.) Gray,H. Gray's Anatomy.1901th edition, 1974

152.) Kupper,T.S. & Fuhlbrigge,R.C. Immune surveillance in the skin: mechanisms and clinical consequences. *Nat. Rev. Immunol.* 4: 211-222, 2004

153.) Foster,C.A. *et al.* Human epidermal T cells predominantly belong to the lineage expressing alpha/beta T cell receptor. *J. Exp. Med.* 171: 997-1013, 1990

154.) Clark,R.A. *et al.* The vast majority of CLA^{+} T cells are resident in normal skin. *J. Immunol.* 176: 4431-4439, 2006

155.) Kaporis,H.G. *et al.* Human basal cell carcinoma is associated with Foxp3^{+} T cells in a Th2 dominant microenvironment. *J. Invest Dermatol.* 127: 2391-2398, 2007

156.) Clark,R.A. *et al.* Human squamous cell carcinomas evade the immune response by down-regulation of vascular E-selectin and recruitment of regulatory T cells. *J. Exp. Med.* 205: 2221-2234, 2008

157.) Hirahara,K. *et al.* The majority of human peripheral blood CD4$^+$CD25^{high}Foxp3$^+$ regulatory T cells bear functional skin-homing receptors. *J. Immunol.* 177: 4488-4494, 2006

158.) Sugiyama,H. *et al.* Dysfunctional blood and target tissue CD4$^+$CD25^{high} regulatory T cells in psoriasis: mechanism underlying unrestrained pathogenic effector T cell proliferation. *J. Immunol.* 174: 164-173, 2005

159.) Dudda,J.C., Perdue,N., Bachtanian,E., & Campbell,D.J. Foxp3$^+$ regulatory T cells maintain immune homeostasis in the skin. *J. Exp. Med.* 205: 1559-1565, 2008

160.) Toma,J.G. *et al.* Isolation of multipotent adult stem cells from the dermis of mammalian skin. *Nat. Cell Biol.* 3: 778-784, 2001

161.) Toma,J.G., McKenzie,I.A., Bagli,D., & Miller,F.D. Isolation and characterization of multipotent skin-derived precursors from human skin. *Stem Cells* 23: 727-737, 2005

162.) Fernandes,K.J. *et al.* Analysis of the neurogenic potential of multipotent skin-derived precursors. *Exp. Neurol.* 201: 32-48, 2006

163.) Fernandes,K.J. *et al.* A dermal niche for multipotent adult skin-derived precursor cells. *Nat. Cell Biol.* 6: 1082-1093, 2004

164.) Adly,M.A., Assaf,H.A., & Hussein,M.R. Expression pattern of p75 neurotrophin receptor protein in human scalp skin and hair follicles: Hair cycle-dependent expression. *J. Am. Acad. Dermatol.* 60: 99-109, 2009

165.) Hunt,D.P. *et al.* A highly enriched niche of precursor cells with neuronal and glial potential within the hair follicle dermal papilla of adult skin. *Stem Cells* 26: 163-172, 2008

166.) Oliver,R.F. Whisker growth after removal of the dermal papilla and lengths of follicle in the hooded rat. *J. Embryol. Exp. Morphol.* 15: 331-347, 1966

167.) Jones,S., Horwood,N., Cope,A., & Dazzi,F. The antiproliferative effect of mesenchymal stem cells is a fundamental property shared by all stromal cells. *J. Immunol.* 179: 2824-2831, 2007

168.) Chunmeng,S. & Tianmin,C. Effects of plastic-adherent dermal multipotent cells on peripheral blood leukocytes and CFU-GM in rats. *Transplant. Proc.* 36: 1578-1581, 2004

169.) Schallmoser,K. *et al.* Human platelet lysate can replace fetal bovine serum for clinical-scale expansion of functional mesenchymal stromal cells. *Transfusion* 47: 1436-1446, 2007

170.) Miltenyi Biotec GmbH. MACS$^®$ Technology - Gold standard in cell separation. 2008 HP: www.miltenyibiotec.com

171.) Kürschner, U. Untersuchung zur Toxizität und Biotransformation an der humanen Keratinozytenzelllinie HaCaT. 2007 (Thesis/Dissertation)

172.) Boukamp,P. *et al.* Normal keratinization in a spontaneously immortalized aneuploid human keratinocyte cell line. *J. Cell Biol.* 106: 761-771, 1988

173.) Graham,F.L., Smiley,J., Russell,W.C., & Nairn,R. Characteristics of a human cell line transformed by DNA from human adenovirus type 5. *J. Gen. Virol.* 36: 59-74, 1977

174.) Scholz, W. Cell adhesion and growth on coated or modified glass or plastic surfaces. 2010
HP: http://www.nuncbrand.com/us/frame.aspx?ID=593

175.) Samuelsson,H., Ringden,O., Lonnies,H., & Le,B.K. Optimizing in vitro conditions for immunomodulation and expansion of mesenchymal stromal cells. *Cytotherapy.* 11: 129-136, 2009

176.) Parish,C.R. Fluorescent dyes for lymphocyte migration and proliferation studies. *Immunol. Cell Biol.* 77: 499-508, 1999

177.) Molecular Probes Inc. CellTrace™ CFSE Cell Proliferation Kit. 2005
HP: http://probes.invitrogen.com/media/pis/mp34554.pdf

178.) Emory Universtiy, Georgia.2010
HP: http://www.emory.edu/home/index.html

179.) Lyons,A.B. Divided we stand: tracking cell proliferation with carboxyfluorescein diacetate succinimidyl ester. *Immunol. Cell Biol.* 77: 509-515, 1999

180.) Lyons,A.B., Hasbold,J., & Hodgkin,P.D. Flow cytometric analysis of cell division history using dilution of carboxyfluorescein diacetate succinimidyl ester, a stably integrated fluorescent probe. *Methods Cell Biol.* 63: 375-398, 2001

181.) Hasbold,J., Lyons,A.B., Kehry,M.R., & Hodgkin,P.D. Cell division number regulates IgG1 and IgE switching of B cells following stimulation by CD40 ligand and IL-4. *Eur. J. Immunol.* 28: 1040-1051, 1998

182.) Hodgkin,P.D., Lee,J.H., & Lyons,A.B. B cell differentiation and isotype switching is related to division cycle number. *J. Exp. Med.* 184: 277-281, 1996

183.) Nordon,R.E., Ginsberg,S.S., & Eaves,C.J. High-resolution cell division tracking demonstrates the FLt3-ligand-dependence of human marrow CD34^{+}. *Br. J. Haematol.* 98: 528-539, 1997

184.) Lyons,A.B. Analysing cell division in vivo and in vitro using flow cytometric measurement of CFSE dye dilution. *J. Immunol. Methods* 243: 147-154, 2000

185.) Gett,A.V. & Hodgkin,P.D. Cell division regulates the T cell cytokine repertoire, revealing a mechanism underlying immune class regulation. *Proc. Natl. Acad. Sci. U. S. A* 95: 9488-9493, 1998

186.) Invitrogen and Dynal. Dynabeads[®] Human T-Activator CD3/CD28. 2009
HP: http://tools.invitrogen.com/content/sfs/manuals/111-31D32D61D_Dynabeads_Human_T-Activator_CD3CD28%28rev005%29.pdf

187.) Fina,L. *et al.* Expression of the CD34 gene in vascular endothelial cells. *Blood* 75: 2417-2426, 1990

188.) Kopher,R.A. *et al.* Human embryonic stem cell-derived CD34^{+} cells function as MSC progenitor cells. *Bone* 47: 718-728, 2010

189.) Peltonen,J. *et al.* Localization of integrin receptors for fibronectin, collagen, and laminin in human skin. Variable expression in basal and squamous cell carcinomas. *J. Clin. Invest* 84: 1916-1923, 1989

190.) Karelina,T.V., Hruza,G.J., Goldberg,G.I., & Eisen,A.Z. Localization of 92-kDa type IV collagenase in human skin tumors: comparison with normal human fetal and adult skin. *J. Invest Dermatol.* 100: 159-165, 1993

191.) Schipani,E. & Kronenberg,H.M. StemBook Cambridge (MA): Harvard Stem Cell Institute, 2008

192.) Ishida,M., Kushima,R., & Okabe,H. Aberrant expression of class III beta-tubulin in basal cell carcinoma of the skin. *Oncol. Rep.* 22: 733-737, 2009

193.) Jouhilahti,E.M., Peltonen,S., & Peltonen,J. Class III beta-tubulin is a component of the mitotic spindle in multiple cell types. *J. Histochem. Cytochem.* 56: 1113-1119, 2008

194.) Blondheim,N.R. *et al.* Human mesenchymal stem cells express neural genes, suggesting a neural predisposition. *Stem Cells Dev.* 15: 141-164, 2006

195.) Caneva,L., Soligo,D., Cattoretti,G., De,H.E., & Deliliers,G.L. Immuno-electron microscopy characterization of human bone marrow stromal cells with anti-NGFR antibodies. *Blood Cells Mol. Dis.* 21: 73-85, 1995

196.) Airas,L. *et al.* CD73 is involved in lymphocyte binding to the endothelium: characterization of lymphocyte-vascular adhesion protein 2 identifies it as CD73. *J. Exp. Med.* 182: 1603-1608, 1995

197.) Arvilommi,A.M., Salmi,M., Airas,L., Kalimo,K., & Jalkanen,S. CD73 mediates lymphocyte binding to vascular endothelium in inflamed human skin. *Eur. J. Immunol.* 27: 248-254, 1997

198.) Airas,L., Niemela,J., & Jalkanen,S. CD73 engagement promotes lymphocyte binding to endothelial cells via a lymphocyte function-associated antigen-1-dependent mechanism. *J. Immunol.* 165: 5411-5417, 2000

199.) Saalbach,A., Haustein,U.F., & Anderegg,U. A ligand of human Thy-1 is localized on polymorphonuclear leukocytes and monocytes and mediates the binding to activated Thy-1-positive microvascular endothelial cells and fibroblasts. *J. Invest Dermatol.* 115: 882-888, 2000

200.) Campioni,D. *et al.* A decreased positivity for CD90 on human mesenchymal stromal cells (MSCs) is associated with a loss of immunosuppressive activity by MSCs. *Cytometry B Clin. Cytom.* 76: 225-230, 2009

201.) Buhring,H.J. *et al.* Phenotypic characterization of distinct human bone marrow-derived MSC subsets. *Ann. N. Y. Acad. Sci.* 1176: 124-134, 2009

202.) Duarte,R.F. *et al.* Functional impairment of human T-lymphocytes following PHA-induced expansion and retroviral transduction: implications for gene therapy. *Gene Ther.* 9: 1359-1368, 2002

203.) Gieseke,F. *et al.* Human multipotent mesenchymal stromal cells inhibit proliferation of PBMCs independently of IFNgammaR1 signaling and IDO expression. *Blood* 110: 2197-2200, 2007

204.) Najar,M. *et al.* Mesenchymal stromal cells promote or suppress the proliferation of T lymphocytes from cord blood and peripheral blood: the importance of low cell ratio and role of interleukin-6. *Cytotherapy.* 11: 570-583, 2009

205.) Selmani,Z. *et al.* Human leukocyte antigen-G5 secretion by human mesenchymal stem cells is required to suppress T lymphocyte and natural killer function and to induce CD4$^+$CD25^{high}FOXP3$^+$ regulatory T cells. *Stem Cells* 26: 212-222, 2008

206.) Wang,Y., Zhang,A., Ye,Z., Xie,H., & Zheng,S. Bone marrow-derived mesenchymal stem cells inhibit acute rejection of rat liver allografts in association with regulatory T-cell expansion. *Transplant. Proc.* 41: 4352-4356, 2009

207.) Yoo,K.H. *et al.* Comparison of immunomodulatory properties of mesenchymal stem cells derived from adult human tissues. *Cell Immunol.* 259: 150-156, 2009

208.) Najar,M. *et al.* Mesenchymal stromal cells use PGE2 to modulate activation and proliferation of lymphocyte subsets: Combined comparison of adipose tissue, Wharton's Jelly and bone marrow sources. *Cell Immunol.* 264: 171-179, 2010

209.) Pfisterer, K. and Elbe-Bürger, A. Establishment of a CFSE-based cell division tracing system to investigate the differentiation of human naive helper T cells. 2010 (Unpublished Work)

210.) Sakaguchi,S., Wing,K., Onishi,Y., Prieto-Martin,P., & Yamaguchi,T. Regulatory T cells: how do they suppress immune responses? *Int. Immunol.* 21: 1105-1111, 2009

211.) Bocelli-Tyndall,C. *et al.* Human bone marrow mesenchymal stem cells and chondrocytes promote and/or suppress the in vitro proliferation of lymphocytes stimulated by interleukins 2, 7 and 15. *Ann. Rheum. Dis.* 68: 1352-1359, 2009

212.) Banas,R.A. *et al.* Immunogenicity and immunomodulatory effects of amnion-derived multipotent progenitor cells. *Hum. Immunol.* 69: 321-328, 2008

213.) Gimmi,C.D., Freeman,G.J., Gribben,J.G., Gray,G., & Nadler,L.M. Human T-cell clonal anergy is induced by antigen presentation in the absence of B7 costimulation. *Proc. Natl. Acad. Sci. U. S. A* 90: 6586-6590, 1993

214.) Tan,P. *et al.* Induction of alloantigen-specific hyporesponsiveness in human T lymphocytes by blocking interaction of CD28 with its natural ligand B7/BB1. *J. Exp. Med.* 177: 165-173, 1993

215.) Webb,L.M. & Feldmann,M. Critical role of CD28/B7 costimulation in the development of human Th2 cytokine-producing cells. *Blood* 86: 3479-3486, 1995

216.) Rulifson,I.C., Sperling,A.I., Fields,P.E., Fitch,F.W., & Bluestone,J.A. CD28 costimulation promotes the production of Th2 cytokines. *J. Immunol.* 158: 658-665, 1997

217.) Guo,F., Iclozan,C., Suh,W.K., Anasetti,C., & Yu,X.Z. CD28 controls differentiation of regulatory T cells from naive CD4 T cells. *J. Immunol.* 181: 2285-2291, 2008

218.) Chagastelles,P.C., Nardi,N.B., & Camassola,M. Biology and applications of mesenchymal stem cells. *Sci. Prog.* 93: 113-127, 2010

219.) Vaculik, C. Characterization and isolation of stem cells in the human dermis. 2008 (Thesis/Dissertation), Medical University of Vienna

220.) Trejo,O., Reed,J.A., & Prieto,V.G. Atypical cells in human cutaneous re-excision scars for melanoma express p75NGFR, C56/N-CAM and GAP-43: evidence of early Schwann cell differentiation. *J. Cutan. Pathol.* 29: 397-406, 2002

221.) Chunmeng,S. & Tianmin,C. Skin: a promising reservoir for adult stem cell populations. *Med. Hypotheses* 62: 683-688, 2004

222.) Javazon,E.H., Beggs,K.J., & Flake,A.W. Mesenchymal stem cells: paradoxes of passaging. *Exp. Hematol.* 32: 414-425, 2004

223.) Schieker,M. *et al.* Human mesenchymal stem cells at the single-cell level: simultaneous seven-colour immunofluorescence. *J. Anat.* 210: 592-599, 2007

224.) Rose,R.A. *et al.* Bone marrow-derived mesenchymal stromal cells express cardiac-specific markers, retain the stromal phenotype, and do not become functional cardiomyocytes in vitro. *Stem Cells* 26: 2884-2892, 2008

225.) Shi,S. & Gronthos,S. Perivascular niche of postnatal mesenchymal stem cells in human bone marrow and dental pulp. *J. Bone Miner. Res.* 18: 696-704, 2003

226.) Skalli,O. *et al.* Alpha-smooth muscle actin, a differentiation marker of smooth muscle cells, is present in microfilamentous bundles of pericytes. *J. Histochem. Cytochem.* 37: 315-321, 1989

227.) Peled,A., Zipori,D., Abramsky,O., Ovadia,H., & Shezen,E. Expression of alpha-smooth muscle actin in murine bone marrow stromal cells. *Blood* 78: 304-309, 1991

228.) Kotoula,V., Papamichos,S.I., & Lambropoulos,A.F. Revisiting OCT4 expression in peripheral blood mononuclear cells. *Stem Cells* 26: 290-291, 2008

229.) Lee,J., Kim,H.K., Rho,J.Y., Han,Y.M., & Kim,J. The human OCT-4 isoforms differ in their ability to confer self-renewal. *J. Biol. Chem.* 281: 33554-33565, 2006

230.) Tschachler,E. *et al.* Sheet preparations expose the dermal nerve plexus of human skin and render the dermal nerve end organ accessible to extensive analysis. *J. Invest Dermatol.* 122: 177-182, 2004

231.) Covas,D.T. *et al.* Multipotent mesenchymal stromal cells obtained from diverse human tissues share functional properties and gene-expression profile with CD146^{+} perivascular cells and fibroblasts. *Exp. Hematol.* 36: 642-654, 2008

232.) Romanov,Y.A., Svintsitskaya,V.A., & Smirnov,V.N. Searching for alternative sources of postnatal human mesenchymal stem cells: candidate MSC-like cells from umbilical cord. *Stem Cells* 21: 105-110, 2003

233.) Sarugaser,R., Lickorish,D., Baksh,D., Hosseini,M.M., & Davies,J.E. Human umbilical cord perivascular (HUCPV) cells: a source of mesenchymal progenitors. *Stem Cells* 23: 220-229, 2005

234.) Foster,K. *et al.* Contribution of neural crest-derived cells in the embryonic and adult thymus. *J. Immunol.* 180: 3183-3189, 2008

235.) Dupin,E., Calloni,G., Real,C., Goncalves-Trentin,A., & Le Douarin,N.M. Neural crest progenitors and stem cells. *C. R. Biol.* 330: 521-529, 2007

236.) Le,B.K., Tammik,L., Sundberg,B., Haynesworth,S.E., & Ringden,O. Mesenchymal stem cells inhibit and stimulate mixed lymphocyte cultures and mitogenic responses

independently of the major histocompatibility complex. *Scand. J. Immunol.* 57: 11-20, 2003

237.) Clark,R.A. & Kupper,T.S. IL-15 and dermal fibroblasts induce proliferation of natural regulatory T cells isolated from human skin. *Blood* 109: 194-202, 2007

238.) Golovina,T.N. *et al.* CD28 costimulation is essential for human T regulatory expansion and function. *J. Immunol.* 181: 2855-2868, 2008

239.) Sansom,D.M. & Walker,L.S. The role of CD28 and cytotoxic T-lymphocyte antigen-4 (CTLA-4) in regulatory T-cell biology. *Immunol. Rev.* 212: 131-148, 2006

240.) Schuster,C. *et al.* HLA-DR[+] leukocytes acquire CD1 antigens in embryonic and fetal human skin and contain functional antigen-presenting cells. *J. Exp. Med.* 206: 169-181, 2009

241.) Bour-Jordan,H. & Blueston,J.A. CD28 function: a balance of costimulatory and regulatory signals. *J. Clin. Immunol.* 22: 1-7, 2002

242.) Goldrath,A.W. & Bevan,M.J. Selecting and maintaining a diverse T-cell repertoire. *Nature* 402: 255-262, 1999

243.) Marrack,P. *et al.* Homeostasis of alpha beta TCR^{+} T cells. *Nat. Immunol.* 1: 107-111, 2000

244.) Surh,C.D. & Sprent,J. Homeostatic T cell proliferation: how far can T cells be activated to self-ligands? *J. Exp. Med.* 192: F9-F14, 2000

245.) Surh,C.D., Ernst,B., Lee,D.S., Dummer,W., & LeRoy,E. Role of self-major histocompatibility complex/peptide ligands in selection and maintenance of a diverse T cell repertoire. *Immunol. Res.* 21: 331-339, 2000

8   Curriculum Vitae

PERSONAL INFORMATION

Name	Karin Pfisterer
Date and Place of Birth	April 16th, 1980; Grieskirchen, Austria
Nationality	Austria
Marital status	domestic partnership
Children	Jakob Vitus Wielscher (born Dec. 8th, 2008)
Office Address	Medical University of Vienna
	Dept. of Dermatology,
	Division of Immunology, Allergy and Infectious Diseases
	Lazarettgasse 19
	1090 Vienna, Austria
	Phone: +43-1-40160-63008
	Fax: +43-1-40160-963005
Home Address	Castellezgasse 2/13
	1020 Vienna, Austria
	Mobile: +43-699-10256410

EDUCATION

since 11/2009	employed as project collaborator
	Department of Dermatology, Medical University of Vienna
2009	maternal leave
01/2008-11/2008	Diploma Thesis in Immunobiology:
	"Human Dermal Mesenchymal Stem Cell Subsets Induce FoxP3 in Naive T cells"
	Department of Dermatology, Medical University of Vienna;
	Supervisor: ao.Prof.Dr. Adelheid Elbe-Bürger
2002	Studies of Genetics/Microbiology, University of Vienna, Austria
2000-2002	Temporary employment abroad (Africa, South America, North America, Europe)
1995-2000	Commercial Academy, Ried i./I., Austria
1990-1995	Humanistic Gymnasium, Ried i./I., Austria
1986-1990	Primary School, Upper Austria

PUBLICATIONS

<u>Pfisterer K.</u>, Vaculik C., Kramer G., Strunk D., Elbe-Bürger A.: Human Dermal-derived Mesenchymal Stem Cells Efficiently Promote the Differentiation of Naive Helper T Cells into Regulatory T cells (**poster abstract**). Jahrestagung der Österreichische Gesellschaft für Dermatologie und Venerologie, Nov. 19-21, 2010, Vienna, Austria

<u>Pfisterer, K.</u>, Vaculik C., Kramer G., Strunk D., Elbe-Bürger A.: Human Skin-derived Mesenchymal Stem Cells Drive the Differentiation of Naive Helper T Cells Towards a Regulatory Phenotype without Provision of Costimulatory Molecules (**selected talk**). Annual Meeting of the Austrian Society for Allergology and Immunology, Dec 3-5, 2010, Vienna, Austria

<u>Pfisterer, K.</u>, Kramer G., Strunk D., Elbe-Bürger A.: Perivascular Mesenchymal Stem Cells from Human Dermis Drive the Differentiation of Naive Helper T Cells Towards a Regulatory Phenotype without Provision of Known Costimulatory Molecules (**manuscript in preparation**).